

NONLINEAR OPTICAL PROPERTIES OF NATURAL DYES BASED ON OPTICAL RESONANCE

Sidiki Zongo

A thesis submitted in partial fulfillment of the requirements for the degree of Magister Philosophiae in the Department of Physics, University of the Western Cape

Supervisor: Prof. M. Maaza (iThemba LABS, Materials Research Department).



Co-supervisors:

Dr. S. Halindintwali (University of the Western Cape, Physics Department)

Dr. L. Kotsedi (iThemba LABS, Materials Research Department)

November 2012

Key words

Nonlinear properties

Resonance

Natural dyes

Optical limiting

Femtosecond laser

Refractive index

Multiphoton absorption



Acknowledgments

I am very thankful to my guide and supervisor, Professor Malik Maaza, for the constant support, suggestions and encouragement that I received from him throughout the period of my MSc work. His support and encouragement have been a source of inspiration to me all the time. I am grateful to my co-supervisors Dr. Sylvain Halindintwali who always showed deep interest in my work. His comments and suggestions have helped me considerably during the period of the research work. My gratitude also goes to Dr Balla N’Gom and Dr. Lebogang Kotsedi, for their advices and support. I would like to thank the MRD staff members for all the help, they rendered. I am happy to acknowledge the African Institute for Mathematical Sciences (AIMS - South Africa), NRF-ithemba LABS, NanoAfnet for the M.Sc. fellowship. I also thank Mr. B. Sone and Mr. S. Kamlish for the help received from them. I am thankful to Remy Boucher, Dr. Mlungisi Nkosi, Dr. Siham Yousuf Alqaradawi for their facilities and particularly Dr. Patience Mthunzi and for her generosity and her optical facilities.

I want to thank, Siaka Lougué, Ousmane Sawadogo and Dechi Taya Joelle. I am grateful for their support and trust. Many thanks go to N. Nyangiwe and Y. zebib for their friendship.

A special thank goes to Prof. Claude Carignan and his wife M. Monique. Their supporting love kept me going through hard times and gave me confidence and courage. I would like to thank once again all the persons who helped me in one way or another for the successful completion of my research work.

I would like to remember with deep sense of gratitude the support received from the parents during the present work.



UNIVERSITY *of the*
WESTERN CAPE

Abstract

Recent research shows that the study of optical properties of organic material natural dyes has gained much consideration. The specific functional groups in several natural dyes remain essential for the large nonlinear absorption expressed in terms of nonlinear optical susceptibilities or other mechanism of absorption such as two photon absorption (TPA), reverse saturable absorption (RSA) or intensity-dependent refractive index characteristic. In this thesis we highlight the optical limiting responses of selected natural dyes as nonlinear response in the femtosecond regime. This technique refers to the decrease of the transmittance of the material with the increased incident light intensity. Three dyes derived from beetroot, flame flower and mimosa flower dyes were investigated. The results showed a limiting behaviour around 795 mW for the beetroot and the flame dye while there is total transmission in the flame dye sample. The performance of the nonlinearity i.e. the optical limiting is related to the existence of alternating single and double bonds (i.e. C-C and C=C bonds) in the molecules that provides the material with the π -electron delocalization, but also it is related to the light intensity. Beside nonlinearity study, crystallographic investigation was carried out for more possible applicability of the selected dyes and this concerned only the mimosa and flame flower dye thin film samples since the beetroot thin film was very sensitive to strong irradiation (i.e. immediately destroyed when exposed to light with high intensity). For more stability, dye solutions were encapsulated in gels for further measurements.

Contents

CHAPTER-1: INTRODUCTION	1
1.1. Definition and Motivation	1
1.2. Objectives and Scope of the Research Project	4
References:	4
CHAPTER-2: NONLINEAR OPTICS	7
2.1. General Description of Nonlinear Optics	7
2.2. Atomistic and Classical Origin	10
2.3. Maxwell's Equations	18
2.4. Polarization and Nonlinear Susceptibility.....	22
2.5. Second Harmonic Generation and Phase-Matching Process	23
2.6. Third Harmonic Generation (THG)	27
2.7. Example of NLO Effects.....	28
2.7.1. Intensity-Dependent Refractive Index (IDRI).....	28
2.7.2 Harmonic Generation and Wave mixing.....	29
2.7.3 Saturable Absorption.....	31
2.8. Optical Limiting.....	34
References:	38
CHAPTER-3: GENERAL DESCRIPTION OF NATURAL DYES	40
3.1. Description of Natural Dyes	40
3.2. Sources of Natural Dyes.....	41
3.3. Natural Distribution and Chemical structure	42
3.3.1 Caratenoids	42
3.3.2 Chlorophyll	44
3.3.3 Flavonoids.....	46
3.3.4. Betalains	48
3.4. Extraction of Natural Dyes	49
3.5. Colour and Stability	51
3.6. Stability Enhancement	52
3.7. Typical Examples of Dyes in Photonics:	53
3.7.1 Dye Lasers Sources.....	53

3.7.2. Dye Solar Cells	58
References:	63
CHAPTER-4: EXPERIMENTS, RESULTS AND DISCUSSION	68
4.1. Samples preparation, Morphological, Elemental and Crystallographic Characterization.....	69
4.1.1 Samples Preparation.....	69
4.1.2 X-Ray Diffraction	72
4.1.3 Atomic Force Microscopy (AFM) and Scanning Electron Microscopy (SEM)-EDX Analysis	75
4.2. Linear and Nonlinear Properties	81
4.2.1. Infrared Spectroscopy and Vibrational Properties.	81
4.2.2. UV-VIS Spectroscopy and Optical Absorption Properties.	85
4.2.3. Nonlinear Optical Properties and Optical Limiting Investigations	97
References:	106
SUMMARY AND CONCLUSION.....	108



Declaration

I hereby, declare that the work contained in this thesis is my original work, and that it has not been submitted anywhere for any award. Where other sources of information have been used, they have been acknowledged and referenced accordingly.

Sidiki Zongo,

November 2012



CHAPTER-1: Introduction

1.1. Definition and Motivation

As it is well established, the nonlinear optical (NLO) response of materials results from modification of their optical properties while interacting with intense pumping electromagnetic waves [Sat-2007, Rob-2007]. The investigation of these NLO properties in specific class of materials remains an important aspect in the field of electromagnetism in general and optics particular. The optical investigation leads to a better understanding of not only the fundamental nature of such an intense light-matter interaction but also induces a large spectrum of photonics applications too [Car-1997]. From technological point of view, NLO materials are currently full integrated components in numerous devices in bulk, micro and nano-scaled forms. The global market for NLO materials was estimated to be about \$856.1 million in 2005 and \$1,656 billion in 2009 with a yearly average growth of about 5-7% [Bus-2005].

From fundamental perspectives, the NLO optical response of a material can lead to experimental conditions that are not attainable by other standard means. As an illustration, one can consider the harmonic conversion of a modern laser illumination to frequencies in which laser radiations are not directly accessible [Ste-2000]. Historically, the NLO response has been achieved with the first experiment of the second harmonic generation (SHG) conducted by Peter Franken and colleagues in 1961 [Kar-2009]. This pioneering experiment was the cornerstone phase which has stimulated a wide interest in the field of NLO optical phenomena. More accurately, an NLO optical response is generated from basic mechanism such as anharmonicity of the alternative single and double bond electrons, molecular orientation local polarization, variation of the refractive index and multiphoton absorption [Rob-2007].

Thus, the use of a generation of lasers that can provide high light intensities permits the investigation and understanding of details and in the molecular and atomic structure of any optical material in various time scale such as the femtosecond and even the attosecond regimes [Ahm-1999]. A large number of NLO effects are observed among them, we can list the Kerr electro-optic effect, Pockel's electro-optic effect, third harmonic generation (THG), the second harmonic generation, general four wave mixing (FWM), self-focusing, Brillouin scattering, Raman scattering, self-phase modulation, self-phase conjugation and two-photon absorption [Ter-2008]. Theoretically, most of these phenomena are fully described by the perturbation theory, in which nonlinear susceptibility is highlighted by applying the Fourier transform of the Green function [Val-2004, Ale-2012].

While there is a wide class of NLO materials [Ele-2000], the current trend is geared towards hybrid systems involving artificial dye-like macro-cycles. As established, the NLO susceptibility describing the nonlinear response exhibited by such dyes is due to the π -electrons' delocalization in the conjugated systems [Leo-2010]. The application of these organic materials in devices is often limited by their stability and their optical bleaching. Hence there is a need to engineer new hybrid NLO systems based on more stable dye; encapsulated natural dye molecules in gel host matrices could be a potential solution.

Natural dyes have long been known for their several and multi-functional applications in colouring of food, leather as well as natural protein fibres-like wool, silk and cotton as major areas of use [Ash-2009]. However, the advent of synthetic dye technologies has considerably reduced the extent of the use of such natural dyes. There is an emerging interest and research work being undertaken by various research groups worldwide on natural dye applications for various reasons, namely [Wah-2004]:

- (i) Green chemistry and environmental protection, which has become a challenge for the chemical industry world-wide,
- (ii) The shift of technology towards practically non-polluting and green based technologies,
- (iii) The viability of natural dyes and the high potential of these to be used as optical materials for industrial and scientific applications.

This growing interest in the application of natural dyes is geared mainly towards the need of developing green novel hybrid photonics. Indeed, several reports [Rek-2009, Bal-2011] have demonstrated that some natural dyes exhibit colossal and ultrafast nonlinear responses. Consequentially, these natural dyes are receiving great attention due to the high degree of electron conjugation. This thesis investigates of linear and nonlinear optical properties of 3 specific natural dyes: namely red-beetroot, orange-flame flower and yellow-mimosa flower dyes.

In chapters 2 and 3, we will give an overview of the theoretical background. This will cover the basic properties of nonlinear optics as well as the physical-chemical characteristics of natural dyes in general. In chapter 4, we will present the samples preparation procedure, the analytical techniques used in the samples characterisation, the results obtained and their discussion. The last part of the thesis will summarize the result of our investigation and presents our recommendations for future work.

1.2. Objectives and Scope of the Research Project

The aim of this research work is to demonstrate the possibility of using natural dyes as NLO materials for optical applications, particularly for optical limiting. More specifically, we focus on three selected natural dyes extracted from plants namely: red-beetroot, orange-butea monosperma commonly called flame of forest and yellow-mimosa dyes. The investigations were carried out following the subsequent phases:

- (i) Literature review on natural dyes and their NLO properties,
- (ii) Dye identification and extraction phase,
- (iii) Elemental analysis,
- (iv) Optical absorption characterization,
- (v) Optical limiting investigations in the femtosecond regime,
- (vi) Demonstration and engineering of stable selected dyes-gel hybrid matrix composites.



References:

- [Sat-2007] K. Sathiyamoorthy, Synopsis of nonlinear optical response of dyes and metalloporphyrin in atypical environments, Department of Physics, Indian Institute of Technology Madras Chennai, India. April 2007.
- [Rob-2007] Robert W. Boyd. The Nonlinear Optical Susceptibility (2007)
- [Car-1997] Carlo Boutron et al. Enhanced Second-Order Optical Nonlinearity of Dye Molecules Adsorbed onto Laponite Particles, Clays and Clay Minerals, Vol, 45, No. 3, 483-485, (1997)
- [Bus-2005] Business Communications Company Inc, Non-Linear Optical Materials and Applications, August (2005)

- [Ste-2000] Steven Richard Vigil, Nonlinear-Optical Studies of Organic Liquids and Polymer optical Fibers, Washington State University, Ph.D. May (2000)
- [Kar-2009] A. Karpierz and George I. Stegeman¹, Nonlinear Optics: A Vibrant Field Mirosław, Photonics Letter of Poland, vol. 1 (4), 145-147 (2009)
- [Ahm-1999] Ahmed Zewail, Nobel Prize lecture, Nobel Foundation, Femtochemistry: Atomic-Scale Dynamics of the Chemical Bond Using Ultrafast Lasers (1999)
- [Val-2004] Valerio Lucarini, Jarkko J. Saarinen, Kai-Erik , Peiponen, and Erik M. Vartiainen, Kramers-Kronig Relations in Optical Materials Research ; Monograph November 14 (2004)
- [Ale-2012] Aleksei Zheltikov, Anne L'Huilier and Ferenc Keszler, Nonlinear Optics, Physics and Astronomy, Part A, 161-251, (2012)
- [Bah-1991] Bahaa E. A. Saleh, , Fundamentals of Photonics Nonlinear Optics Carl Teich John Wiley and Sons, Inc. ISBNs: 0-471-83965-5 (Hardback); 0-471-2-1374-8 (Electronic) (1991)
- [Ter-2008] Francesca Terenziani, Claudine Katan, Ekaterina Badaeva, Sergei Tretiak, Mireille Blanchard-Desce, Enhanced Two-Photon Absorption of Organic Chromophores: Theoretical and Experimental Assessment, Advanced Materials. 20, 4641-4678 (2008)
- [Ele-2000] Electro-optics handbook, R.W. Waynant and M.N. Ediger, Editors, McGraw Hill Inc, ISBN 0-07-068716-1 (2000)
- Leonardo De Boni, Daniel S. Corrêa and Cleber R. Mendonça, Nonlinear Optical Absorption of Organic Molecules for Applications in Optical Devices, Advances in Lasers and Electro Optics (2010)
- [Leo-2010] Leonardo De Boni, Daniel S. Corrêa and Cleber R. Mendonça, Nonlinear Optical Absorption of Organic Molecules for Applications in Optical Devices, Advances in Lasers and Electro

Optics (2010)

- [Ash-2009] Ashis Kumar Samanta and Priti Agarwal, Application natural Dyes on textiles, Indian Journal of fibre & Textile Research. Vol.34, 384, (2009)
- [Wah-2004] S. Waheed and A. Alma Studies of Some natural Dyes, Jour.Chem.Soc.Pak. Vol.26, No .3, 255(2004)
- [Rek-2009] R.K. Rekha and A. Ramalingam, Non-linear characterization and optical limiting effect of carmine dye, Indian Journal of Science and Technology, Vol.2 No. 8 2009)
- [Bal-2011] G. Balaji, R.K. Rekha and A. Ramalingam, Nonlinear Characterization of Safranin O Dye for Application in Optical Limiting , Acta Physica Polonica A , Vol. 119 (2011)



CHAPTER-2: Nonlinear Optics

2.1. General Description of Nonlinear Optics

While the objective of this chapter is to give an overview on nonlinear optical properties of materials, it is worth starting by highlighting the basic foundations of electromagnetic wave and matter interaction. Under normal conditions, most of a material's responses to an applied electric field exhibit linear characteristics. As a consequence, physical properties in general and optical characteristics specifically can entirely be described using linear optical properties. Thus, the interaction of an applied electric field with material at low light intensities leaves the optical properties of such material unchanged. In others words, the optical properties of the material are independent of light intensity. In that case, the superposition principle holds true and the light waves do not interact with each other while passing through the sample. This is illustrated in figure 1. (a), which shows that the behaviour of a light wave when exiting a medium at low frequency and low intensities does not produce any new frequencies. The scattered and the incident waves have the same frequencies but not necessarily the same propagation direction.

In contrast to the linear optical regime, the nonlinear optical phenomena occur as a consequence of the modification of optical properties, such as the refractive index and the speed of light in the nonlinear system because of its interaction with intense incident light. In such conditions, the superposition principle is thus no longer valid and light can be used to control light [Bah-1991]. Figure 1. (b) is an illustration of an interaction in which new frequencies are generated after the medium is excited using intense light. The NLO response is therefore described [Sat-2007] as the consequence of intense light interaction with matter, causing the modification of optical properties of such matter interacting within the

optical field.

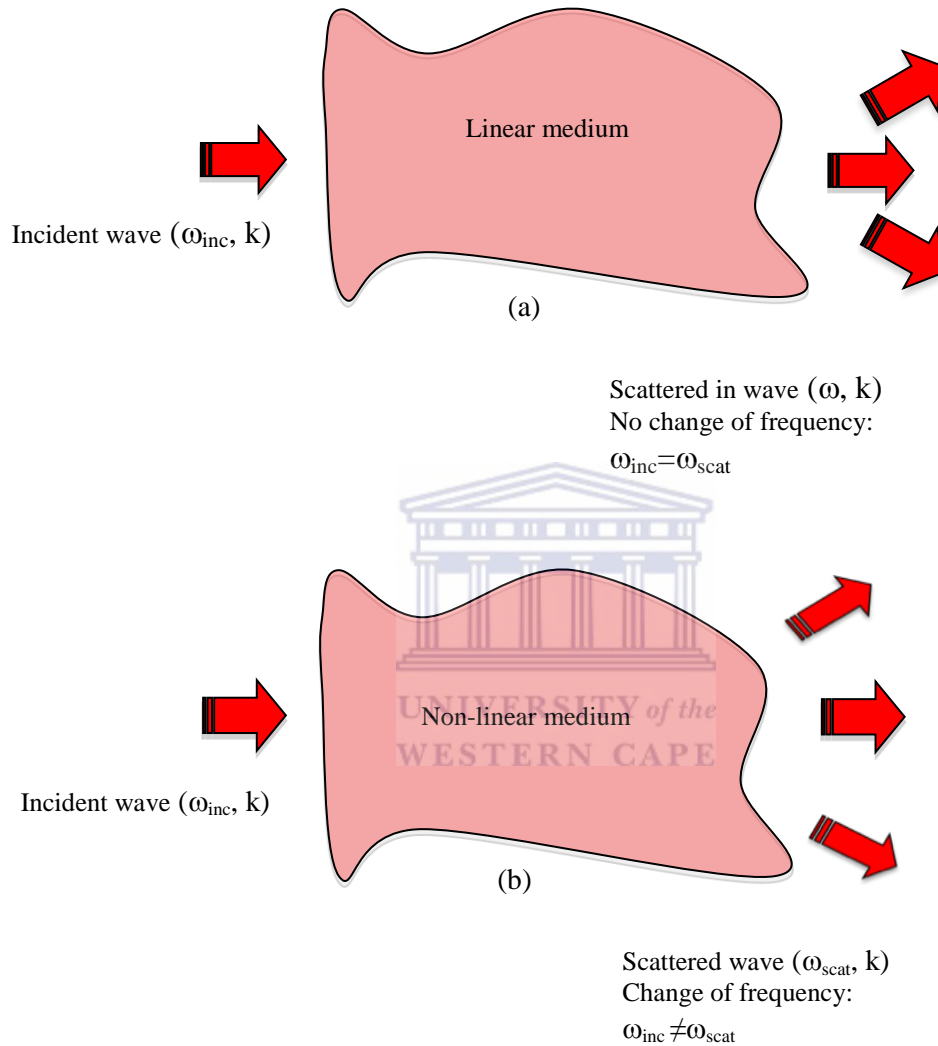


Figure 1: The excited material and or its free electrons oscillate linearly with the exciting electromagnetic wave: (a) behaviour of a light wave when exiting a medium at low frequency; (b) generation of new frequencies after the medium is excited using intense light.

Such a behavior can be exemplified by the pioneering experiment of Franken et al whose schematic is given in figure 2. In 1961, *Franken et al.*

[Fra-1961] have discovered that certain materials such as crystalline quartz and glass could literally double the frequency of a laser light passing through them. In the demonstration outlined in figure 2 an intense beam generated from a ruby laser at a wavelength of 694.3 nm in the red was focused on a quartz crystal. The beam exiting the crystal was analyzed by a spectroscope that recorded spectral components of the exiting beam on a photographic plate. Most of the source light passed through the crystal unchanged, very a small portion was converted to light of exactly double the frequency (half the wavelength) or 347.1 nm [Sur-2012] which lies in ultraviolet portion of the electromagnetism spectrum. Since this discovery, much work has been carried out regarding nonlinear optical materials and techniques have been devised to exploit this phenomenon in an efficient way. Nowadays, the second harmonic light finds application in popular devices such as laser pointers that exploit this technique in generating green light by doubling the infrared output from a tiny diode-pumped neodymium solid-state laser (which normally has an output in the infrared).

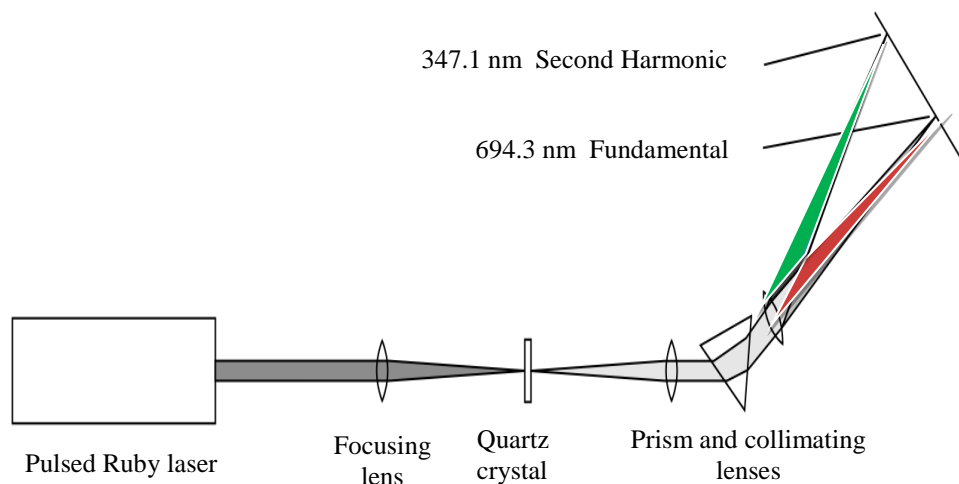
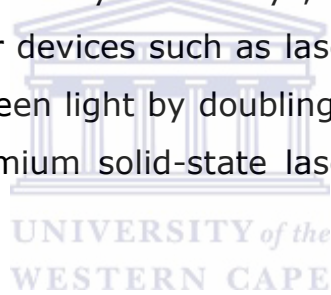
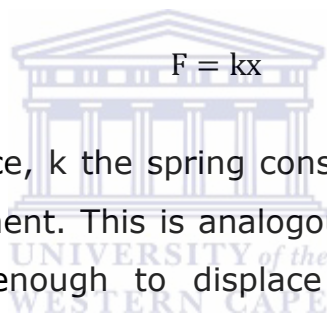


Figure 2: Pioneering Franken et al experiment demonstrating the generation of higher harmonics [Mar-2004].

2.2. Atomistic and Classical Origin

Most effects encountered in general physical system are linear as modeled by the standard Hooke's law in mechanics. Basic physics shows us that effect such as the deflection of a steel ruler on a table under the influence of a weight is directly proportional to the weight applied to it. If a given weight deflects the ruler, doubling the applied weight will cause a double deflection. The ruler is modeled as a simple spring in which the deflection is governed by the applied force. The relationship between this applied force and the stretching of the spring along the x-direction is given by [Mar-2004, Raj-2004]


$$F = kx \quad (2.1)$$

where F is the applied force, k the spring constant of the material, and x the deflection or displacement. This is analogous to a molecule where the force applied is strong enough to displace the electrons from their equilibrium position, but not strong enough to ionize the molecule [Ben-2010]. Like most physical relationships, the deflection of the ruler is linear with respect to the force applied. If, however, the ruler is subjected to a large force, the deflection is no longer linear. Therefore, the relation in Eq (2.2) is written with higher order terms as follows: [Mar-2004, Raj-2004]:

$$F = k_1x + k_2x^2 + k_3x^3 + k_4x^4 + \dots \quad (2.2)$$

The appearance of high-order terms such as x^2 , x^3 , and beyond into the equation suggests that the relationship between the applied force and the depletion is no longer linear. It is important to mention that this nonlinear behavior occurs only when large forces are applied to the material. When forces are low (i.e. the deflection of the ruler is small compared to the length of the ruler), the relationship is quite linear as seen in Eq. (2.1). As the force is increased, though, stresses will be induced in the material,

which will cause permanent damage, for example bending the ruler, but before this happens, nonlinear behavior will be observed.

Most of optical materials behave in a similar way. When light with low intensity is applied, the optical phenomena are quite linear, but when an intense light is used, a nonlinear behavior is observed. Consider for example the structure of a quartz crystal: a lattice with atoms placed at regular patterns. Electrons in the crystal are held to the nucleus of each atom by a force similar to a spring. When low and moderate light intensities interact within such a crystal, electrons behave in a linear manner [Mar-2004]. When an intense electric field strikes an atom, valence electrons in the shell move to one side of the atom, and the electron shell becomes eccentric and offset. Therefore, the optical field on interaction within atoms makes the entire material becomes polarized on a localized level. This is a macroscopic charge polarization "P" of the material, and the amount of charge polarization depends on the strength of the applied electric field according to $P = \alpha E$. where α is the coefficient of polarizability for the material and E is the applied electric field in V/cm. This is a linear relationship, which is similar to the previous relationship between force and deflection seen in Eq. (2.1) and is applied for low applied forces such as those encountered everyday: the intensities of light sources such as sunlight and most artificial lights. Because of this, nonlinear effects are not seen when, for example, red light passes through quartz. In the presence of a weak electric field a polarization is produced that is in step with the applied electric field. This polarization and re-radiation of photons results in a slowing of the velocity of light through the crystal (this is the origin of the index of refraction of the material), but no change occurs in the nature of the light passing through the crystal.

Now, when a light with high intensity shines on optical material, nonlinear effects are observed for the same reason that the ruler exhibits nonlinear

behavior for a large force. The charge polarization becomes nonlinear which can be described as a geometric series [Mar-2004]:

$$P = \alpha_1 E + \alpha_2 E^2 + \alpha_3 E^3 + \alpha_4 E^4 + \dots \quad (2.3)$$

The accomplishment of the nonlinear polarization requires an intense electric field. Therefore, the nonlinearity of charge polarization becomes apparent, and high-order terms such as α_2 and α_3 contribute to the polarization. When normal light sources with electric fields below 100 V/cm is applied, only linear optical effects can be observed. Considering that electric fields in range of 10^9 V/cm [Mar-2005] are required to induce nonlinear effect, there are only few sources with enough electric field that can generate nonlinear effects. As examples: a focused laser beam can provide an electric field ranging from 10^6 to 10^7 V/cm on a crystal while a modern amplified femtosecond laser can reach electric field strengths of $>10^9$ V/cm [Mar-2005]. Even higher intensities, with even higher electric fields, can be found inside the cavities of most lasers (where the intra-cavity intensities are often 100 times the external intensity). Consequentially, nonlinear optical phenomena can be easily induced by laser beam-matter interaction.

For a classical description, an electron attached by a spring like-model to an infinitely massive positive charge (the nucleus) under the influence of a sinusoidal oscillating electric field $E(t) = E_{\text{incident}}(t)$ associated to the incident electromagnetic wave as shown in figure 3.

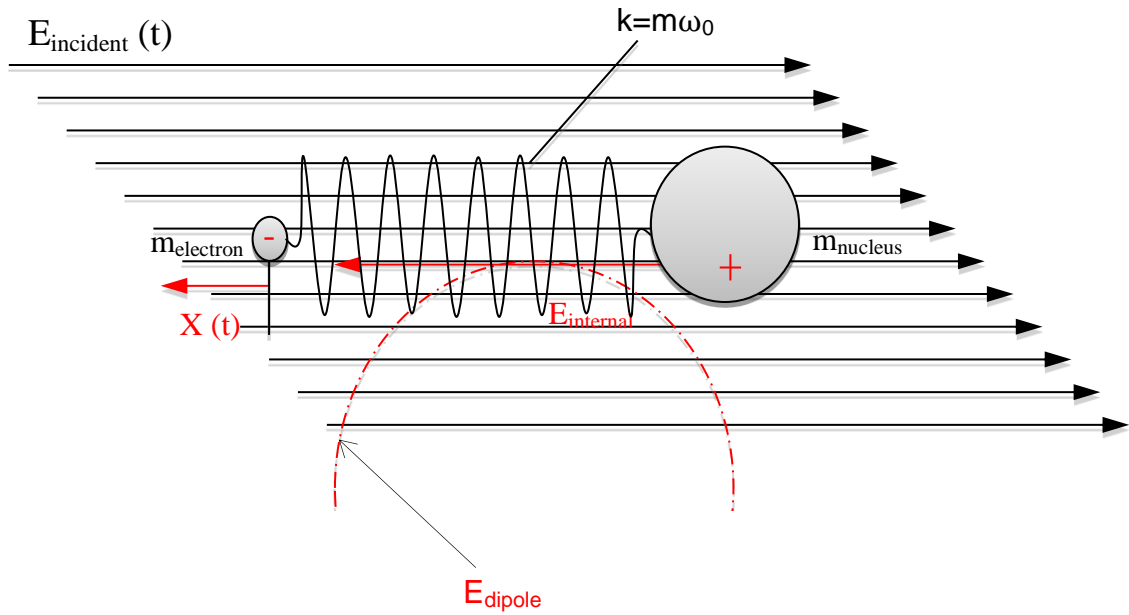


Figure 3: The excited material and or its free electrons oscillate linearly with the exciting electromagnetic wave [Gar-2000].



Considering only one dimension, Newton's equation of motion for the system depicted in figure 3 is:

$$\frac{m d^2 x}{dt^2} + \frac{\eta dx}{dt} + m \omega_0^2 x = e E(t) \quad (2.4)$$

where m is the mass of the electron, x is the distance the electron has moved from its equilibrium position, η is some resistance term or damping term and ω_0 is the resonant frequency of the electron. The oscillating macroscopic polarizability is then given by the solution $x(t)$ of the above equation as:

$$P(t) = N d(t) = N e x(t) \quad (2.5)$$

where N is the number of oscillators per unit volume and d is the dipole moment. For a sinusoidal excitation i.e. $E = E_0 \cos(\omega t)$, where ω_0 is the optical frequency, the solution to x in the linear equation above can be written as:

$$x_0 = \frac{eE_0}{m} [\omega_0^2 - \omega^2 + i\Gamma\omega]^{-1} \quad (2.6)$$

with $\Gamma = \eta / m$. This leads to a complex polarizability of the form

$$P(t) = [Ne^2 E(t)] [\omega_0^2 - \omega^2 + i\Gamma\omega]^{-1} \quad (2.7)$$

The polarizability is linear in the electric field and can be written as $P = \chi E$ where χ is the complex linear susceptibility tensor. This linear relationship between P and E results in an index of refraction and absorption coefficient that is independent of the electric field. Although this simple oscillating spring model seems to predict field-independent indexes and absorption coefficients, and many other observed optical behaviour, it fails to explain the phenomena associated to very strong electric field $E(t)$ as the Hooke's law for very large force in the spring model. Indeed, in general, the charges responding to the oscillating electric field have been moved from some equilibrium point and try to return to that point when the field

is removed. This is called stable equilibrium and can be thought of as a potential well that has a minimum point. The potential V can be expanded about the minimum point located at $r=0$:

$$V(r) = V_{(r=0)} + \frac{dV}{dr_{(r=0)}} r + \frac{d^2V}{dr^2_{(r=0)}} \frac{r^2}{2!} + \frac{d^3V}{dr^3_{(r=0)}} \frac{r^3}{3!} + \dots \quad (2.8)$$

Since the first two terms can be set to zero at $r=0$, the potential becomes:

$$V(r) = \frac{d^2V}{dr^2(r=0)} \frac{r^2}{2!} + \frac{d^3V}{dr^3(r=0)} \frac{r^3}{3!} + \dots \quad (2.9)$$

Inducing a force of:

$$F(r) = \frac{d^2V}{dr^2(r=0)} r + \frac{d^3V}{dr^3(r=0)} \frac{r^2}{3} + \dots \quad (2.10)$$

The first term in this last equation is Hooke's law and is the dominant term for small deviations of the electron from the equilibrium position. With larger perturbations, associated with larger electric fields such as the ones generated by focused laser beams or femtosecond laser sources, the restoring force must include higher-order terms and results in a more complicated nonlinear behavior. A comparison of the anharmonic and harmonic potential wells is illustrated in figure 4.

For a general restoring force derived from a nonparabolic stable equilibrium potential well, the force equation about the minimum potential is given by:

$$\frac{m d^2x}{dt^2} + \nu \frac{dx}{dt} + m\omega_0^2 x + \sum_{i=1}^N D_i x^{i+1} = eE(t) \quad (2.11)$$

For small anharmonic contributions, the solution is of the form:

$$x(t) = \sum_{i=1}^N \frac{x_i \exp(ij\omega t)}{2} + cc \quad (2.12)$$

By equating the coefficients of $\exp(i\omega t)$, the second-order term x_2 can be found oscillating at $2\omega_0$ and is given as:

$$x(t) = \frac{-De^2E_0^2}{2m^2[(\omega_0^2 - \omega^2) + i\omega\eta]^2(\omega_0^2 - 4\omega^2 + 2i\omega^2\eta) + \dots} \quad (2.13)$$

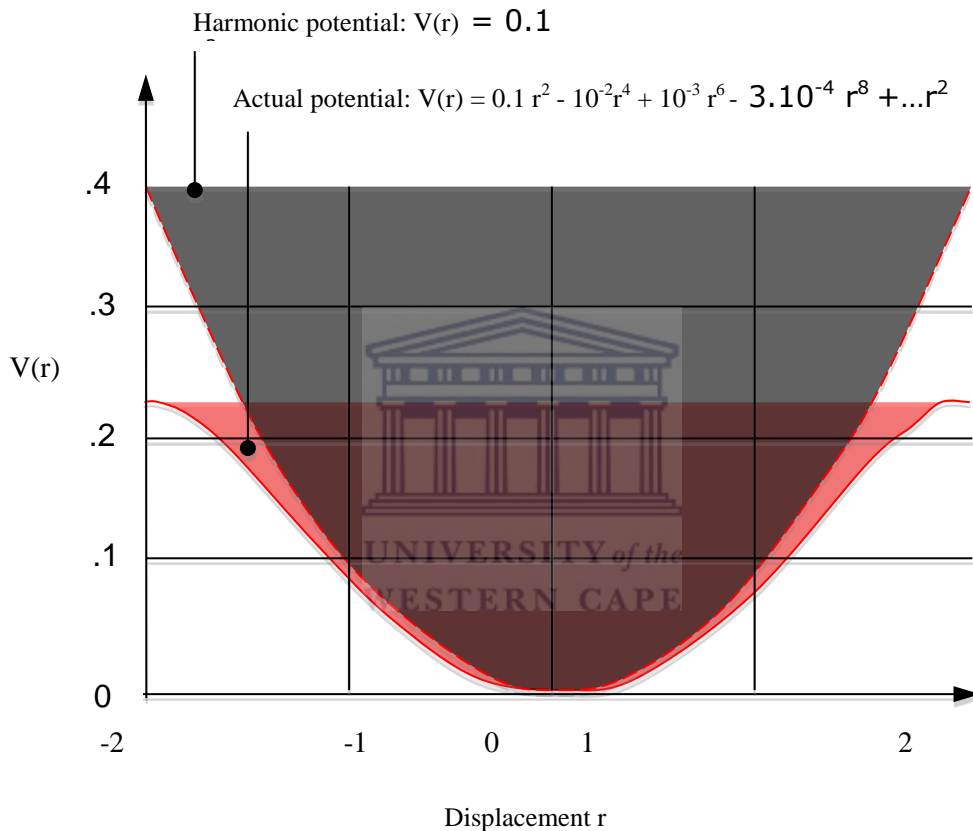


Figure 4: A symmetric potential well is shown for a molecular system by the solid line. The equation for this potential is given as $V = 0.1r^2 - 10^{-2}r^4 + 10^{-3}r^6 - 3 \cdot 10^{-6}r^8$. As a comparison, a harmonic potential of $V = 0.1r^2$ is also shown by the dotted line [Gar-2000].

In addition to the $\omega = \omega_0$ resonance there is also a resonance at $\omega = \omega_0 / 2$. The anharmonic terms result in a nonlinear polarizability which, in general, for three dimensions is written as [Gar-2000]:

$$P_i(x_p) = \chi_{ij}^{(1)} E_j + \chi_{ijk}^{(2)} E_j E_k + \chi_{ijkl}^{(3)} E_j E_k E_l + \dots \quad (2.14)$$

where E corresponds to the total applied electric field. The first term results from a linear restoring force i.e. the harmonic potential well and describes linear, low-intensity, optical interactions with materials. The second term, which includes the second harmonic term, has a second-order susceptibility $\chi_{ijk}^{(2)}$ and two electric fields E_j and E_k . This term results from an anharmonic potential well and is only found in crystals without inversion symmetry. In fact, all the even-numbered, higher-order susceptibilities are eliminated in materials that have a center of inversion as it will be demonstrate in the section 2.3. The third-order term, and all associated higher odd-ordered terms, is observed in all materials, assuming that the material or the medium will not suffer from laser-induced damage first. In the classical approach which is modelled as a spring, seen in figure 3 above, the electron is held stable by the attraction of positive nucleus. With an application of electric field, the electron is deviated from its equilibrium position and results in the charges experiencing the anharmonic region of the potential well and determines the relative importance of the nonlinear terms.

The linear susceptibility is proportional to the square of the expectation value of the dipole. In fact, the n^{th} -order susceptibility is proportional to the dipole multiplied by $n+1$ or $\chi^{(n)}$ is proportional to d_{21}^{n+1} . Since the dipole moment multiplied by an electric field is the energy $\hbar\omega$, the dipole moment can be written as a resonance frequency divided by some characteristic field strength which binds the charges $d_{21} \propto \omega_0/E_{\text{int}}$. Comparing terms in the polarization vector yields:

$$\frac{P^{n+2}}{P^n} = \frac{\chi^{(n+2)} E^{n+2}}{\chi^{(n)} E^n} = d_{21}^2 E^2 \propto \left(\frac{E}{E_{\text{int}}} \right)^2 \quad (2.15)$$

From this equation, it can be seen that when $(E/E_{\text{int}})^2 \ll 1$, the polarization vector will rapidly converge. For materials transparent to optical radiation, $E_{\text{int}} \sim e / 4\pi\epsilon_0(1\text{\AA})^2 \sim 10^9 \text{ V / cm}$ and, since most laser pulses cannot achieve such electric fields, the expansion is in general valid. Therefore, away from resonance, the third-order susceptibility is much smaller in magnitude than the second-order susceptibility, which in turn is much smaller than the linear susceptibility. In addition to the index of refraction and absorption coefficients that depend on the optical electric field, nonlinear effects often introduce new radiation frequencies. The polarization vector frequency ω_p , describes the material frequency response to the incident electric fields. When the susceptibility tensor is independent of the optical electric field, i.e. in the linear optical regime, the polarization vector frequency ω_p is equal to the incident frequency. This is the material response at normally encountered optical intensities. As an example, in the solution to the classical dipole case above, with the introduction of an anharmonic potential well, the response included a term oscillating at twice the incident frequency. A convenient way to characterize the different types of optical nonlinearities could be the possibilities to combine frequencies with the nonlinear susceptibility terms.

2.3. Maxwell's Equations

As mentioned above, the NLO phenomena are, in general, described in terms of nonlinear susceptibilities [Wen-2007] involving strong interaction between the electric field of the probe light source and the material. As mentioned previously, such light's propagation through the medium creates a nonlinear displacement of charges and their distribution within the atomic constituents, giving rise to an induced local and macroscopic polarizations that depends on the order of the applied field degree. This

polarization is usually written as a power series expansion and given by the simplest formula [Rob-2000]:

$$P(t) = \epsilon_0[\chi^{(1)}E_1 + \chi^{(2)}E_2 + \chi^{(3)}E_3 + \dots] \quad (2.16)$$

Nonlinear responses can be classified into two categories, namely: (i) intrinsic and (ii) extrinsic nonlinearities [Nie-1993]. In the case of intrinsic nonlinearity, the principle of superposition is violated due to the interaction of one or more light waves in the optical material. Extrinsic nonlinearity, meanwhile, results from the modification of the composition of a sample that occurs as the consequence of light absorption or emission [Nie-1993]. In both intrinsic and extrinsic cases, the optical properties of the material depend not only on its molecular structure, but also on the intensity of the interacting light. The formulation of the light interaction is, in general, governed by Maxwell equations describing the electromagnetic phenomena. In addition to these observations, the following three main conditions need to be satisfied:

- (i) Energy conservation,
- (ii) Momentum conservation, and
- (iii) Dispersion relation

For a better understanding of electromagnetic phenomena involved in the study of optics, Maxwell developed [And-2011, Man-2006] a theory which allows the mathematical description of the optical and electromagnetic response in both linear and nonlinear approaches. The foundation of this theory is based on equations referred to as Maxwell equations. In the Gaussian unit, Maxwell's equations relate to the space and time derivatives of the applied magnetic and electric fields through homogeneous, non-magnetic and non-conductive media and can be expressed as follows [Ste-2000, Man-2006]

$$\nabla \cdot D(r, t) = 4\pi\rho(r, t) \quad (2.17)$$

$$\nabla \cdot B(r, t) = 0 \quad (2.18)$$

$$\nabla \times E(r, t) = \frac{1}{c} \frac{\partial}{\partial t} B(r, t) \quad (2.19)$$

$$\nabla \times H(r, t) = \frac{4\pi}{c} J(r, t) + \frac{1}{c} \frac{\partial}{\partial t} D(r, t) \quad (2.20)$$

where r and t are 3-dimensional coordinate vectors and time, respectively.

B = magnetic induction (teslas or webers/square meter; T or W b m⁻²)

D = electric flux density (coulombs/square meter; Cm⁻²)

H = magnetic field intensity (amperes/meter; A m⁻²)

E = electric field. The magnetic induction $B(r, t)$ and electric displacement, $D(r, t)$, are related to the electric and magnetic flux density, respectively, by the following formulae:

$$B(r, t) = H(r, t) + 4\pi M(r, t) \quad (2.21)$$

and

$$D(r, t) = E(r, t) + 4\pi P(r, t) \quad (2.22)$$

this can be expressed in the form:

$$D(r, t) = E(r, t) + 4\pi \int_{-\infty}^t j(\varepsilon) d\varepsilon \quad (2.23)$$

where $P(r, t)$ and $M(r, t)$ are induced polarization and magnetization of the medium, respectively.

J is the induced current density (amperes/square meter A m⁻²), which can be expressed as a series expansion multipoles:

$$J = \frac{\partial}{\partial t} ((P - \nabla \cdot Q) + (Q \times M)) \quad (2.24)$$

where P and Q indicate the electrical dipole and quadruple polarization (in coulombs (C)) , respectively.

In the approximation of the electric field, only the first right-hand term in Eq. (2.24) is considered. Thus, Eq. 2.23 becomes

$$D(r, t) = E(r, t) + 4\pi P(r, t) \quad (2.25)$$

where P can be expressed as a sum of linear and nonlinear polarizations.

$$P(r, t) = P_L(r, t) + P_{LN}(r, t) \quad (2.26)$$

In this case, the linear polarization describes the linear optic phenomena, whereas the nonlinear polarization describes the nonlinear optic phenomena. The combination of the above equations leads to the simplified nonlinear wave equation [Boy-2007],

$$\nabla^2 E - \frac{\epsilon^{(1)}}{c^2} \frac{\partial^2 E}{\partial t^2} = \frac{1}{\epsilon_0} \frac{\partial^2 P_{NL}}{\partial t^2} \quad (2.27)$$

where $\epsilon^{(1)}$ defines a scalar quantity.

This equation exhibits the form of a driven wave equation; the nonlinear response of the medium acts as a source term appearing on the right-hand side of this equation, leading to the generation of new waves with new k-vector, polarization and frequencies. In the absence of this source term, solutions of Eq. 2.27 are in form of a free wave propagating with velocity n/c where n represents the linear index of refraction that satisfies $n^2 = \epsilon^{(1)}$

2.4. Polarization and Nonlinear Susceptibility

The response of atoms or molecules of material on interaction with optical field may be seen in two ways [Gua-2008]: (i) transition of a certain amount of atoms or molecules from their eigenstates to another state; and (ii) the perturbation of normal distribution or motion of electric charges within atoms or molecules. The first type of response usually occurs in a resonance interaction, while the second is predominant in a near or non-resonance interaction. The induced nonlinear polarization, in turn, will act as a new source that can generate new waves. This mechanism describes the fundamental process of the optical field-induced dipole assumption that the induced dipolar moment of i^{th} molecule is P_i , the total induced polarization P_{NL} is defined as a summation of P_i over the various orders moment of a molecular system and the generation of new optical waves.

$$P_{NL}(t) = \sum_{n=2}^{\infty} P_i^{(n)}(t) \quad (2.28)$$

The n^{th} order is defined as a multiple convolution, shown below:

$$P_i^{(n)}(t) = \int_{-\infty}^t \mathcal{G}_{ij_1 \dots j_n}^{(n)}(t \dots t_1) E_{j_1}(t_1 - t_n) dt_n \quad (2.29)$$

where the Green function \mathcal{G} is symmetric in time variable and temporal causality principle. To simplify, the polarisation can be written as:

$$P_i(x_p) = \chi_{ij}^{(1)} E_j + \chi_{ijk}^{(2)} E_j E_k + \chi_{ijkl}^{(3)} E_j E_k E_l + \dots \quad (2.30)$$

This relation is valid when the response of the media is instantaneous. In general, the polarizability P is the result of the electric fields located

throughout space and time as indicated in equation Eq. (2.29). The polarizability is given as the product of the susceptibility and the fields integrated over space and time. However, for slowly varying field amplitudes only the susceptibility is integrated and the susceptibility is given in terms of the frequency response as follow [Wen-2003]:

$$\begin{aligned}
 P_{NL}^{(n)}(\omega_i) = & \chi_{lm}^{(1)} E(\omega_i) \\
 & + 2\chi_{lmn}^{(2)}(\omega_i; \omega_j; \omega_k) E_m(\omega_j) E_n(\omega_k) \delta(\omega_i; \omega_j + \omega_k) + \\
 & 6\chi_{lmno}^{(3)}(\omega_i; \omega_j; \omega_k; \omega_h) E_m(\omega_j) E_n(\omega_k) E_o(\omega_h) \delta(\omega_i; \omega_j, \omega_k, \omega_h)
 \end{aligned}
 \tag{2.31}$$

where the indexes i, j, k, \dots indicate the Cartesian components and $\omega_i, \omega_j, \omega_k, \dots$ represent the desired frequencies. The susceptibilities are associated with the response of the material to the field. From Eq. (2.31), it can be seen that the radiation at a new frequency could be generated by an intense electric field. Moreover, the various orders of susceptibilities lead to a good description of the generation of new optical waves as well as the nonlinear coupling between different incident waves through to the nonlinear polarization. Depending on the intensity of the applied electric field, some important mechanisms may contribute to nonlinear polarization in the optical medium and are referred to as the distortion of the molecular cloud, the molecular reorientation and the induced population change [Woh-2005].

2.5. Second Harmonic Generation and Phase-Matching Process

The second harmonic generation occurs as a second order nonlinear phenomenon resulting from the interaction of light within nonlinear optical media. Considered as a specific case of the sum-difference wave generation, it has been experienced for the first time in the work

conducted by Franken in 1961 [Wen-2003]. This seminal work remains an important tool in understanding many NLO phenomena. As we saw in section 2.3, the nonlinear response is described by the $n^{(th)}$ order nonlinear susceptibility. The SHG is thus described by second-order nonlinear susceptibility through nonlinear polarization, the equation for which is given in its simplest form by:

$$P^{(2)}(\omega) = \chi^{(2)}(\omega)E^{(2)}(\omega) \quad (2.32)$$

In this nonlinear process, only non-centrosymmetry media can emit second-order nonlinear optic signals. This can be demonstrated if Eq. (2.32) is rewritten as follows

$$P^{(2n)}(\omega) = \chi^{(2n)}(\omega)E^{(2n)}(\omega) \quad (2.33)$$

where $n=1, 2, 3, \dots$

The sign of $P^{(2n)}$ is reversible in centrosymmetric only if the direction of the applied field is reversed [Eri-2001]. We have

$$-P^{(2n)}(\omega) = \chi^{(2n)}(\omega)(-E^{(2n)}(\omega)) \quad (2.34)$$

$$-P^{(2n)}(\omega) = \chi^{(2n)}(\omega)(E^{(2n)}(\omega)) \quad (2.35)$$

Hence,
$$-P^{(2n)} = P^{(2n)} \quad (2.36)$$

which is possible only if $\chi^{(2n)} = 0$ Consequently, only non-centrosymmetric materials are involved in the process shown in figure 6. In this process, one considers two laser beams at the frequencies $\omega_1 = \omega_2 = \omega$, with collinear or non-collinear geometry on interaction with nonlinear medium. The new frequency $\omega_1 = \omega_2$ collected is the result from their interaction

converted in a second harmonic wave and could be the sum or difference of frequencies. The new wave vector difference between the two waves is given by Eq. (2.37). Taking the propagating wave in the complex form and inserting the nonlinear wave equation Eq. (2.27) we can derive the second harmonic intensity-dependent refractive index [Nie-1993, Eri-2001] given by Eq. (2.38). The refractive index can be understood more readily if one considers that the propagation of intense light is accompanied by an orientation of the electric charge along the electric field:

$$\Delta k = k_{2\omega} - 2k_{\omega} \quad (2.37)$$

$$I_2(L) = \frac{512\pi^2}{n_1 n_2 \lambda_1^2 c} |\chi_{eff}|^2 I_1^2 L^2 \left(\sin\left(\frac{\Delta k \cdot L}{2}\right) / \left(\frac{\Delta k \cdot L}{2}\right) \right)^2 \quad (2.38)$$

where the parameter L defines the propagation length of the nonlinear medium, providing a maximum [SHG] efficiency. χ_{eff} Corresponds to the effective nonlinear susceptibility, n represents the refractive index which can change with the increasing wavelength λ , c represents the speed of light. Generally, $\Delta k \neq 0$ and not all contributions to the harmonic generation arrive in phase but, for a perfect mismatching, the intensity has a maximum at $\Delta k = 0$ which corresponds to the momentum conservation, which is given by $p = \hbar k$ and has damped oscillation at non-zero values as shown figure 5. (b); additionally, the amplitude increases rapidly and this so-called phase matching condition shows that the generated wave and the polarization maintain a same phase relation. However, if no phase matching is observed, this means that there is a weak interaction regime. In this case, the amplitude of the SHG signal is low at the exit of NLO medium [Thi-2009].

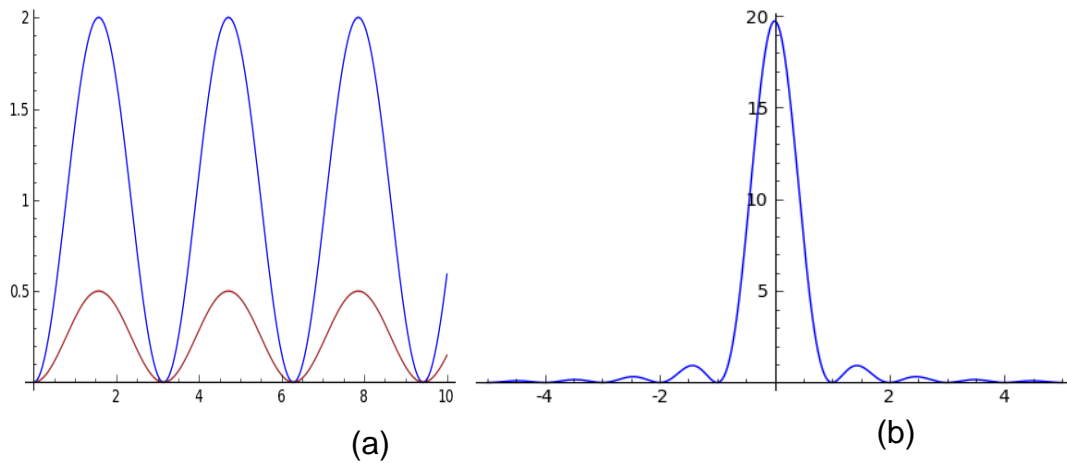


Figure 5: (a) The second harmonic intensity as function of the length of the nonlinear medium for two values of L ; (b). Perfect mismatch (i.e. $\Delta k = k_1 + k_2 + k_3 = 0$) between three waves interacting within the distance L .

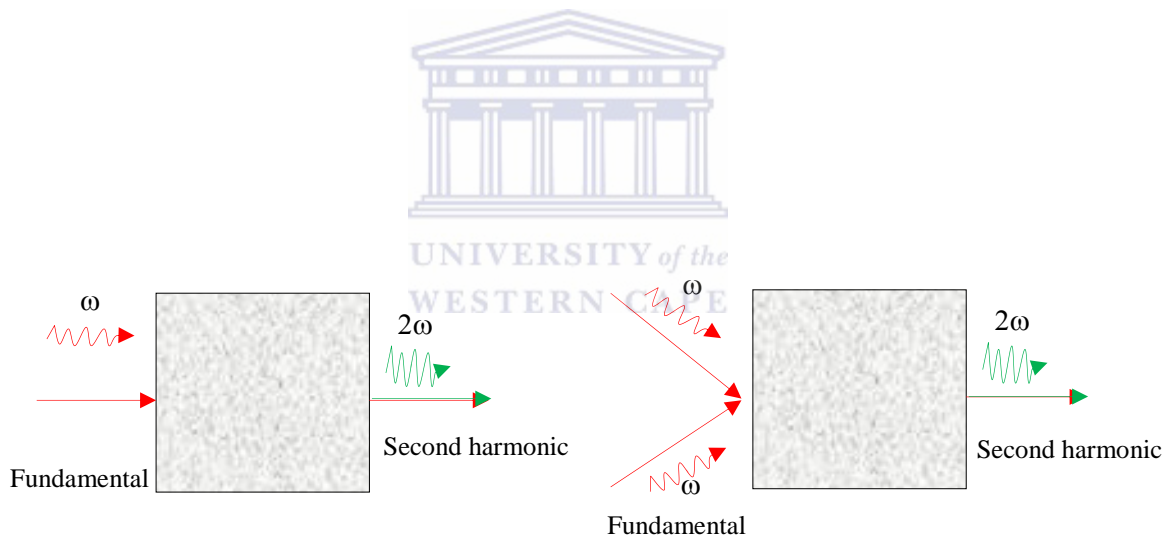


Figure 6: Second harmonic generation.

In an anisotropic medium, the phase matching can be achieved by utilizing birefringence associated with different propagations in order to offset the natural dispersion of the medium. However, it is sometimes difficult to achieve the phase-matching process in material with small birefringence because of the refractive dispersions in this material. Therefore, a suggested approach is quasi phase-matching (QPM), which is

based on the spatial refractive index, the wave guide structure or nonlinear susceptibility in periodic fashion [Nie-1993].

2.6. Third Harmonic Generation (THG)

The third-order nonlinear susceptibility is the lowest nonlinear order for all optical material that can exhibit a third order nonlinear effect. Let us consider an intense laser beam passing through a third-order nonlinear medium, which could be a liquid, gas or a solid material. The induced polarization of Eq. (2.31) is, in general, given its simplest form by the following equation [Eri-2001]:

$$P_i^{(3)} = \epsilon_0 \chi_{ijkl}^{(3)} E_j(\omega_3) E_k(\omega_2) E_l(\omega_1) \quad (2.39)$$

If for example, the polarization is along the x axis, the nonlinear optical response is entirely due to the non-resonant interaction, and thus the polarization will have the x component only, the tensor elements in y and z axes are both zero. The nonlinear polarization acts as source radiation, the intensity of which is given by [Eri-2001]. The third-order nonlinear polarization describes many nonlinear optical phenomena such as Four Waves Mixing (FWM), Self-Phase Modulation (SPM), Self-Focusing, Stimulated Raman Scattering and the Kerr Electro-Optic effect or Optical Kerr Effect (OKE). In the later, OKE, for example, which is present in almost all optical material, the third order oscillates at the frequency of the probe field. If the optical interaction is purely non-resonant, the third-order nonlinear polarization is entirely real, while in the case of a resonant interaction, both real and imaginary parts are considered. Although both components oscillate at the same frequency, the term is shifted out-phase of the imaginary part compared to the real part and the incident probe field. On the other hand, the new wave generated by the polarization is itself phase shifted relatively to the oscillation of the source polarization.

Consequently the real component signal is phase shifted compared to the probe field, whereas, the signal associated with the imaginary part is either in phase or shifted due to the emission or the absorption of light, respectively. The process of third harmonic generation has been demonstrated successfully in many optical materials in solid, liquid and gaseous state [Tha-1983]

2.7. Example of NLO Effects

2.7.1. Intensity-Dependent Refractive Index (IDRI)

The nonlinear response of material is sometimes characterized by the measurement of the refractive index, which can be understood by considering the propagation of an intense light through the nonlinear material. It is accompanied by an orientation of the electric charge along the electric field. The intensity-dependent refractive index occurs as the most important parameter in the process [Ulr-2002]. The refractive index of the sample changes with the intensity of light. This change can either be induced by the beam itself (self-phase modulation) or refractive index that is not independent of wavelength. It tends to vary with wavelength between the absorption resonances. Assuming that only one resonance is near the optical frequency and that the local field felt by the electron is close to that incident field, the index of refraction can therefore be approximated from the Eq. (2.40) as [Man-2006]

$$n(r,t) = n_0(r,t) + \Delta n[I(r,t)] \quad (2.40)$$

where n_0 represents the linear refractive index, which is dominant in the nonlinear response at low intensities. $\Delta[I(r,t)]$ corresponds to the component of the refractive index that depends on the intensity $I(r,t)$. The

refractive index is found to be proportional to the real part of the third-order nonlinear susceptibility [Ulr-2002]. Hence, for weak absorption, small local field correction, and only one dominant nearby resonance, the index of refraction and the absorption coefficient are independent of the optical electric field, as is observed at low optical intensities, and given as:

$$n^2 \sim 1 + \text{Re}(\chi)/\epsilon_0 \quad (2.41)$$

and

$$\alpha \sim I\omega \text{Im}(\chi)/nc\epsilon_0 \quad (2.42)$$

2.7.2 Harmonic Generation and Wave mixing

Harmonic generation and frequency mixing are generally used to generate coherent radiation in nonlinear optic processes. Two or more light waves interact in a nonlinear system to produce a variety of frequencies, some of which could be additive whilst others could involve a wave attenuating the amplitude of another. An interesting case is that of the three wave mixing process, in which two optical waves, ω_1 and ω_2 , interact, giving rise to the generation of a third one (new wave or new colour) at sum-or difference frequency $\omega_3 = \omega_1 \pm \omega_2$. This mixing of waves is also known as up-conversion or down-conversion, and is sensitive to the incoming frequencies [Eri-2001, Cla-2003]. The mixing of the three waves can also be viewed as photon interactions in which energy and momentum are conserved, as follows:

$$\hbar\omega_1 + \hbar\omega_2 = \hbar\omega_3 \quad (2.43)$$

$$\hbar k_1 + \hbar k_2 = \hbar k_3 \quad (2.44)$$

where k_i , $i=1,2,3$ are the wave vectors. The "+" sign is rather used than the "-" sign when the resonance condition is treated in terms of quantum mechanics. In this approach, a photon with energy $\hbar \omega_1$ and momentum $\hbar k_1$ and another one $\hbar \omega_2$ and momentum $\hbar k_2$ interact with each other, via the medium nonlinearities. That leads to their annihilation. This annihilation creates a new photon of energy $\hbar \omega_3$ (see figure 7. (a)) and momentum $\hbar k_3$, satisfying the conditions for energy and momentum conservation. In the classical approach, the "-" sign is preferred, giving rise to the following [Bah-1991]

$$\hbar \omega_3 + \hbar \omega_2 = \hbar \omega_1 \quad (2.45)$$

$$\hbar k_3 + \hbar k_2 = \hbar k_1 \quad (2.46)$$

UNIVERSITY of the
WESTERN CAPE

The quantum mechanics meaning behind these equations is that two photons with energy $\hbar \omega_3$ and $\hbar \omega_2$ and momentum $\hbar k_3$, $\hbar k_2$ are created when a photon with energy $\hbar k_1$ is annihilated, via the nonlinear medium.

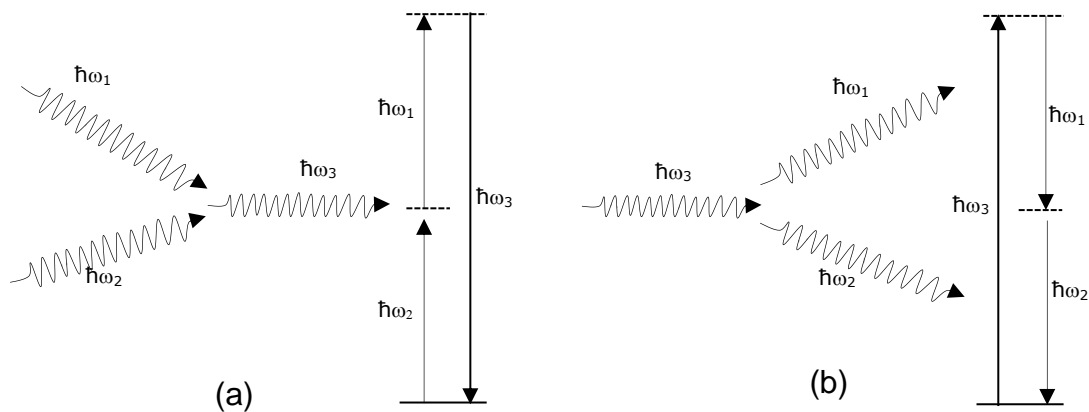


Figure 7: Diagram of a wave interacting with a nonlinear medium. (a) Annihilation of two photons at low frequencies. That leads to the creation of a new photon at a high frequency. (b) Annihilation of one photon at high frequency and the creation of two low-frequencies [Bah-1991].



2.7.3 Saturable Absorption

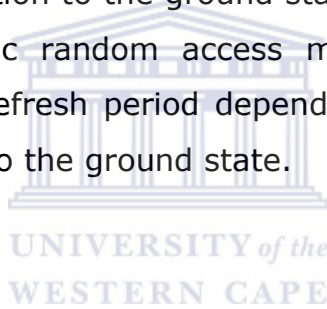
Consider an optical system in which only specific frequency is absorbed by each atom, but in which the absorption of different frequencies involves different atoms. After the photon absorption by an atom, this atom is promoted from its ground state to an excited state. The motion of the atom from the excited state to the ground state requires an average period and during this period, the atom can no longer absorb photons. However, if the radiation is very intense, the absorption of the entire system can be saturated. In other terms, the saturable absorption takes place because of the depletion of the ground state population. This phenomenon is characterized by the parameter called saturation intensity I_{sat} . The consequence of saturable absorption is the modification of the absorption coefficient. The intensity dependant absorption coefficient is written as [Nie-1993, Unn-2003, Mar-1998]

$$\alpha(I) = \frac{\alpha_0}{1 + I/I_{\text{sat}}} \quad (2.47)$$

α_0 is the linear absorption coefficient at low intensities and I_{sat} is the saturation intensity. The saturation intensity is defined as the intensity required to reduce the absorption to one-half of the nonlinear absorption at low intensities. This is given as follows:

$$I_{\text{sat}} = \frac{\Delta E}{\sigma \tau} \quad (2.48)$$

ΔE is the energy difference between the ground state and the excited state, σ is the absorption cross-section of the ground state and τ represents lifetime for the return of the population to the ground state. Saturable absorption can be applied as the dynamic random access memory (DRAM), a type of computer memory whose refresh period depends upon the time taken from excited state to relax back to the ground state.



2.7.4. Multiphoton and Excited State Absorption

The multiphoton and excited state absorption can induce a variety of optical phenomena, depending on the electronic configuration of the system. The absorption coefficient changes as the function of the intensity of the laser beam depends on the cross-section between the different energy levels and their lifetime. The principles and mechanism of multiphoton and excited state absorption are based on the concept of intermediate states. The basic steps can be represented schematically as shown in figure 8. (B), which illustrates how photons can be absorbed simultaneously by a single molecule through intermediate states [Gua-2008]. In the case multiphoton absorption MPA (i.e. 2PA, 3PA, 4PA ...) as shown schematically in figure 7. (B), the requirement for energy conservation can be satisfied under the resonance

condition, $E_f - E_g = nhv$ where E_f and E_g represent the energy at the final and ground state respectively, and $n=2, 3, 4...$ When nanosecond, picosecond or femtosecond laser pulse is used as source of excitation, MPA in general and direct 2PA in particular is assumed to be predominant where intensity-dependent of the nonlinear absorption or excitation is observed as shown in figure 8. (A).

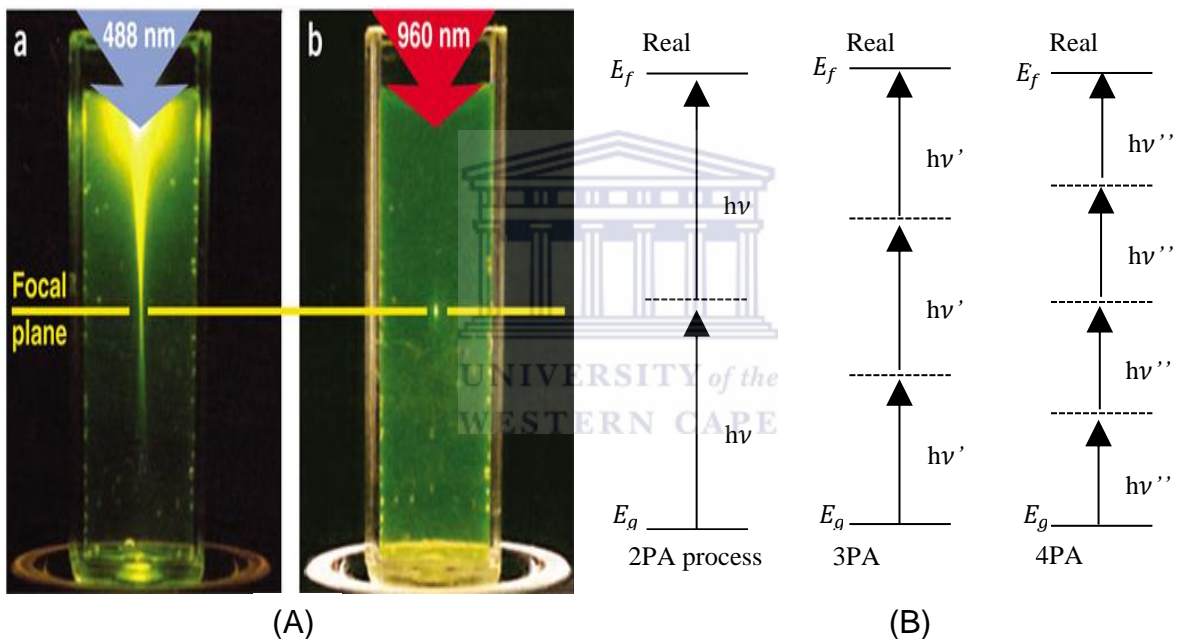
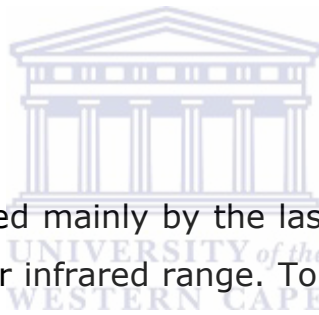


Figure 8: (a) Single-photon excitation of fluorescein by focused 488nm light (b) Two-photon excitation using focused femtosecond pulses of 960 nm light. [Wil-2003].

2.8. Optical Limiting

In relation to the above mentioned nonlinear optical phenomena of intensity-dependent refractive index (IDRI), saturable absorption and multiphoton excited state absorption, the optical limiting is an important, if not a paramount property for applications of nonlinear optical materials in laser safety and tunable laser attenuation. An optical limiting device is by definition an optical system which controls the optical transmission versus the incident light source. These optical limiting systems are thus required in the 3 spectral standard bands:

- (i) Band I: 400 nm - 2.5 μm
- (ii) Band II: 3-5 μm
- (iii) Band III: 8-13 μm



The human eye is concerned mainly by the laser sources emitting in band I i.e. in the visible and near infrared range. To appreciate the requirement for the laser eye protection by using adequate beam stoppers such as optical limiting systems, one could consider the case of a simple laser pointer of 2 mW. If the beam enters the eye, it will be focused by the cornea and lens to a spot of the order of 16 μm on the retina. If so, the irradiance on the retina is about Power/area $\sim 1000 \text{ W/cm}^2$; this is far above the human eye's threshold for infrared radiations specifically. The most common used solid state laser source in the band I is the Nd: YAG. This laser source emits at 1064 nm in the nano or picosecond regimes as well as in a continuous mode. In addition to this laser source, Optical Parametric Oscillators (OPO) and Ti-Sapphire femto-second lasers sources are potential eye damaging laser sources in view of their frequency tunability and power. They emit in the range of 420-680 nm and 670-1020 nm respectively. In both cases, the intense infrared emissions are the most damaging sources. Hence, developing adequate optical limiting

systems is of a prime consideration in the field of lasers sciences and related technologies.

An ideal laser optical limiting, which in fact based on a nonlinear optical process, should obey at least the following criteria:

- Efficiency over a wide spectral frequency range, specifically in the range of transparency the ocular media (400-1400 nm),
- Wide temporal efficiency; from picosecond pulsed laser to continuous laser sources,
- Neutral optical colorimetry i.e. preserve the colour vision with a large optical transmission for low intensities,
- Should exhibit an elevated damage threshold,
- Elevated efficiency even for very high repetition rates
- Should have a tunable optical transmission consequentially, and considering the above mentioned criteria, one could mention the various optical limiting systems used currently:

(i) Passive protection optical limiting systems:

This optical limiting systems family includes absorbing, interferential and holographic filters. Even if their optical limiting efficiency is very high, unfortunately these systems have a series of drawbacks: their efficiency is limited to a fixed wavelength and cannot handle high repetition laser sources,

(ii) Active protection optical limiting systems:

In this configuration, the optical limiting component is associated to rapid response detector which triggers the functioning of the optical limiter once the intensity input has reached a threshold.

(iii) Photo-induced optical limiting system: In this ideal case, the nonlinear optical material, itself, reduces its optical transmission when the incident beam intensity is above the threshold. The ideal optical the incident beam intensity is above the threshold. The ideal optical behaviour of these photo-active can be described by the trend of figure 9. (a) and 9 (b).

The focus of this MSc dissertation will be oriented on this last class of optical limiters based on selected natural dyes. Therefore, the optical limiting behaviour will appear as a nonlinear response of the investigated dyes. As it will be demonstrated later in the experimental chapter, their optical limiting due to their nonlinear optical characteristics are exemplified by figure 9. (a) and 9. (b). Figure 9 (a) reports the variation of the transmitted intensity versus the intensity of the incident beam. Before the so called "Limitation threshold", the intensity of the transmitted beam increases linearly with the intensity of the incident beam "Linear regime". Once the limitation threshold is reached, the intensity of the transmitted beam stabilizes throughout a plateau which should be smaller or equal to the Maximum Permissible Exposure (MPE). Once the intensity of the incident beam reaches the damaging threshold, then the transmitted beam intensity decreases in a stochastic way. Figure 9.(b) is another description of an ideal optical limiting NLO material. It depicts its optical transmission versus the incident beam intensity; the optical transmission T is nearly constant until the limitation threshold where it decreases linearly. Once the damage threshold is reached, the optical transmission starts to fluctuate stochastically. Naturally, an ideal NLO optical limiter should present

- An identified limitation threshold always smaller than the MPE in the investigated spectral range,
- A linear photo-induced optical density above the limitation threshold, and
- An elevated damage threshold.

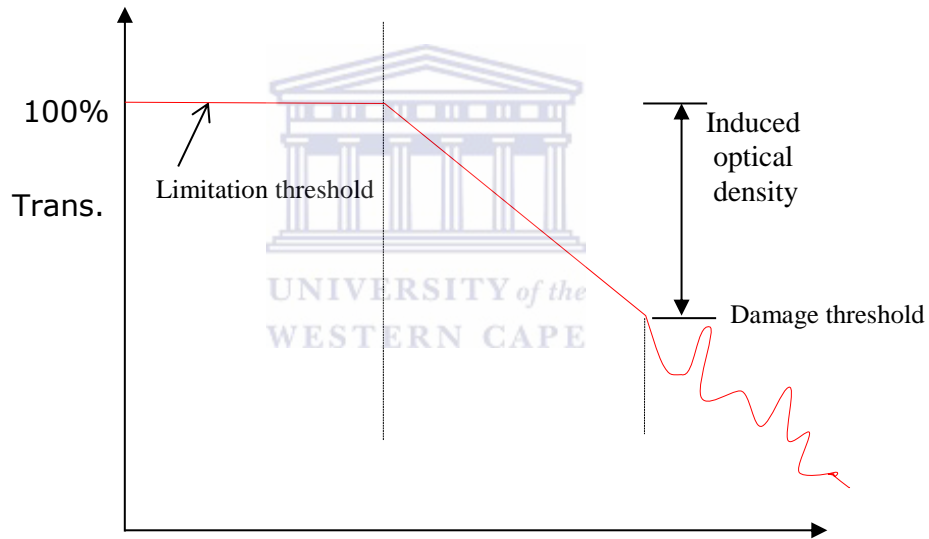
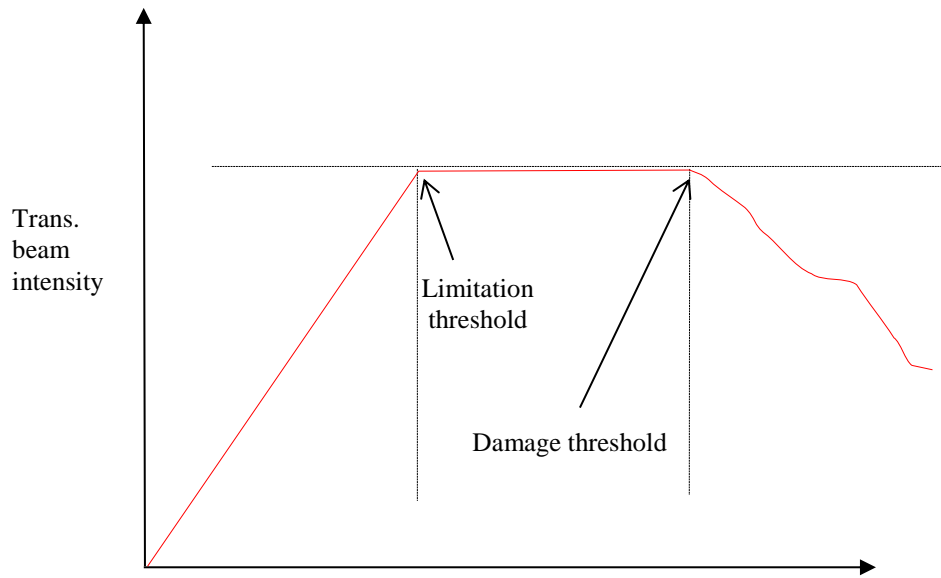


Figure 9: Characteristics of optical limiter: (a) variation of the transmitted intensity versus the intensity of the incident beam. (b) Depicts the optical transmission versus the incident beam intensity.

References:

- [Bah-1991] Nicolaa B. Bahaa E. A. Saleh, Nonlinear Optics, Carl Teich JohnWiley & Sons, Inc. ISBNs: 0-471-83965-5 (Hardback), (1991)
- [Sat-2007] K. Sathiyamoorthy, Synopsis of nonlinear optical response of dyes and metalloporphyrin in atypical environments, Chennai, India. April 2007
- [Fra-1961] P. A. Franken, A. E. Hill, C. W. Peters, and G. Weinreich, Generation of Optical Harmonic, Physical Review vol.7, (4), (1961)
- [Sur-2012] S. Suresh, A. Ramanand, D. Jayaraman and P. Mani Review on Theoretical Aspect of Nonlinear Optics, Rev. Adv. Mater. Sci. 30 175-183, (2012)
- [Mar-2004] Mark Csele, Fundamentals of Light Sources and Lasers, ISBN 0-471-47660-9, John Wiley & Sons, Inc., (2004)
- [Raj-2004] V. Rajendran, A. Marikani, Nonlinear Materials; Material Science (2004)
- [Ben-2010] Benjamin R. Anderson, Nathan J. Dawson, Sheng-Ting Hung, Nonlinear Optics, (2010)
- [Mar-2005] Marc Smits, Multi Active Electron Effects in the Strong-Field Ionization of Transition Metal Atoms and Clusters (2005)
- [Gar-2000] Gary L. Wood and Edward J. Sharp, "Nonlinear Optics", McGraw-Hill Optical and Electro-Optical Engineering Series, R.E. Fischer and W.J. Smith, Series Editors, (2000)
- [Wen-2007] Wendell T. Hill and Chi H. Lee, Light-Matter Interaction: Atoms and Molecules in External Fields and Nonlinear Optics, (2007)
- [Woh-2005] Manfred Wohlecke, Klaus Betzler; Nonlinear optics, 2005
- [Rob-2000] Robert J. Kruhlak, Characterization of Molecular Excited States for Nonlinear Optics, (2000)

- [Nie-1993] Wenjiang Nie, Optical Nonlinearity: Phenomena, Application and Material, Adv. Mater. Vol.5, 520, (1993)
- [And-2011] Andreas Trügler, Optical properties of metallic nanoparticles, (2011)
- [Man-2006] Manthos G. Papadopoulos, Andrzej J. Sadlej, Jerzy Leszczynski, Nonlinear-optical Properties of Matter: From Molecules to Condensed Phases,(2006)
- [Boy-2007] Robert W. Boyd. The Nonlinear Optical Susceptibility (2007)
- [Gua-2008] Guang S. He and Song H. Liu, Physics of Nonlinear Optics, 2008
- [Wen-2003] Wendell T. Hill and Chi H. Lee, Light-Matter Interaction: Atoms and Molecules in External Fields and Nonlinear Optics, (2003)
- [Thi-2009] Thierry Verbiest, Koen Clays, and Vincent Rodriguez, Second-order Nonlinear Optical Characterization Techniques: An Introduction, CRC Press, (2009)
- [Eri-2001] Eric Vauthey, Introduction to nonlinear optical spectroscopic techniques for investigating ultrafast processes, Dpt. of physical chemistry, University of Geneva, Switzerland
- [Cla-2003] Claude Rulli, Femtosecond Laser Pulses: Principles and Experiments, Second Edition, Springer, (2003)
- [Tha-1983] M. Thalhammer and A. Penzkofer Measurement of Third-Order Nonlinear Susceptibilities by Non-Phase Matched Third-Harmonic Generation, Appl. Phys. B 32,137-143, (1983)
- [Ulr-2002] Ulrich Gubler, Christian Bosshard, Molecular Design for Third-Order Nonlinear Optics, Advances in Polymer Science,vol.158, (2002)
- [Wil-2003] Williams and W. W. Webb, Nature Biotechnology 21, 1369-1377 (2003)

CHAPTER-3: General Description of Natural Dyes

3.1. Description of Natural Dyes

In this chapter, an overview of natural dyes and their characteristics for optical applications is presented. The sources of these dyes, as well as their molecular structures, which could be the most important elements for an eventual study, will be discussed.

An initial consideration when working with a dye is its colour. In a general sense, colour can be regarded as a combination of physical characteristics and chemical aspects involving the transmission, refraction, absorption and scattering of light. Natural dyes have historically been known for their use in food and textiles. Currently, natural dyes are being investigated for novel applications because of optical properties that they may exhibit.

Based on the property of solubility, there is a difference between dyes and pigments. Whereas dyes in general are classified as organic compounds and are soluble in water and/or organic solvents, pigments are usually inorganic materials or minerals and are insoluble in both of the abovementioned liquid media. Natural dyes, which can be regarded as a lake of pigments, have long been widely used for either colouring or painting materials. This is illustrated by the use of anthraquinones and their hydroxy derivatives as red dyes and pigment lakes from prehistoric times [Mar-2009]. However, with the advent of synthetic dye technology, the use of natural dyes has declined rapidly. Recently, investigations of natural dyes are being undertaken around the world for novel applications in addition to their food and textile applications. The utilisation of natural dyes as novel technological materials is encouraged compared to the use of synthetic dye, which have adverse effects on the environment [Est-2024, Mah-2010], such as water pollution caused by uncontrolled or poorly regulated industrial processes.

3.2. Sources of Natural Dyes

Plants have been identified as the main sources of natural dyes [Nor-2009]. However, the extraction of natural dyes from plant sources presents challenges such as conservation and is sometimes related to molecular polarity. There are no specific methods; it could depend on the goal. Other challenges are related to the availability of the dye source, which is a significant problem as most of the plant sources are seasonal. This problem of the low availability of particular plants during certain seasons, as well as possibly high variability is to undertake a large-scale planting program, once a suitable plant source has been identified. On the other hand, natural dyes are less stable (i.e. they degrade quickly) and then cannot be kept for a long time. Other natural dye sources include insects (e.g. cochineal beetles and lac scale insects) and minerals (e.g. ferrous sulphate, ochre and clay), as well as animal (e.g. some species of mollusk or shellfish). In addition to those from animal and plant sources [Che-2010], natural colourants can also be obtained from certain microbial sources such as chlorella (e.g. red carotenoid pigments) [Boa-2005]. The latter type of dye source has several advantages, namely: (i) production processes are flexible; and (ii) these processes can more easily be controlled compared to those involving plant and animal sources. Microbes in general produce dyes such as chlorophyll and carotenoids, as well as unique pigments [Boa-2005]. The abovementioned diversity of sources could allow natural dyes to be found widely throughout the world during precise moment, even though the extraction process may present difficulties, some of which have been mentioned above.

3.3. Natural Distribution and Chemical structure

Natural dyes are from a variety of sources and are structurally diverse. They can be classified into four major groups [Naz-2002]. Each of which will subsequently be discussed in more detail: (i) carotenoids; (ii) chlorophylls; (iii) flavonoids; and (iv) betalain.

3.3.1 Caratenoids

The most important group of tetraterpenoids are carotenoids, a family of pigments synthesized by plants and microorganisms [Rao-2007]. Carotenoids are responsible for the yellow-orange and red colour of many flowers, fruits, vegetables, roots and autumn leaves. Explicitly, carotenoids are classified further into two main groups: (i) hydrocarbon carotenoids, usually called carotene; and (ii) those containing oxygen, which are termed xanthophylls. Both groups of carotenoids exhibit similarities in structure, for example, it can be observed in figures 10 and 11 [Ala-2006] a polyisopropenoid structures and a series of a minimum of 10 alternative single and double bonds that are centrally located. These chromophores (i.e. conjugated system) are responsible for light absorption in the visible range, which serves as a basis for the identification and quantification of compounds. In addition to carotenoids of being utilised in the food industry, it can be noted that these types of dyes are potentially promising candidates for large nonlinear optical behaviour such as the large nonlinear susceptibilities involved in photonic applications [Abd-2012]. Even though, carotene was among the first [Mac-1993] organic compound with an extended π -electron structure to be investigated for organic third-order susceptibility $\chi^{(3)}$. If carotenoids

are found to be promising for nonlinear optical applications, it can be noted the disadvantage of these dyes is their intermittent availability as they are seasonal.

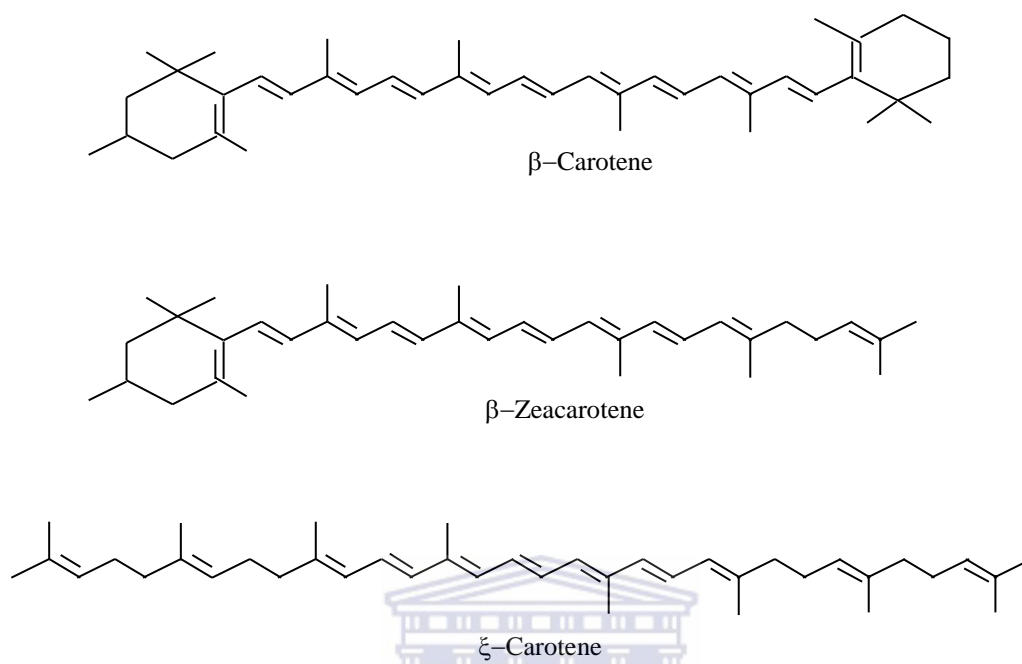


Figure 10: Basic structures of some Carotene [Del-2001].

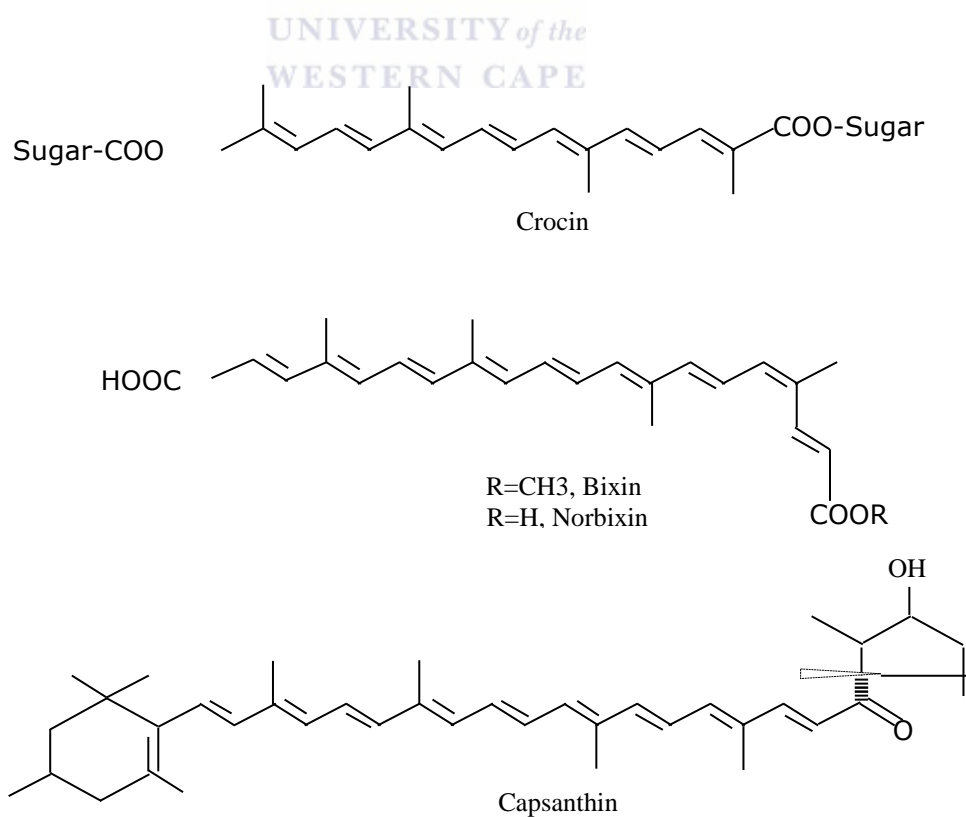


Figure 11: Basic structures of some xanthophylls [Del-2001].

In addition to their high potential to be utilised in the food and textile industries, these types of dyes are promising candidates for novel applications. The long conjugated system in the chemical structure of these dyes could be an important factor for large third-order nonlinear susceptibility that is required for photonic applications [Abd-2012]. Such applications include all optical switching, data processing, and sensor and eye protection. The production of these dyes is also limited by climate factors (i.e. Humidity, temperature, oxygen and nitrogen concentrations in water and air). Another disadvantage is that, there is a lack of availability of precise technical knowledge on extraction. Moreover, natural dyes exhibit sometimes a low colour fastness performance [Ash-2011]. Approximately 750 different types of carotenoids have been identified [Hye-2007] with the same pigments but with significant differences in the ratios of individual pigments. The orange varieties, for example, contain the largest amount (44% of the total carotenoids in Double Esterel orange, while the yellow varieties contain the large amount of oxygenated derivatives is estimated at 97% of carotenoids in the Double Esterel jaune [Ade-2003].

3.3.2 Chlorophyll

The most important group of tetrapyrrols are chlorophylls, which represent the most abundant pigment in nature. Chlorophylls are found in plants, algae and the marine environment. These pigments are involved in essential life and natural processes, notably photosynthesis on earth. Chlorophylls present a cyclic conjugated system of double bonds with central magnesium ion and the presence of some functional groups as substitutes results in derivatives such as Chlorophyll a, b (see figure 12).

Natural chlorophyll in general is very limited in its use as colourant because of the liability of it coordinate central magnesium. In other terms, chlorophyll is unstable. Despite this instability, they are known as very effective photoreceptors [Ber-2002], because of the networks of alternating single and double bonds which is responsible of a strong absorption of light in the visible portion. Moreover, a mixing with other colourants (e.g. anthocyanin) [Noo-2011] or chemical modification can lead to an enhancement of the stability as well as a highly efficiency for photo-conversion in technological applications such as sensitizers. As other plant pigments, chlorophylls are also diversely distributed according to the area and this because of climate factors such as humidity, temperature and the oxygen and nitrogen concentrations in water and air.

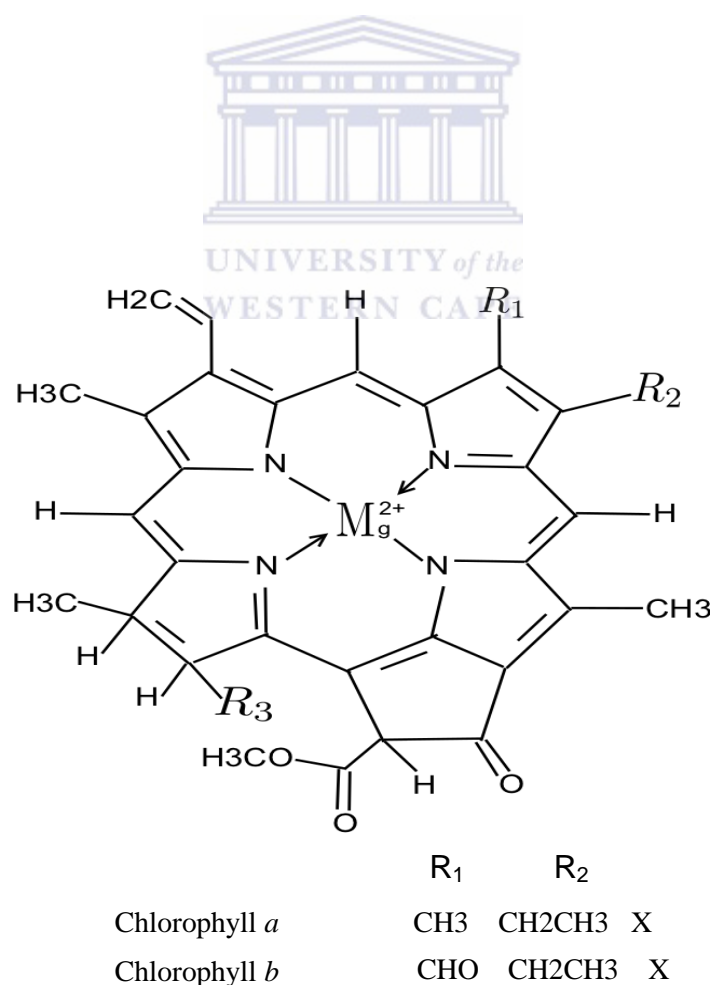


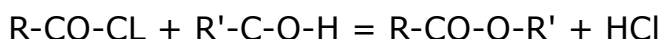
Figure 12: Basic structure of chlorophyll [Hug-1991]

3.3.3 Flavonoids

Flavonoids constitute an important group of natural dyes used in the food industry, because of the varieties of colours that they exhibit. These compounds are responsible for, or contribute to, the attractive colour that many fruits and vegetables exhibit, from a white/cream colour; to red, purple, blue and yellow products such as chalcones, aurones, flavonol and flavone that co-occur with carotenoids. The most common flavonoid component is anthocyanin, which has a chemical structure based on a C_{15} skeleton arranged in the pattern $C_6 - C_3 - C_6$ unit, which is responsible for the attractive orange-red and violet colour that appears in many flowers and fruits. The large quantity of anthocyanin is related to the great diversity of derivatives that can result from glycosylation and acylation reactions [Ala-2006]. The glycosylation reaction involves a glycosyl donor attached to a glycosyl acceptor forming a glycoside. Possible glycosylation are:

- N-linked glycosylation
- O-linked glycosylation
- C-linked glycosylation
- Glycation

while the acylation consists in a reaction in which the hydrogen atom in organic compound is replaced by an acyl (R-CO) group. A typical acylation is the reaction of acetyl chloride with an alcohol



Anthocyanins are naturally polar, and are soluble in water as well as in various types of organic solvent. The heterocyclic structures shown in figure 13 are responsible of light absorption in the visible region of the electromagnetic spectrum. The unbound electron contained in these structures requires less energy to be excited. This process of excitation

will therefore lead to the process of light absorption particularly in the visible range. An increase in the double-bond conjugations or hydroxylation (i.e. an introduction of a hydroxyl (OH) group in an organic compound) can induce high wavelength absorption. The major anthocyanidins pelargonidin (orange/red), cyanidin (pink) and delphinidin (blue/violet) have different hydroxylation patterns [Nic-2009], which can influence the optical and chemical properties of these compounds. Other factors, such as R-group conjugation, may greatly affect the absorbance of light. In addition to the water soluble property, the concentration and type of anthocyanin varies considerably according to the plant source. It can be noted as colourant red cabbage, purple carrot, red radish and the grape pomace. The natural production of anthocyanins is estimated to be 10^9 tons/year [Aok-2002].

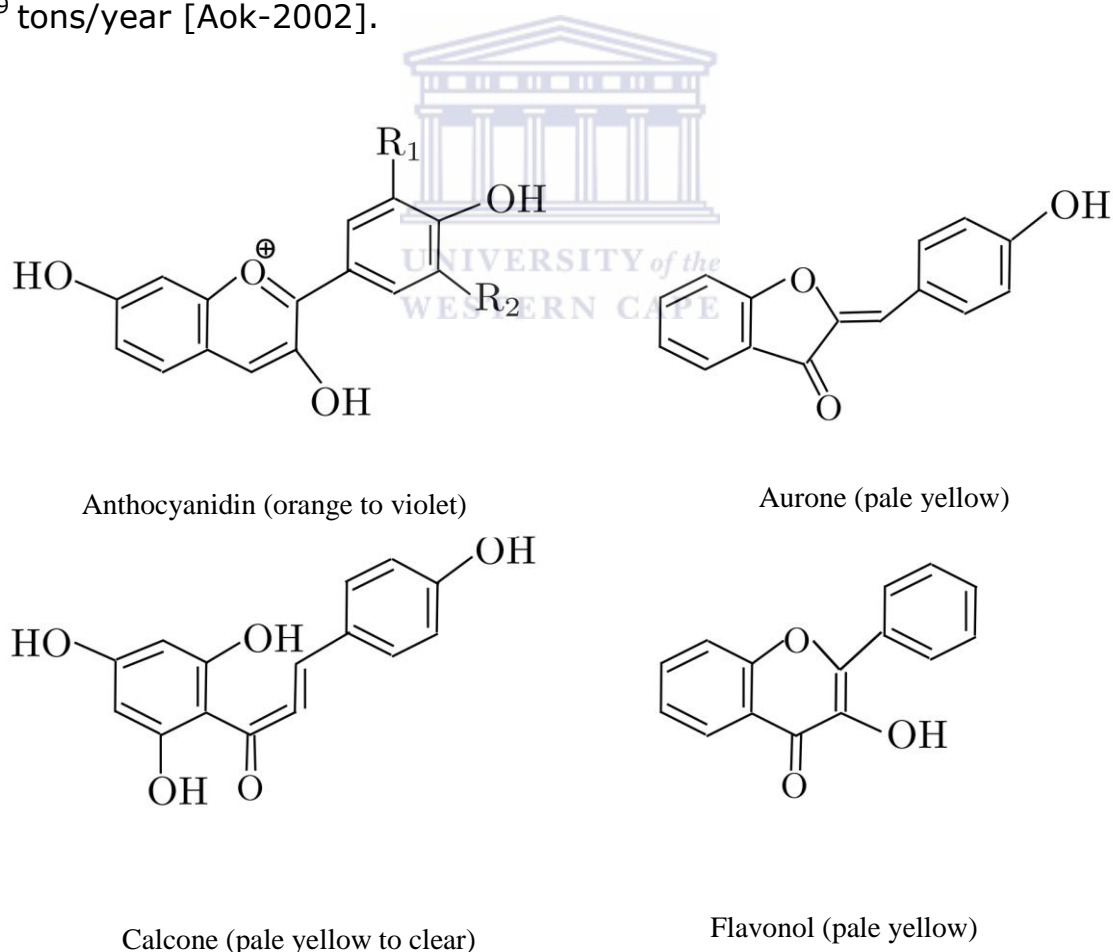


Figure 13: Basic structures of flavonoids where R₁, R₂ = H, OH and/or OCH₃ [Øyv-2006].

3.3.4. Betalains

Betalain dyes have recently gained more interest in the food industry. Found in only 10 families [Ant-2004] of the Caryophyllales which are flowering species, betalains are nitrogenous chromoalcaloids and their presence excludes the anthocyanin (i.e. both of them cannot coexist). The most important compound of betalains is referred to as the betacyanin of red colour found in roots, leaves, fruits and other plant tissues. Betalains are water soluble and are also nitrogen-containing compounds derived from the amino acid tyrosine [Hen-2009, Naz-2002] and demonstrate strong light absorption. Depending on the betalamic acid conjugation (i.e. chromophore), betalains can be classified into two main groups, namely: (i) betacyanin and (ii) betaxanthin with cyclo-DOPA (cyclo-L-3,4 dihydroxyphenylamine) derivative or free amino acid/amine [Naz-2002]. In other terms, the red-violet betacyanin (figure 14 (b)) is derived from betalamic acid and cyclo-DOPA (see figure 14 (a)), while the yellow-orange betaxanthin is derived from betalamic acid condensed with an amino acid or amine (figure 14 (c)). These two colours are observed under basic and acidic conditions, respectively. An important common source, is the beetroot in which betanin ($C_{24}H_{27}N_2O_{13}$) contributes up to 75-90% [Kap-2009, Rab-2009] of the total colouring matter. This pigment, like other betacyanins such as isobetanin and betanidin, is susceptible to changes induced in colour by both pH and temperature [Rab-2009].

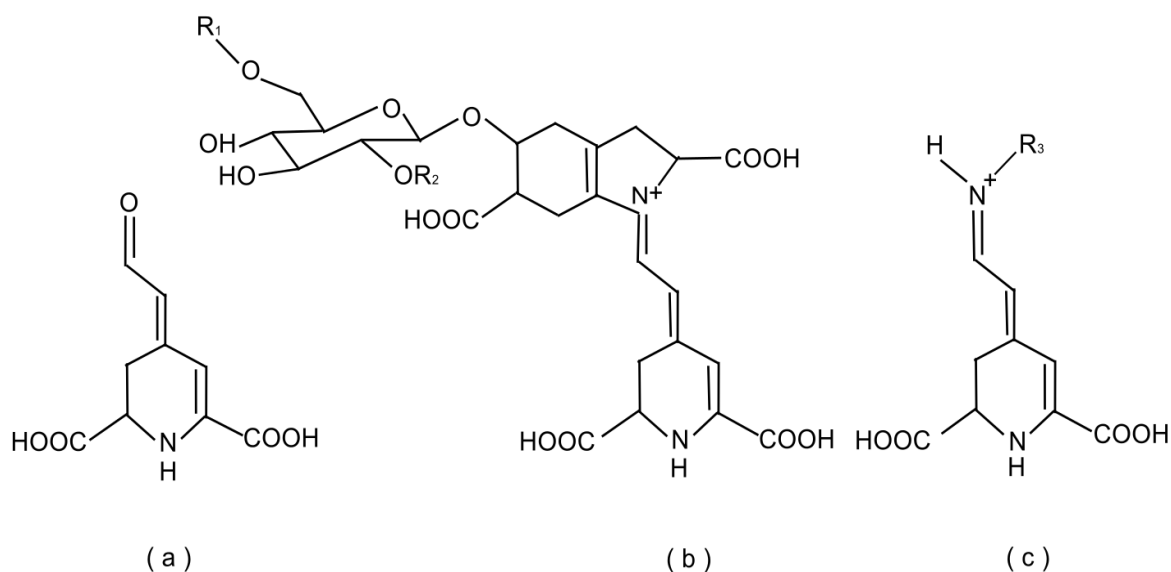


Figure 14: General structure of Betalamic acid (a), Betacyanins (b) and Betaxanthin (c). Betanin: $R_1 = R_2 = H$, $R_3 =$ amine or amino acid group [Hen-2009].



3.4. Extraction of Natural Dyes

Extraction constitutes the first step for any natural dye exploitation. Depending on the nature and source of the dye and its intended purpose, the choice of extraction technique is of great importance. Another significant consideration is the choice of solvent to be used in the extraction process, which is determined by the polarity of the dye. The extraction efficiency of these dyes depends on many factors, such as the type of medium used (aqueous/organic solvent or acids/ alkyl), the pH of the medium, temperature, time duration and type of solvent [Jin-2010]. Most of the dyes from different origin can be extracted using commonly aqueous [Ash-2011] method i.e. by pure water extraction involving with or without addition of organic compounds. Certain dyes can be precipitated by slight acidification with hydrochloric acid or with acidified

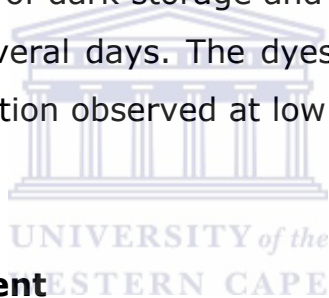
acetone or ethanol (0.4% to 1% HCl) [Del-2003]. Careful attention needs to be paid during the extraction process, because the colour of the dye can be altered or its denaturation can occur due to changes induced the parameters listed above. Indeed, the temperature occurs as the main factor that influences extraction efficiency. The physicochemical properties of water can be affected when the temperature varies. Thus, it can be seen that water dielectric constant decreases as the temperature decreases from high to ambient, hence, the reduction of its polarity. That contributes to the enhancement of the solubility of the organic compounds [Nur-2011]. Many tones of colourant can be extracted since the intensity of the colour could depend on variations in temperature. At very low temperatures, there may be less variation in dye colour, but such variation may become important with increased duration of exposure. Water or organic solvents are used to extract natural dyes, depending on the nature of the dyes and also the aim and the application. In our case for example, we aim to study the optical properties of these dyes. Therefore, either water or specific organic solvent will play an important role in the extraction process. Most commonly used organic solvents in natural dyes extraction are methanol, ethanol and acetonitrile [Mag-2004]. However some of them have been found to be good while others may contribute to degradation of the dyes depending domain of applications. For example, the redness of anthocyanin is increased through interaction with a larger number of methoxyl groups, while the red colour changes to a more bluish colour if more hydroxyl group are involved instead [Del-2003]. It was found that ethanol is not suitable for dye extraction if such dye is used as sensitizer in stability of the Dye-Sensitized Solar Cell (DSSC) [Kel-2011], while polar solvents such methanol, acetone and acetonitrile exhibit the highest extraction efficiency [Fei-2012] of dyes with phenolic compounds. The use of these solvents can sometimes lead to a better resistance to a change in colour than the boiling process in which the temperature is more involved. It is also important to note that the high temperature can destroy the

chemical bonds of the dye compounds. Solvents may also significantly influence the linear and nonlinear properties of dyes [Sun-2000]. Organic solvents, in particular, have the ability to modify the wavelength of the absorbance maximum. Although the use of organic solvents contributes to efficient and precise results in terms of colour variations and long lifetime, in dye extraction processes, it can nevertheless be noted that the use of these solvents presents some disadvantages; they remain frequently toxic or harmful to human and environment, sometimes large quantities of solvent are involved and may be relatively expensive [Shi-2012].

3.5. Colour and Stability

Natural dyes possess colour because these compounds [Tan-2010]; (i) possess a basic chemical structure consisting of alternating double and single bonds; (ii) possess a chromophore; (iii) absorb light in the visible part of the electromagnetic spectrum; and (iv) exhibit electron resonance, which is a stabilizing force in organic compounds. In addition to the chromophore, most dyes also contain a group known as an auxochrome, which plays the role of colour helper [Tan-2010] such as carboxylic acid, sulfonic, amino and hydroxyl. As mentioned in section 3.3, the combination of various factors such as extraction temperature and time; the presence of metal ions, enzymes, oxygen, ascorbic acid, sugar and sugar metabolites; and water activity [Rod-2011] have a great impact on the colour of a natural dye. Variations in colour, for example, can be observed following an increase in temperature. *K. Woo et al.* [Woo-2011] reported that the treated dye, for example, lost 30% of its colour in the initial stage storage at 80°C. *Nursyamirah et al.* [Nur-2011] have shown that the crude dye extracted at 50°C with a bluish tint totally changed to purple at 100°C and that the redness decreases while the yellowness effect becomes more dominant which gives yellow-orange as the temperature increases. In a general case, the intensity of the colour may decrease as

the temperature increase. Extraction efficiency and colour changes can also be influenced by the nature and concentration of the solvent used. For example, it is not likely that the use of methanol, acetone or ethanol as solvents result in the same kind of colour change. This is mainly due to the different chemical (e.g. acylation) interactions that could potentially occur during the extraction process. In addition to the solvent effect on colour, it is often possible to observe the colour change when the dyes are exposed to ultraviolet (UV) and visible light. There may be ready discolouration [Yos-2009] or the light exposure can accelerate destruction of the dye. This degradation by light is due to the excitation of the electron of the chromophore to a more energetic state, which can lead to higher reactivity or lower activation of the molecule [Woo-2011]. However, under conditions of dark storage and low temperature (4°C), the colour is conserved for several days. The dyes are thus relatively stable, with no significant degradation observed at low temperature.



3.6. Stability Enhancement

Various measures can be undertaken to address the abovementioned limitations with regard to the stability of natural dyes. These measures include avoiding unfavourable conditions for certain applications and improving stability through formulation, several examples of which will be presented below. Dyes, for example, could be formulated to enhance the stability of a colourant, which could be achieved by mixing colourants or adding other compounds such as auxochromes. This can be illustrated stable yellow colourant from Gardenia is obtained with mixing sugar (e.g. lactose and dextrin) and spray drying the mixture [Boa-2005].

Another example is formulating natural dyes in powder form through a drying process, instead of a formulating the dyes in a liquid state, so that the shelf-life is prolonged. The dye could also be encapsulated in a transparent material such as gels. Likewise, stability can also be improved

by a process of co-pigmentation [Sun-2000, Jea-1998] of an organic molecule or pigment (e.g. Batacyanin) and a co-pigment (flavonoids, simpler phenolic or aliphatic acids) molecule that involves chemical mechanisms such as inter or intra-molecular co-pigmentation, self-association [Jea-1998].

3.7. Typical Examples of Dyes in Photonics:

3.7.1 Dye Lasers Sources

The so called dye lasers form a specific family of coherent lasing sources. They are considered as an established technology which has reached its maximum yet. They appear as main investigation tool in the high resolution spectroscopy in the visible range. Discovered in the late sixties following the research of *Sorokin* and *Lankard* [Sor-1966], the dye lasers cover a very broad spectral emission capability from the near UV (~ 390 nm) to the near infrared ($\sim 1 \mu\text{m}$). Moreover, the dye lasers have an attribute of multi-colour emission. More than 200 organic dyes are used in this family of laser sources. Figure 14 shows the approximate spectral domain that can be observed using major families of laser dyes: Cormarins, Xanthene and Oxazines as well as the major dye absorptions (inset). They can be pumped by coherent sources such as excimers, Argon-Krypton, and doubled Nd: YAG lasers or incoherent sources such as flash-lamps. These types of laser can be utilized both in continuous or pulsed regimes. In the continuous regime, their output power can vary from 100 mW to several Watts. In the case of the (liquid or solid) dye based lasers, the dye molecules are subjected to a UV or Visible radiations where the vibrational sub-levels of the singular excited state S_1 are populated by optical pumping from the fundamental vibrational level S_0 (figure 16). The excited vibrational sub-levels have a short lifetime of 10^{-12}s ; they relax in a non radiative way towards the lowest vibrational level of the single S_1

state. This level de-excites in a radiative way to the various vibrational levels of the fundamental state S_0 or non-radiatively towards the triplet state T_1 which has a life time of about 1 ms. Hence, the trapped dye molecules in the triplet state absorb, generally, the laser wavelength, limiting therefore the laser efficiency in the continuous regime. For a considered dye solution, the laser emission takes place in a large spectral range. Each dye covers only a limited range of wavelengths (figure 15), with peakoutput roughly in the middle of that range for a mono-mode type dye laser functioning, a spectral selection is required allowing a monochromatic emission over the band gain. Other dye in general give lower power levels, as does the Rhodamine dye used in dye lasers. Therefore, the suitable wavelength can be selected from 570 to 660nm. Figure 17 shows a dye laser while table.1 reports typical characteristics of selected dye laser sources.



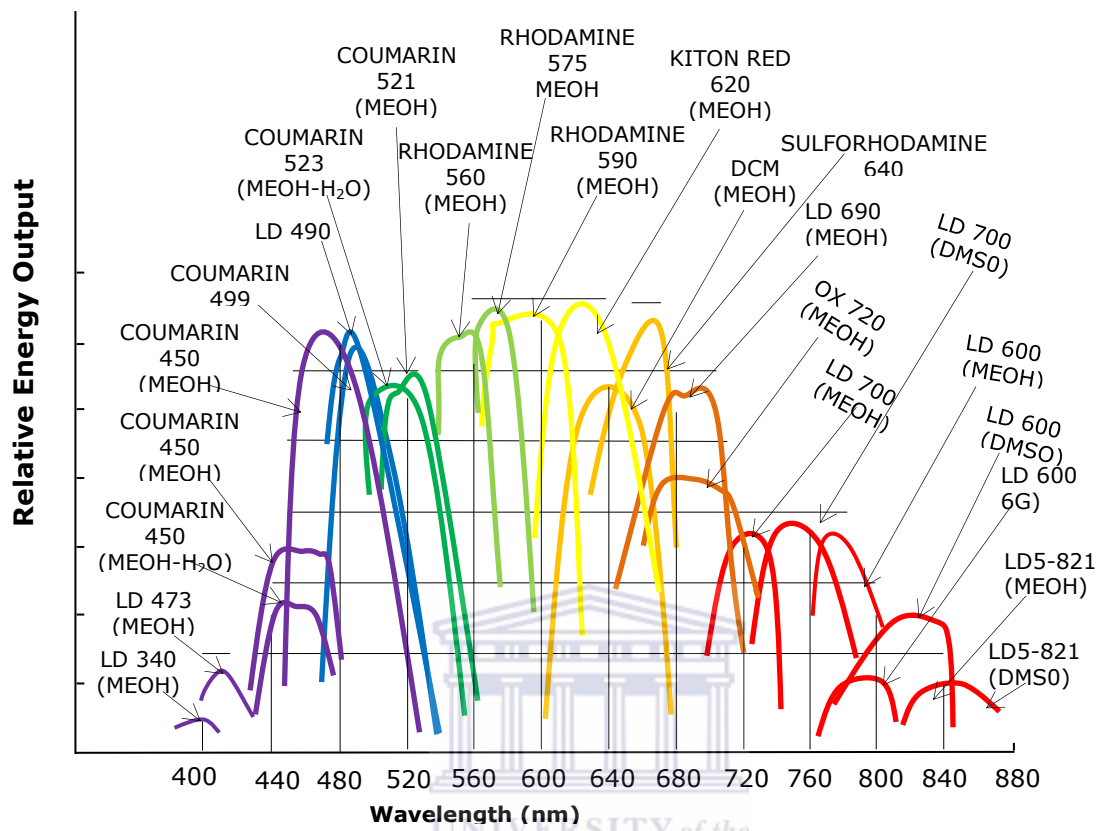


Figure 15: Dye spectral emission characteristics of some common laser dyes [Hen-2005]

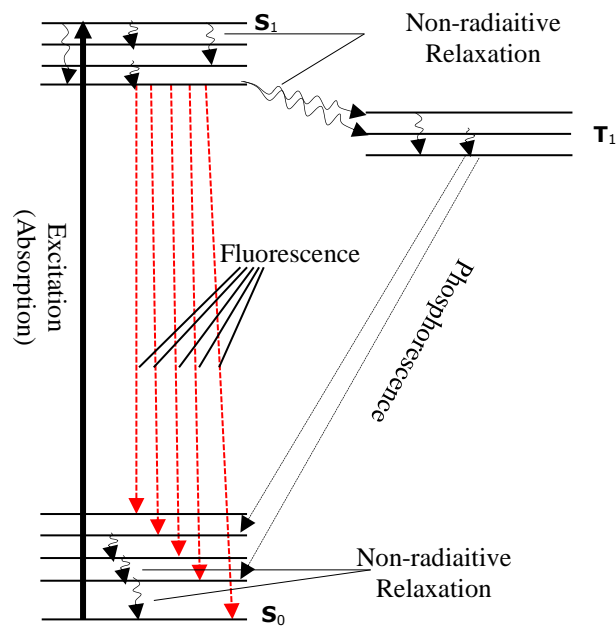


Figure 16: Typical energy levels structure in a laser dye [Jef-1992].

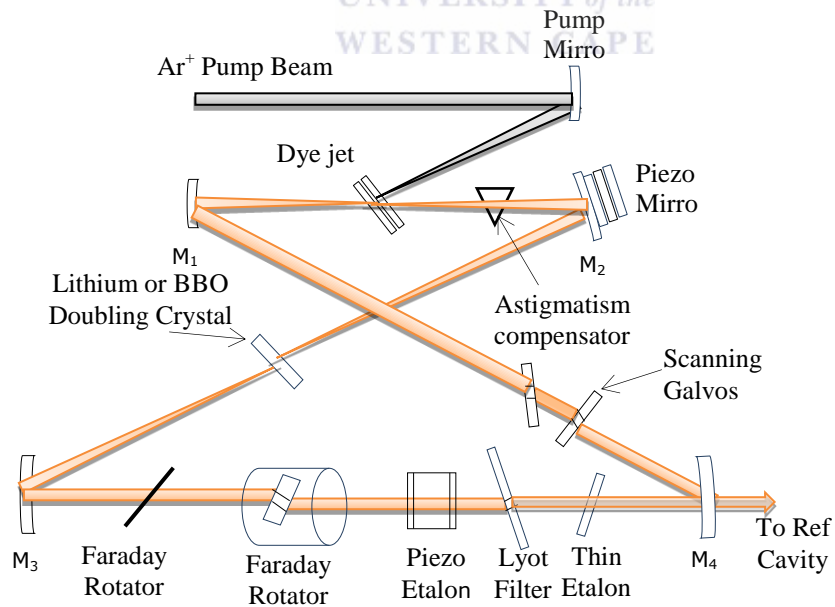


Figure 17: Configuration of high resolution Ring Dye Laser with travelling wave inside the laser cavity [Jef-1992].

Table 1: Characteristics of Selected Laser Dyes plus Titanium-Sapphire for Different Pump Sources [Jef-1992].

Dye output, Dye Name	Wavelength, nm			Maximum	
	Range	Peak	Pump Sources	Pump, WW(at peak)	
Polyphenyl 2		383	Short-UV Argon	3.4	0.25
Stilbene 1		415	UV Argon	6.0	0.42
Stilbene 3	408-453	425	Nitrogen	-	-
(Stilbene 420)	410-454	424	XeCl	-	-
	412-444	424	Nd-YAG 335 nm	-	-
	414-465	435	UV Argon	7.0	1.0
Coumarin 102		477	Kr,407-415 nm	4.8	0.58
(coumarin 480)	454-510	470	Ar ultraviolet	-	-
	457-520	478	Flashlamp	-	-
	457-517	478	XeCl	-	-
	459-508	475	Nd-YAG, 335 nm	-	-
	453-495	470	Nitrogen	-	-
		518	Kr,407-415 nm	4.6	0.38
Coumarin 30	529-585	540	Ar, 455-514 nm	23	3.6
Rodhamin 110	529-570	541	Cu, 511 nm	-	-
(Rodhamin 560)	530-580	554	Flashlamp	-	-
	541-583	563	Nd-YAG, 332 nm	-	-
	542-578	555	XeCl	-	-
Rodhamin 6G	546-592	562	Nd-YAG, 335 nm	-	-
(Rodhamin 590)	563-625	586	Flashlamp	-	-
	563-607	585	Cu, 511 nm	-	-
	566-610	583	XeCl	-	-
	568-605	579	Nitrogen	-	-
	573-640	593	Ar,455-514	24	5.6
Dicyanomethylene	598-677	644	Cu, 511 nm	-	-
	600-677	635	Flashlamp	-	-
	600-695	637	Nitrogen	-	-
	607-676	635	Nd-YAG, 335 nm	-	-
	610-709	661	Ar,455-514 nm	20	2.9
Ti-Sapphire		790	Ar,455-514 nm	20	3.6
Styryl 9	775-865	818	Nd-YAG, 335 nm	-	-
	784-900	822	Argon	-	-
	810-860	841	Flashlamp	-	-
Infrared dye 140	866-882	875	Nd-YAG, 335 nm	-	-
	875-1015	960	Kr, 753-799 nm	3.0	0.2
	876-912	884	XeCl	-	-
	900-995	936	XeC	-	-
	906-1018	964	Nitrogen	-	-

3.7.2. Dye Solar Cells

Another example of successful application of dyes in general and natural dyes specifically is in the so called Grätzel Dye Solar Cells (DSCs) technology based on the Ru polypyridile complexes, since the pioneer communication of *Grätzel et al.* in 1991 [Gra-1991]. In parallel, a growing interest on the use of alternatives to Ru did occur with the achievement leading to highly efficient DSCs based on material such as organic dyes containing polythiophene unit [Eu-2010] in addition to its low cost of production. Figure 18 shows a typical DSC. In general DSCs are composed of a Nano-crystalline porous semiconductor electrode-absorbed dye, a counter electrode, and an electrolyte containing iodide and tri-iodide ions. The dye, upon absorption of a photon $h\nu$, is promoted from its ground state to an electronically excited state which lies energetically above the conduction band edge of the semiconductor nanoparticles. An electron is therefore injected into the TiO_2 conduction band. The deactivation reaction is a relaxation of the excited states, which occurs in competition with the electron injection into the TiO_2 . The collection efficiency of the photo-injected electrons at the anode back contact is hindered by two major recombination processes: back electron transfer and the TiO_2 conduction band electron capture by the oxidized redox couple. These two processes are in competition with the oxidation of iodide and tend to reduce the current production of the cell. In the external circuit, the injected electrons give a current flow and provide for the reduction of iodine at the counter electrode. An efficient sensitizer should absorb light over a broad range from the visible to the near-infrared and, the energy of its electronic excited state should lie energetically above the conduction band edge of the TiO_2 . Thermal and photochemistry stability are other essential characteristics of dyes used in DSCs. Consequentially, the synthetic or natural dye as the sensitizer component plays a major role in absorbing

sunlight and transforming solar energy into electric energy via the creation of an electron-hole pair by band gap excitation of the semiconductor. Several metal complexes and organic dyes have been synthesized and utilized as sensitizers. The highest efficiency of DSCs sensitized by Ru-containing compounds absorbed on nano-crystalline TiO₂ was found to be in the range of 11–12% [Chi-2006, Bai-2008]. Although such DSCs have provided a relatively high efficiency, there is a need for alternative materials as there are several disadvantages of using organic dyes as these later have often presented problems as well, such as complicated synthetic routes and low yields. Recently, several groups worldwide are targeting the usage of natural dyes in flowers, leaves, and fruits because they are environmentally friendly, non-toxic and biodegradable. Moreover, natural present a great interest due to their cost efficiency and extraction by simple procedures. Therefore, dyes such as cyanine, carotene, tannin and chlorophyll [Sir-2006, Góm-2010, Esp-2005, Kum-2006] are becoming a popular subject of research for synthesizers. The use of red Sicilian orange juice shows a conversion efficiency of 0.66% [Cal-2008] while a conversion of 0.7%. [Won-2007] was achieved by *Wongcharee et al.* by using a rosella as sensitizer in their DSC. *Roy et al.* reported that when Rose Bengal is used dye as sensitizer, the short circuit current and open circuit voltage J_{sc} and V_{oc} respectively of their DSC reached 3.22 mA cm⁻² and 0.89 V, respectively, resulting in 2.09% conversion efficiency [Roy-2008]. An additional list of 20 natural dyes [Hui-2011] sensitizers which were extracted from plants with their photochemical parameter are reported in table 2. The photoelectro-chemical performance of the DSCs based on these dyes containing cyanine, carotene, chlorophyll, etc..., showed that the V_{oc} ranged from 0.337–0.689 V, whereas J_{sc} was in the range of 0.14–2.69 mA cm⁻². Recently, a research on anthocyanin and betalains as sensitizer was carried out by *Calogero et al.* [cal-2012]. This research group also reported the DSC's result with natural dyes extracted from wild Sicilian prickly pear, blackberry, red Sicilian orange, mulberry, radicchio, eggplant

and giacche grape. For example, Sicilian prickly pear, eggplant and radicchio have shown a monochromatic incident photon to current efficiency (IPCE) varying from 40% to 69% table 3 [Cal-2012]. Short circuit photocurrent densities (J_{sc}) up to 8.8 mA/cm², and open circuit voltage (V_{oc}) ranging from 316 to 419 mV, which were obtained from these natural dyes under 100 mW/cm² (AM 1.5) simulated sunlight, while the best solar conversion efficiency achieved was 2.06%.

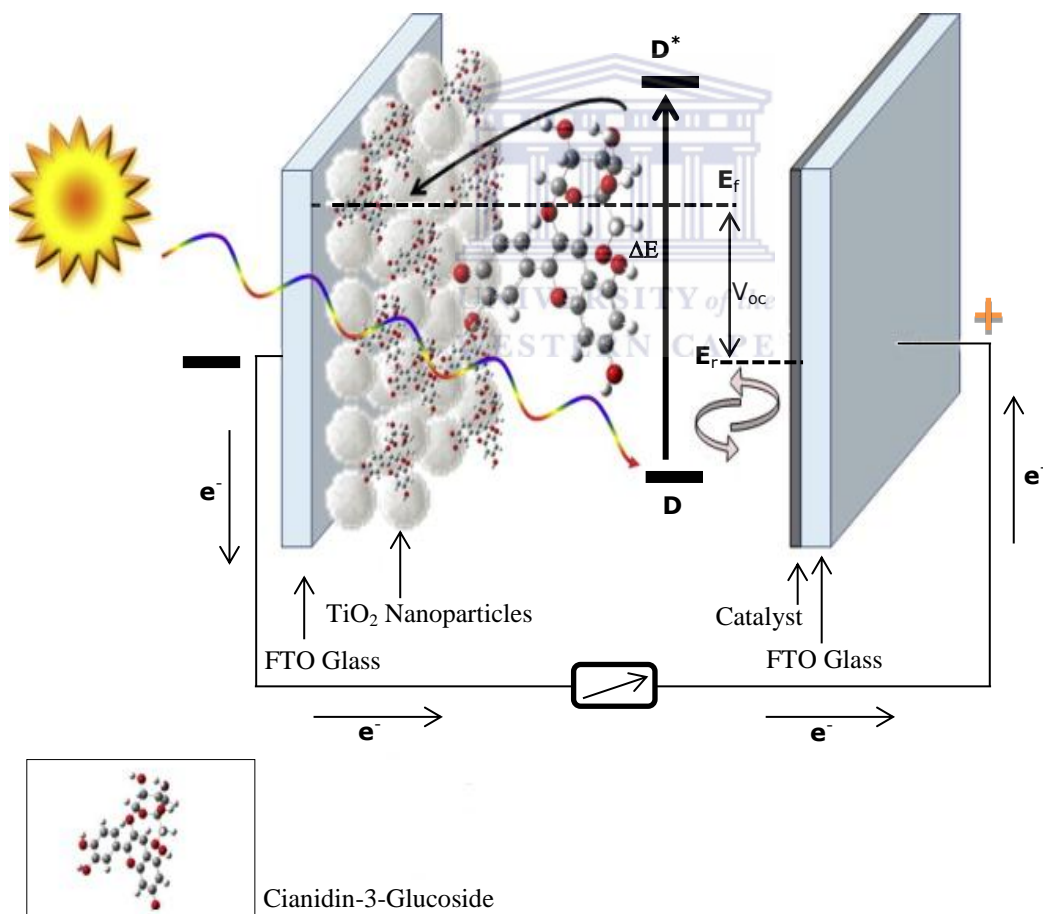


Figure 18: Typical Grätzel Dye Solar Cell based on nano-TiO₂ in which the dye consists of Cyanidin-3-glucoside [Pie-2010].

Table 2: [Hui-2011] Photoelectrochemical parameters of the DSCs sensitized by natural dyes extracted with (a) ethanol, (b) water, and (c) 0.1 M HCl-ethanol. N719 was extracted with the mixture of (d) acetonitrile and tert-butyl alcohol; (e) λ_{\max} in the visible light range is shown.

Natural dye	λ_{\max}^e (nm)	J_{sc} (mA cm ⁻²)	Voc (V)	FF	η (%)
Begonia ^a	540	0.63	0.537	72.2	0.24
Tangerine peel ^a	446	0.74	0.592	63.1	0.28
Rhododendron ^a	540	1.61	0.585	60.9	0.57
Fructus lycii ^a	447, 425	0.53	0.689	46.6	0.17
Marigold ^a	487	0.51	0.542	83.1	0.23
Perilla ^a	665	1.36	0.522	69.6	0.50
Herbartemisiae scopariae ^a	669	1.03	0.484	68.2	0.34
China loropetal ^a	665	0.84	0.518	62.6	0.27
Yellow rose ^a	487	0.74	0.609	57.1	0.26
Flowery knotweed ^a	435	0.60	0.554	62.7	0.21
Bauhinia tree ^a	665	0.96	0.572	66.0	0.36
Petunia ^a	665	0.85	0.616	60.5	0.32
Lithospermum ^a	520	0.14	0.337	58.5	0.03
Violet ^c	546	1.02	0.498	64.5	0.33
Chinese rose ^c	516	0.90	0.483	61.9	0.27
Mangosteen pericarp ^a	/	2.69	0.686	63.3	1.17
Rose ^b	/	0.97	0.595	65.9	0.38
Lily ^b	/	0.51	0.498	66.7	0.17
Coffee ^b	/	0.85	0.559	68.7	0.33
Broadleaf holly leaf ^b	/	1.19	0.607	65.4	0.47
N-719 ^d	515	13.74	0.773	57.6	6.11

Table 3: IPCE% maximum values, measured at λ_{max} for some selected dyes adsorbed on TiO₂ multilayer structures (13.3 μm thick, including a scattering layer) [Cal-2012].

Dyes	Electrolyte	λ_{max} (nm)	IPCE (%)
N719	A6979	550	89
N719	A6141	550	86
Sicilian prickly pear (H ⁺)	A6979	450	69
Blackberry (H ⁺)	G1	550	46
Blackberry (H ⁺)	A6979	550	44
Red Sicilian orange concentrated juice (H ⁺)	A6979	550	42
Red Sicilian orange concentrated juice	G1	550	40



References:

- [Mar-2009] Maria J. Melo; History of natural dyes in ancient Mediterranean world. Handbook of natural Colorants, (2009)
- [Est-2024] Esther Forgacs, Tibor Cserhati, Gyula Oros, Removal of synthetic dyes from wastewaters: a review, Environment International 30 953 – 971 (2004)
- [Mah-2010] S. Mahesh, G. Vijay Kumar and Pushpa Agrawal, Studies on the utility of plant cellulose waste for the bioadsorption of crystal violet dye; Journal of Environmental Biology; 31 277-280 (2010)
- [Nor-2009] H. Norasiha. A.M. Mimi Sakinah¹, C.M. Rohaida, Characterization of β -Cyclodextrin Complexes with Natural Dye, (2009)
- [Che-2010] B. Chengaiah K. Mallkarjuna Rao, K. Mahesh Kuma, M. Alagusundaram, C. Madhusudhan Chetty. Medical Importance of Natural dyes- A Review. International Journal of PharmTech Research CODEN (USA): Vol.2, No.1, pp 144-154, (2010)
- [Boa-2005] NIIR Board of Consultant & Engineering Natural Dyes and Pigment, Asian Paci Business Press, 448, (2005)
- [Naz-2002] Md. Nazmul Hossain Bhuiyan, katsusuke Murakami and Taiji Adachi, Variation in betalain content and factors affecting the biosynthesis in Portulakasp, 'jewel' cell cultures, Plant Biotechnology, 19 (5) 369-376, (2002)
- [Rao-2007] A.V. Rao, L.G. Rao, Carotenoids and human health, Pharmacological Research 55, 207216, (2007)
- [Ala-2006] Alan Mortensen, Carotenoids and other pigments as natural Colorants, Pure Appl. Chem., Vol. 78, No. 8, pp. 1477-1491, (2006)
- [Abd-2012] Abdoulghafar Omari, Iwan Moreels, Francesco Masia, Wolfgang Langbein, Paola Borri, Dries Van Thourhout, Pascal Kockaert, 6 and Zeger Hens, Role of interband and

- photoinduced absorption in the nonlinear, *Physical Review B* 85, 115318, (2012)
- [Del-2001] Delia B. Rodriguez-Amaya, *a Guide to Carotenoid Analysis in Foods*
- [Mac-1993] Maciek E. Orczyk, Marek Samoc, Jacek Swiatkiewicz, and Paras N. Prasad, Third-order nonlinearity of canthaxanthin carotenoid, *J. Chem. Phys.* 98 (4), 15, (1993)
- [Ash-2011] Ashis Kumar Samanta and Adwaita Konar, *Dyeing of Textiles with Natural Dyes*. In *Tech Open book*, (2011)
- [Hye-2007] Hyesun P. McNulty, Jungsoo Byun, Samuel F. Lockwood b , Robert F. Jacob a , R. Preston Mason, Differential effects of carotenoids on lipid peroxidation due to membrane interactions: *Biochimica et Biophysica Acta* 1768, 167-174, (2007)
- [Ade-2003] Adela Pinteá, Constantin Bele, Sanda Andrei, Carmen Socaciu, HPLC analysis of carotenoids in four varieties of *Calendula officinalis* L. flowers, *Acta Biol Szeged* 47(1-4):37-40, (2003)
- [Ber-2002] Berg JM, Tymoczko JL, Stryer L, *Light Absorption by Chlorophyll induces Electron Transfer*, *Biochemistry*. 5th edition. New York: W H freeman, (2002).
- [Noo-2011] M. M. Noor, M. H. Buraidah, S. N. F. Yusuf, M. A. Careem, S. R. Majid, and A. K. Arof, Performance of Dye-Sensitized Solar Cells with (PVDF-HFP)-KI-EC-PC Electrolyte and Different Dye Materials; *International Journal of Photoenergy*, (2011)
- [Hug-1991] H. Scheer, *Structure and Occurrence of Chlorophylls*
- [Nic-2009] Nick W. Albert, David H. Lewis, Huaibi Zhang, Louis J. Irring G., Paula E. Jameson and Kevin M. Davies, Light-induced Vegetative Anthocyanin Pigmentation in *Petunia* *Journal of Experimental Botany*, vol 60, 2191-2202, (2009)
- [Aok-2002] Aoka, G., Dao, L., Anthocyanins. In: Hurst, W.J. (Ed.), *Methods of analysis for Functional Foods and Nutraceuticals*. CRC (2002)

- [Øyv-2006] Flavonoids : chemistry, biochemistry, and applications, Øyvind M. Andersen and Kenneth R. Markham. Published in 2006 by CRC Press, Taylor & Francis Group (2006)
- [Ant-2004] Antonio Piga, Cactus Pear: Fruit of Nutraceutical and functional importance, (2004)
- [Hen-2009] Henriette M.C. Azeredo, Betalains: properties, sources, applications, and stability, International Journal of Food Science & Technology, 44, 2365-2376, (2009)
- [Jef-1992] Jeff Hecht, Dye laser beam characteristic, the Laser Guidebook, 2nd Ed (1992)
- [kap-2009] V P Kapoor, K Katiyar, P Pushpangadan and N Singh, Development of Natural Dye Based Sindoor, (2009)
- [Rab-2009] M.S. Rabasovica , D. Sevica, , M. Terzicb , S. Savic-Sevica , B. Murica , D. Pantelica and B.P. Marinkovica, Measurement of Beet Root Extract Fluorescence Using TR-LIF Technique, Proceedings of the International School and Conference on Photonics, Phonic A09, Acta Physica Polonica A, Vol. 116 (4), 570 (2009)
- [Jin-2010] Jin Dai, and Russell J. Mumper; Plant Phenolics: Extraction, Analysis and Their Antioxidant and Anticancer Properties, Molecules, 15, 7313-7352, (2010)
- [Del-2003] Francisco Delgado-Vargas and Octavio Paredes-Lopez, Natural Colorants for Food and Nutraceutical, by CRC Press LLC(2003)
- [Nur-2011] Nursyamirah Abd Razak, Siti Marsinah Tumin and Ruziyati Tajuddin, Effect of Temperature on the Color of Natural Dyes Extracted Using Pressurized Hot Water Extraction Method, American Journal of Applied Sciences 8 (1): 45-49, (2011)
- [Mag-2004] Magdalena Biesaga, Anna Wach, Krystyna Pyrzyńska, Chromatographic Identification of Dyes Extracted from Plants and archeological Textiles; Proceedings Book (2004)
- [Kel-2011] Kelvin Alaba Aduloju, Mohamed Basiru Shitta and Simiyu Justus, Effect of Extracting Solvents on the Stability and

- Performances of Dye-Sensitized Solar Cell Prepared Using Extract from Lawsonia Inermis, *Fundamental J. Modern Physics*, Vol. 1, 2, 261-268 (2011)
- [Fei-2012] Fei He, Na-Na Liang, Lin Mu, Qiu-Hong Pan, Jun Wang, Malcolm J. Reeves and Chang-Qing Duan, Anthocyanins and Their Variation in Red Wines I. Monomeric Anthocyanins and Their Color Expression, *Molecules*, 17, 1571-1601, (2012)
- [Sun-2000] Wenfang Sun, Michael M. McKerns, Chris M. Lawson, Solvent Effect on the Third Order Nonlinearity and Optical Limiting Ability of a Stilbazolium-like Dye. *SPIE* (2000)
- [Shi-2012] S.R. Shirsath, S.H. Sonawane P.R. Gogate; Intensification of extraction of natural products using ultrasonic irradiations -A review of current status, Vol. 53 10-23; 37 (2012)
- [Tan-2010] Tania Carreón-Valencia, King-Thom Chung, Silvia de Sanjosé, Harold S. Freeman, Shoji Fukushima, Some Aromatic Amines, Organic Dyes, and Related Exposures, *IARC vol 99*, (2010)
- [Rod-2011] Rodrigo N., Diego T. Santos, Maria Angela A. Meireles, Non-thermal stabilization mechanisms of anthocyanins in model and food systems - An overview, *Food Research International*, Vol. 44, 499-509, (2011)
- [Woo-2011] K.K. Woo, F.H. Ngou, L.S. Ngo, W.K. Soong and P.Y. Tang, Stability of Betalain Pigment from Red Dragon Fruit (*Hylocereus polyrhizus*). *American Journal of Food Technology*, 6: 140-148. (2011)
- [Yos-2009] Yoshiumi Kohno, Reina Kinoshita, Shuji Ikoma, Keiko Yoda, Masashi Shibata, Ryoka Matsushima, Yasumasa Tomita, Yasuhisa Maeda, Kenkichi Kobayashi, Stabilization of natural anthocyanin by intercalation into montmorillonite, *Applied Clay Science* 42, 519-523 (2009)
- [Jea-1998] Jean-François Gonnet, Colour effects of co-pigmentation of anthocyanins A calorimetric definition using the revisited-I.

CIELAB scale; *Food Chemistry*, Vol. 63, No. 3, pp. 409415 (1998)

- [Sor-1966] Sorokin P PandLankard J R, Stimulated emission observed from an organic dye, chloro-aluminumphthalocyanine. *IBM J. Res. Develop.* 10:162-3, 1966.
- [Hen-2005] Henry R. Aldag, David H. Titterton, *From Flashlamp-Pumped Liquid Dyes Lasers to Diode- Pumped Solid-State Dye Lasers*, SPIE photonics West (2005)
- [Gra-1991] B. O'Regan, M. Grätzel, A low-cost, high-efficiency solar cell based on dye- sensitized colloidal TiO₂ films, *Nature* 353, 737–740(1991)
- [Eu-2010] Eugenia Martinez-Ferrero, Ivan Mora Seró, Josep Albero, Sixto Giménez, Juan Bisquert and Emilio Palomares, Charge transfer kinetics in CdSe quantum dot sensitized solar cells *Phys. Chem. Chem. Phys.*, 12, 2819–2821 (2010,)
- [Chi-2006] Y Chiba, A. Islam, Y. Watanabe, R. Komiya, N. Koide, L.Y. Han, Dye-sensitized solar cells with conversion efficiency of 11.1%, *Jpn. J. Appl. Phys.* 45 (2006) L638–L640
- [Bai-2008] R. Buscaino, C. Baiocchi, C. Barolo, C. Medana, M. Grätzel, Md.K. Nazeeruddin, G. Viscardi, A mass spectrometric analysis of sensitizer solution used for dye- sensitized solar cell, *Inorg. Chim. Acta* 361 798–805 (2008)
- [Sir-2006] P.M. Sirimanne, M.K.I. Senevirathna, E.V.A. Premalal, P.K.D.D.P. Pitigala, V. Sivakumar, K. Tennakone, Utilization of natural pigment extracted from pomegranate fruits as sensitizer in solid-state solar cells, *J. Photochem. Photo-biol. A* 177 (2006) 324–327.
- [Góm-2010] N.M. Gómez-Ortíz, I.A. Vázquez-Maldonado, A.R. Pérez-Espadas, G.J. Mena- Rejón, J.A. Azamar-Barrios, G. Oskam, Dye-sensitized solar cells with natural dyes extracted from achiote seeds, *Sol. Energ. Mat. Sol. C* 94 (2010) 40–44.

- [Kum-2006]G.R.A. Kumara, S. Kaneko, M. Okuya, B. Onwona-Agyeman, A. Konno, K. Tennakone, Shiso leaf pigments for dye-sensitized solid-state solar cell, *Sol. Energ. Mat. Sol. C* 90 (2006) 1220–1226.
- [Cal-2008] G. Calogero, G.Di. Marco, Red Sicilian orange and purple eggplant fruits as natural sensitizers for dye-sensitized solar cells, *Sol. Energ. Mat. Sol. C* 92 1341–1346(2008)
- [Won-2007]K. Wongcharee, V. Meeyoo,S. Chavadej, Dye-sensitized solar cell using natural dyes extracted from rosella and blue pea flowers, *Sol. Energ. Mat. Sol. C* 91 566–571, (2007)
- [Roy-2008]M.S. Roy, P. Balraju, M. Kumar, G.D. Sharma, Dye-sensitized Solar cell based on Rose Bengal dye and nanocrystalline TiO₂, *Sol. Energ. Mat. Sol. C* 92 (2008) 909–913.
- [Pie-2010] Pietro Calandra, Giuseppe Calogero, Alessandro Sinopoli, and Pietro Giuseppe Gucciardi, Metal Nanoparticles and Carbon-Based Nanostructures as Advanced Materials for Cathode Application in Dye-Sensitized Solar Cells, *International Journal of Photoenergy* Vol. (2010), Article ID 109495, 15 pages doi:10.1155/2010/109495
- [Hui-2011]Huizhi Zhou, Liqiong Wu, YurongGao, Tingli Ma, Dye-sensitized solar cells using 20 natural dyes as sensitizers, *Journal of Photochemistry and Photobiology A: Chemistry*, 219 188–194(2011)
- [Cal-2012] Giuseppe Calogero, Jun-Ho Yum, Alessandro Sinopoli, Gaetano Di Marco, Michael Grätzel, Mohammad Khaja Nazeeruddin, Anthocyanins and betalains as light-harvesting pigments for dye-sensitized solar cells, *Solar Energy* 86 1563–1575 (2012)

CHAPTER-4: EXPERIMENTS, RESULTS and DISCUSSION

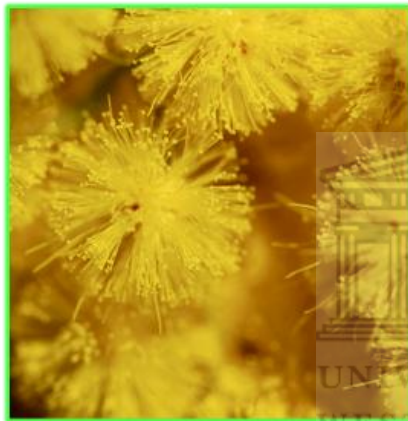
4.1. Samples preparation, Morphological, Elemental and Crystallographic Characterization

4.1.1 Samples Preparation

The mature and fresh flowers of the two considered natural dyes i.e. flame flower and mimosa flower (see figure 19 (a)) were collected in the Western Cape Province in South Africa during winter (early spring-2011), while the fresh beetroot was obtained from a trading market in the same period. Both the flowers and the beetroot were cleaned with de-ionized cold water ($< 18.2 \text{ M}\Omega$), and then the flowers were immediately boiled. The beetroot was thereafter crushed and filtered before the boiling process. The extract of each sample was filtered using a standard filter paper and separated from the residue compounds. Three different types of samples were synthesised from each of the 3 natural dyes: (i) solutions consisting of the dye in H_2O (figure 19 (b)), (ii) dye solution embedded in a nano-porous gel host matrix (figure 20) as well as in (iii) in a thin film configuration. In addition to and for elemental and crystallographic investigations, powders of the 3 considered dyes were synthesized using the freeze drying process. More specifically, the liquid samples were kept cool at a temperature of $\sim 4^\circ\text{C}$ in a refrigerator for further use, while the powder was kept in desiccators. The water extraction method was used in order to make sure that the colour is safe from any chemical interference reaction. To keep the extracted dyes solutions fresh, they were sealed in cleaned amber Schott glass bottles and kept in the fridge at about $\sim 2^\circ\text{C}$.



Flame flower



Mimosa yellow
flower



Beetroot



(a)

(b)

Figure 19: (a) Selected natural dyes from flame flower, mimosa flower and beetroot; (b) Dyes in solution.



Figure 20: Dyes in gels.

4.1.2 X-Ray Diffraction

In this section we report the results that concern the flame and the mimosa dyes for which it was possible to do the XRD and SEM-EDX measurements compared to the beetroot sample which was useless for these experiments because it becomes immediately black when exposed to light.

The XRD patterns of each dye were examined. From the peaks position of the XRD spectra shown in figure 21 and 22, it can be observed that the flame flower dye crystallographic patterns showed peaks at $2\theta = 29.45, 40.60, 50.02, 50.88, 65.5, 74.88$ and 87.5 which have the corresponding reflections (200), (220), (222), (400), (420), (422), respectively. In the case of mimosa flower dye, the powder sample showed the same patterns (figure 22) as seen the case of the flame dye. However, its thin film did not show any particular peaks but rather amorphous characteristics. This means the crystallization was not completed on the thin film or the crystals may be very small in diameter. The powder is found to be well crystallized compared to the thin film. The phases identified by correlation [Moh-2009] with the standard XRD cards indicate a crystalline structure that is similar to that of KCl. The lattice parameter corresponding to this crystallographic structure is about $a = 6.29310\text{\AA}$. Moreover, (200) reflection peaks is particularly strong in intensity relative to the others in the flame dye as well as in the mimosa dye.

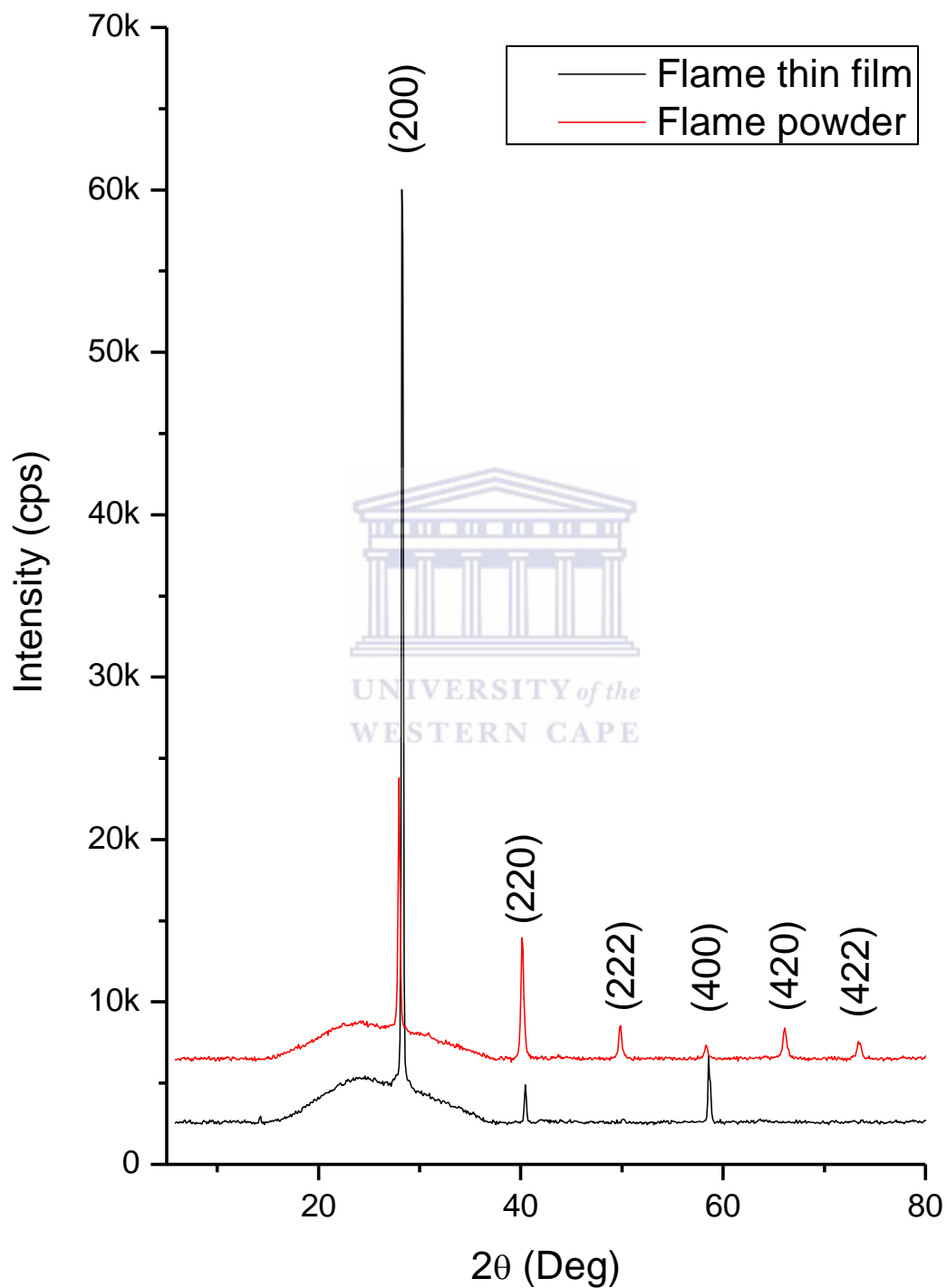


Figure 21: XRD patterns of flame dye on glass and in powder form.

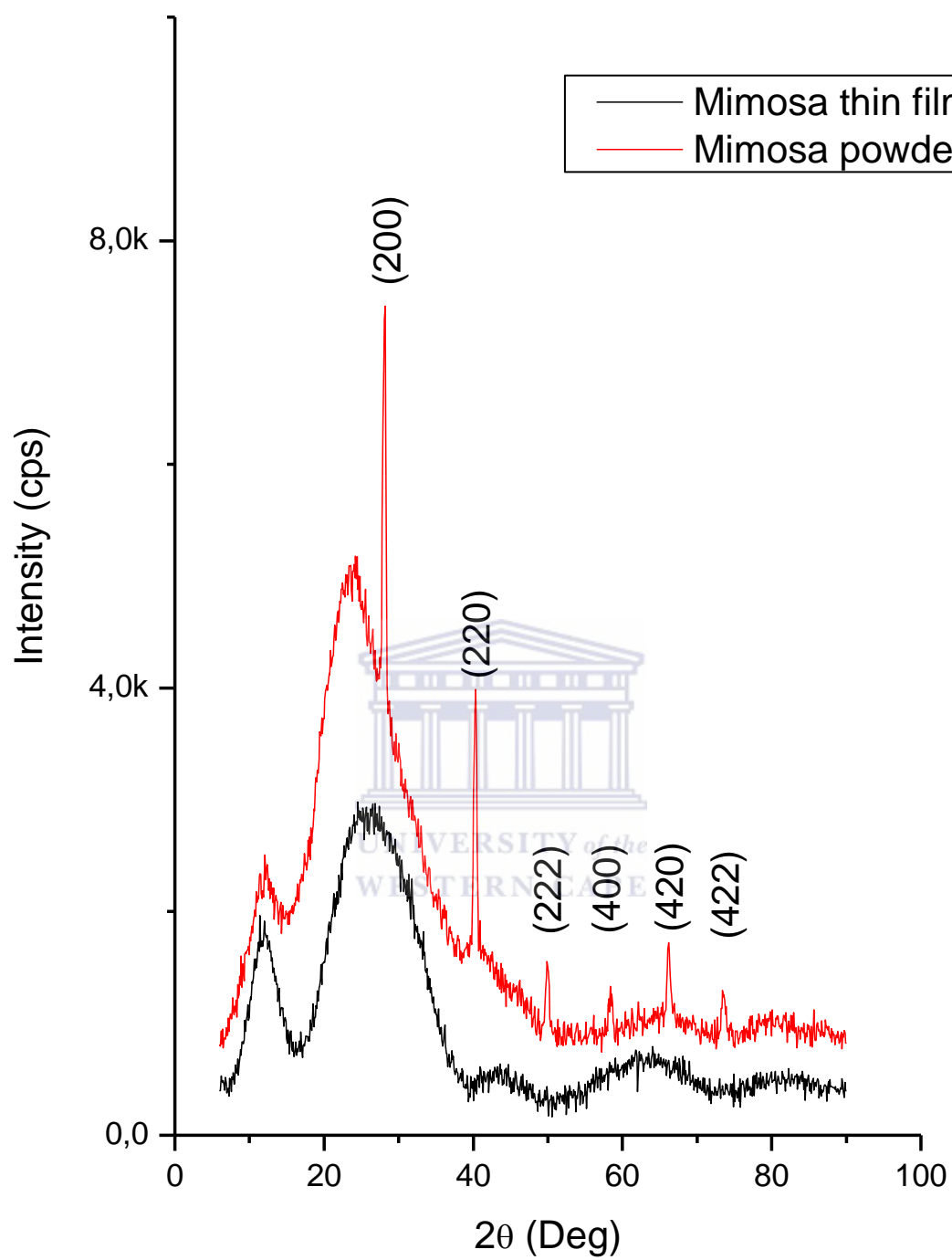


Figure 22 : XRD patterns of mimosa dyes on glass and in powder form.

4.1.3 Atomic Force Microscopy (AFM) and Scanning Electron Microscopy (SEM)-EDX Analysis

The AFM images in figures 23 and 24 indicate a localization of the crystals while the used in conjoint of SEM and EDS techniques enabled information regarding the morphological structure of crystals imaged. With different magnifications, it was possible to observe the texture and the shapes of crystals in the thin film. The SEM image of flame thin film shows in somewhat a well granulated texture of crystals in figure 25 (a) which is magnified in (25 b). The SEM of mimosa thin film on contrast presents plate-like crystals with regular shapes (triangular and rectangular shapes). The distribution of crystals showed in figure 26 (a) with the magnification in 26 (b) shows segregation between the bigger and smaller crystals with less strain among them. On the other hand, they are agglomerated with particle sizes in increasing with the direction. It is evident that the formation of these crystals in both flame and mimosa dye samples may be complex to explain. However, the evolution of the size and the morphology as well as the orientation can be described. According to [Ale-2001], there are three stages which can describe the evolution of the crystal: (i) the isolated growth which is characterized by the free growing of the starting nuclei; (ii) competitive growth, when crystal compete for space and when the selection of crystal orientation is occurring as well as (iii) parallel growth, the final stage where those with proper direction continue to grow. The crystallization phenomenon can therefore lead to an aggregation of crystals with individual preferential orientation. This is supported by the work done by *PB Barna* [Bar-1995]. He also suggested that the growth of particles may be influenced by the impurity species. The presence of impurities may strongly modify the form of crystals during the coalescence phase in the discrete growth of individual crystal [Bar-1995]. Broad and deeper grain boundary (GB) grooves develop after impurity phase grows over the surface neighbouring crystals. In that case, the time-dependent of grooves depth is the form [Mat-2007],

$$d = d_0 t^\alpha \quad (5.1)$$

where $\alpha = 1/2$ in the case of evaporation and condensation. When a crystal grows, it might have different grain size and orientations. Initially, the crystals grow freely and those with faster growth rate are grouped around those with slow growth rate as shown in figure 25 (a). In certain direction, some crystals are buried by neighbouring crystal. This mechanism leads to a reduction in the number of crystalline domains that are not preferentially oriented and in the increase in their size. On the other hand, the size of grains may be reduced during the coalescence phase which takes place when the growing adjacent discrete crystals approach and touch each other [Bar-1995]. For a better understanding of the mechanism of the evolution of the crystals, it is important to note that the main parameters that can be varied are correlated [Ale-2001] to: (1) the starting crystals morphology; (2) the orientation of crystals; the relative growth rate of different crystals; (3) the nucleation density on the substrate and (4) the substrate morphology. Taking in consideration of the peaks recorded using EDS, the nature of some chemical compound that could be involved in the crystals were identified (figure 27 and 28). The signal of oxygen (O) may be due to the glass while the peaks of potassium (K), the Sulphur (S) and the huge amount of Chlorine (Cl) could probably be from the dye layers. The element of K and Cl are in general found in plants because of the fact that the KCl compounds are used in plants as important nutrients. The AFM mapping was carried out to show the possibly crystal formation. During the crystallization phase, these elements may segregate to give the nanocrystals that have been characterized.

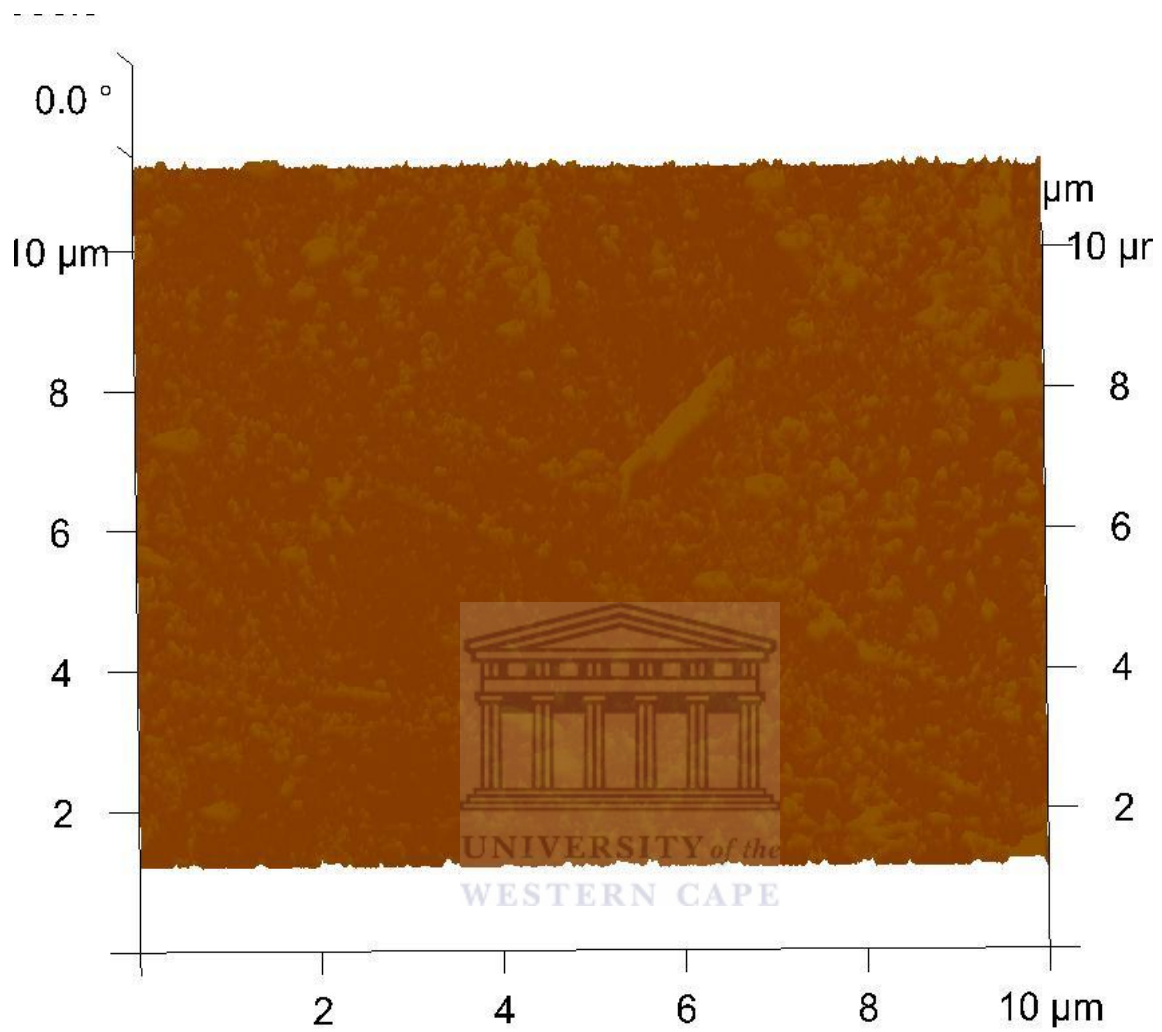


Figure 23: AFM image of flame dye.

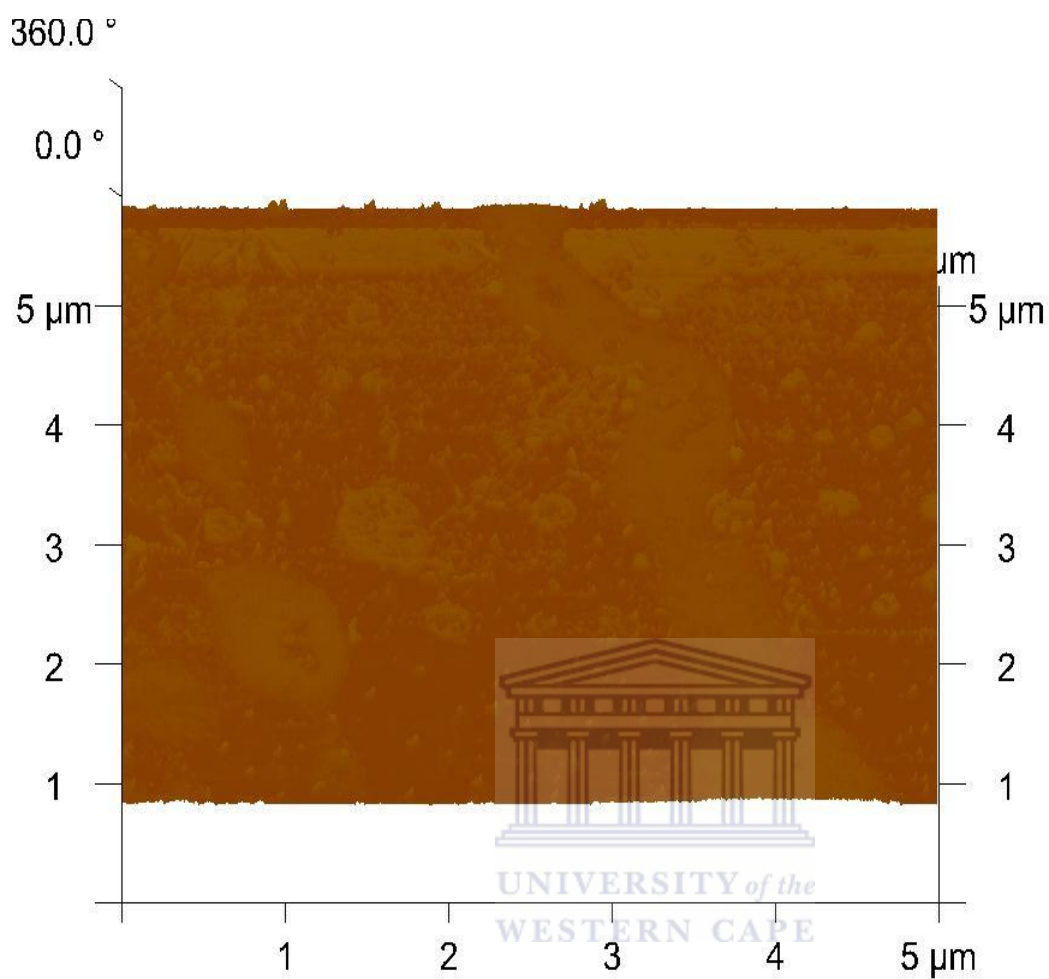


Figure 24: AFM image of mimosa.

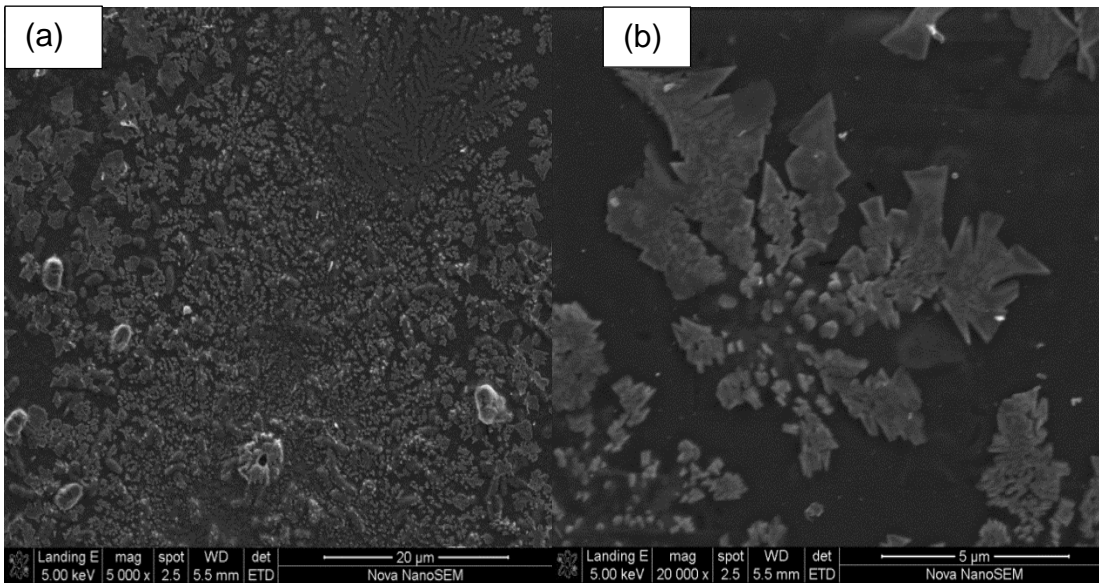


Figure 25: SEM image of flame dye on glass: (a) distribution of crystals; (b) represents the magnification of a portion of (a).

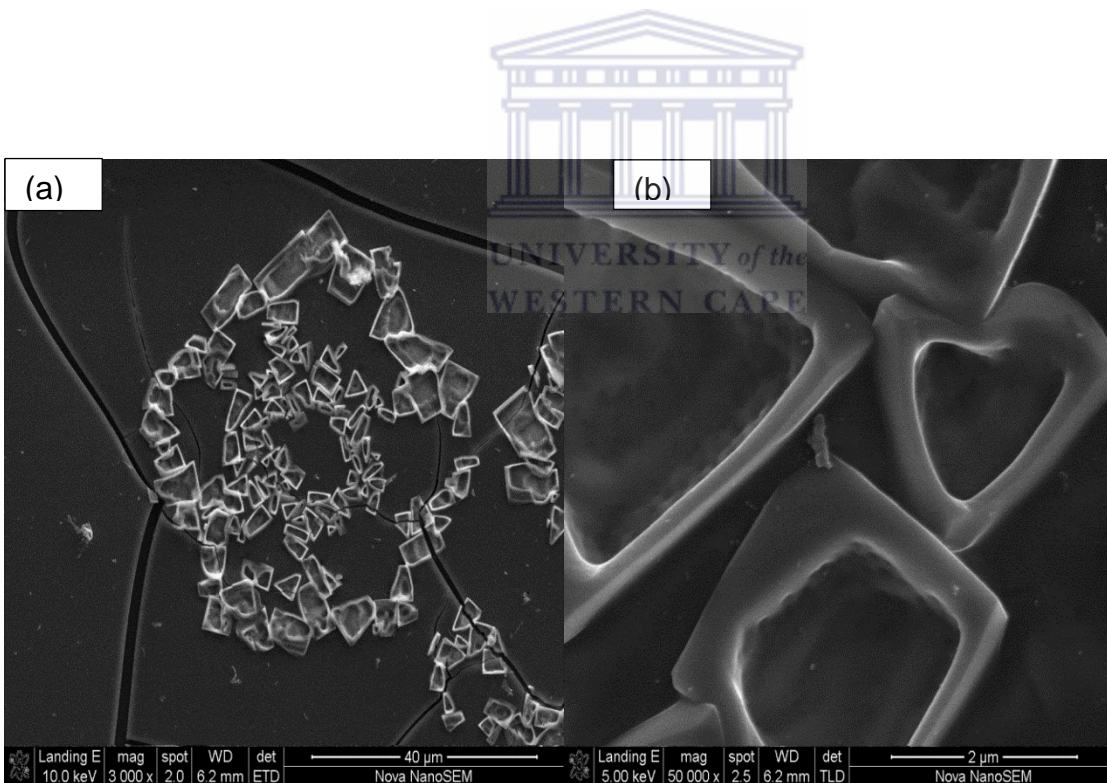


Figure 26: SEM image of mimosa dye on glass: (a) segregation of crystals; (b) represents the magnification of a portion of (a).

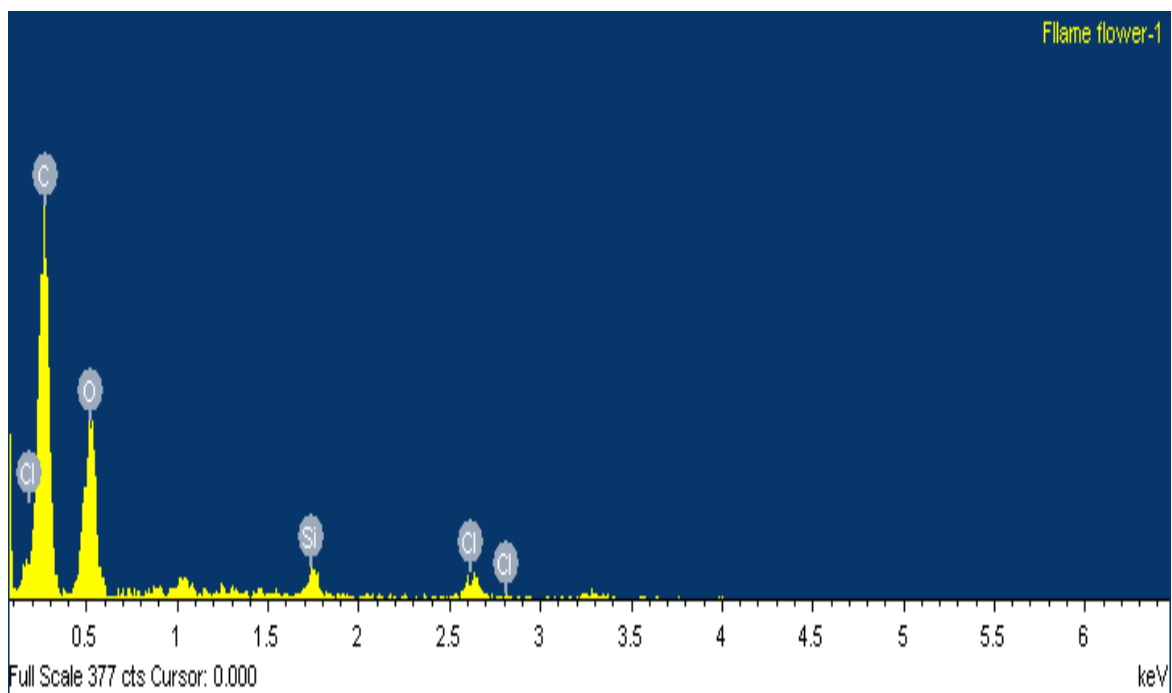


Figure 27: EDX spectrum of flame dye.

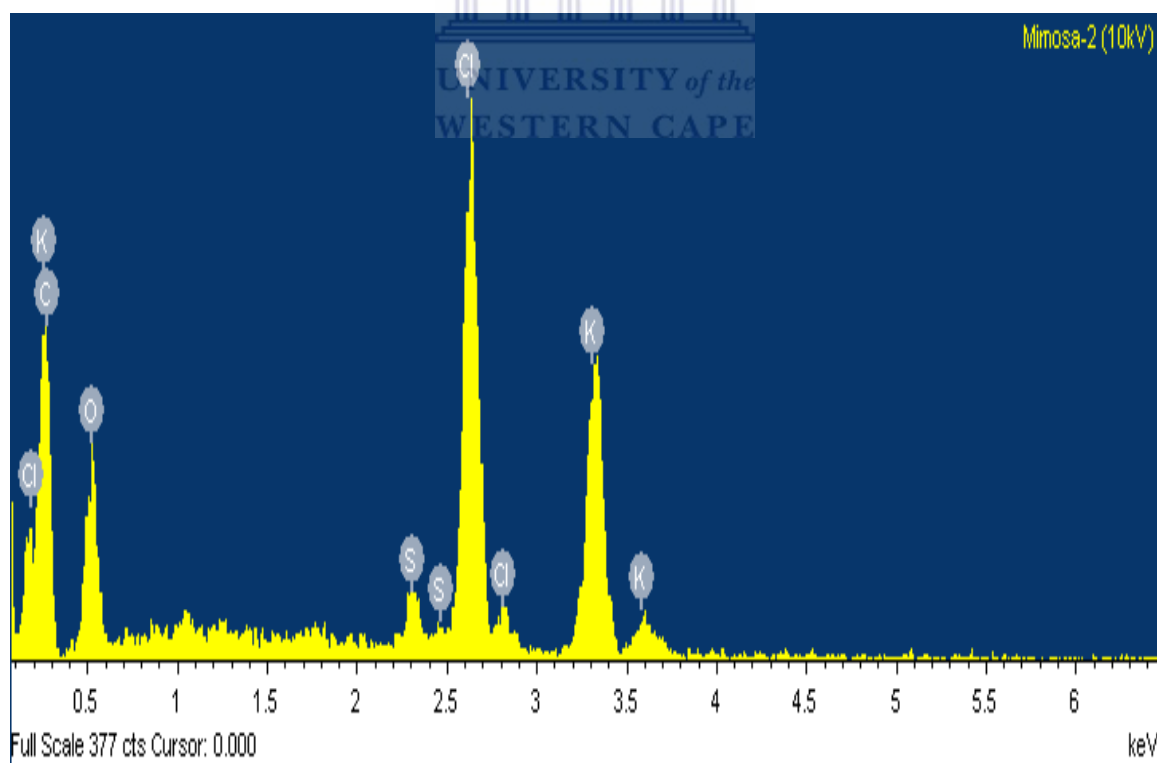


Figure 28: EDX spectrum of mimosa dye.

4.2. Linear and Nonlinear Properties

4.2.1. Infrared Spectroscopy and Vibrational Properties.

Fourier Transform Infra-Red (FTIR) spectroscopy technique is usually one of the most referred techniques used to give a correct assignment of the observed spectral characteristic of functional groups corresponding to different absorption bands which are responsible of the absorption bands. In our experiments, FTIR experiments were carried out at room temperature within the so called Attenuated Total Reflection (ATR) geometry. The IR-ATR transmittance measurements were carried out on a modified Perkin Elmer Paragon 1000, equipped with a wide band MCT mid-IR detector connected to an FTIR spectrophotometer. The IR-ATR measurements were performed in the spectral range of 300-4000 cm^{-1} .

The corresponding FTIR spectra of the studied solutions dyes are presented in figure 29, while table 4 summarizes the various IR absorption peaks due to the investigated dyes in solution form. In all of the three FTIR spectra, the most important absorption peaks were observed. The absorption occurring at the same wavelength may indicate the possibility of common functional groups in all the dyes. More precisely, the following vibration peaks have been observed. The broad and strong absorption band centered around 3435 cm^{-1} for mimosa, 3436 cm^{-1} for beetroot and 3465 cm^{-1} for flame, could be characteristics of the O-H or the N-H stretching modes. The peak centred at 2067 cm^{-1} for beetroot and mimosa and for flame flower at 2077 cm^{-1} is indicative of the $\text{C}\equiv\text{C}$ symmetry stretching vibration. The strong absorption peak at 1635 cm^{-1} represents $-\text{C}=\text{O}$ asymmetric stretching vibration mode in carboxyl groups [Jun-1968]. Finally, the peak centered around 650 cm^{-1} can be ascribed without any doubt to $\text{CH}=\text{CH}$ stretching vibration [Kek-2012]. In addition to the common peaks that are observed in all the three dyes, the beetroot solution dye itself presents two additional absorption peaks localized approximately at 1054 cm^{-1} and 997 cm^{-1} . An IR spectrum near 1000 - 1100

cm^{-1} has been reported to originate from cyclopentadienyl complexes of transition elements possessing an unsubstituted ring. The peak at 1054 cm^{-1} has been observed to be characteristic of coordinated amine group and associated with C-NO₂ of aromatic rings [Ade-2009], while the peak at 997 cm^{-1} can be attributed to C-N stretching of aromatic NO₂ compounds. The $\nu_{\text{asym}}\text{C}=\text{O}$ has been reported in the literature to be dependent on the inductive effect of the constituents, such as electron withdrawing which increase $\nu_{\text{asym}}\text{C}=\text{O}$ and electron releasing, which decrease its relative value to that of the ligands [Nak-1970]. Hence, the little variations in the spectra observed from one sample to another might be due to some substituent that may be present in the samples (e.g. NO₂ or C₆H₅ groups). In one of the studies reported in the literature [Fer-1971], IR broad peaks in region of $3300 - 3550 \text{ cm}^{-1}$ could be assigned to OH stretching frequency of coordinated water which is certainly related to air humidity. It has also been reported [Oka-1981] that in the anhydrous complexes, the band between $3080 - 3600$ implies the presence of (-N-H) and also the range $1230 - 1260 \text{ cm}^{-1}$ has been observed to be characteristic of coordinated amine group and associated with $\nu(\text{C}-\text{N})$ which also occurs at 1276 cm^{-1} , yet this last band was not observed in none of the three solutions. Hence IR broad and strong absorption band centered at 3435 cm^{-1} for mimosa, 3436 cm^{-1} for beetroot and 3465 cm^{-1} for flame are likely due to a combination N-H and mainly to O-H stretching mode of amine group and water molecules in the samples. This observation is evident in the sense that the dyes were extracted in water. One should point out that the absence of the others absorption peaks in the range $1230 - 1260 \text{ cm}^{-1}$ is characteristic of coordinated amine group and associated with $\nu(\text{C}-\text{N})$ which occurs at 1276 cm^{-1} on the flame and mimosa FTIR spectrum suggests that there may be no C-NO₂ and/or N-H chemical functional groups in the flame and mimosa dye. This is supported by the fact that the absorption bands which are associated to the combination of the O-H and the N-H stretching modes are less broadened both in the flame and mimosa solution dye than of the beetroot. A recent study carried out by *Keka Sinha et al.* [Kek-2012], on the FTIR analysis of the extracted natural dye of the flame flower shows distinct peaks at $3300, 2117, 1640$ and 652 cm^{-1} . These bands were attributed respectively to -OH, C \equiv C, -

C=O, CH=CH chemical functional groups but not to amine groups. The current IR-ATR spectral analysis shows the presence of different chemical functional groups like $-C\equiv C-$, $-C=O$, O-H, N-H, C-NO₂ and CH=CH. These functional groups remain essential for the large nonlinear absorption expressed in terms of nonlinear optical susceptibilities or other mechanism of absorption such as two photon absorption (TPA), reverse saturable absorption (RSA) or intensity-dependent refractive index characteristic.

Table 4: Tentative assignment of functional groups

Samples	Bands (cm ⁻¹)	Chemical functional Group
Beetroot dye	3436 1635 2067 1054 997 650	O-H; N-H; C≡C; C=O; C-NO ₂ (Aromatic rings) C-N (stretching of aromatic NO ₂ compounds) CH=CH
Mimosa Dye	3435 2067 1635 650	O-H; C≡C; C=O; CH=CH
Flame dye	3465 2077 1635 650	O-H; C≡C; C=O; CH=CH

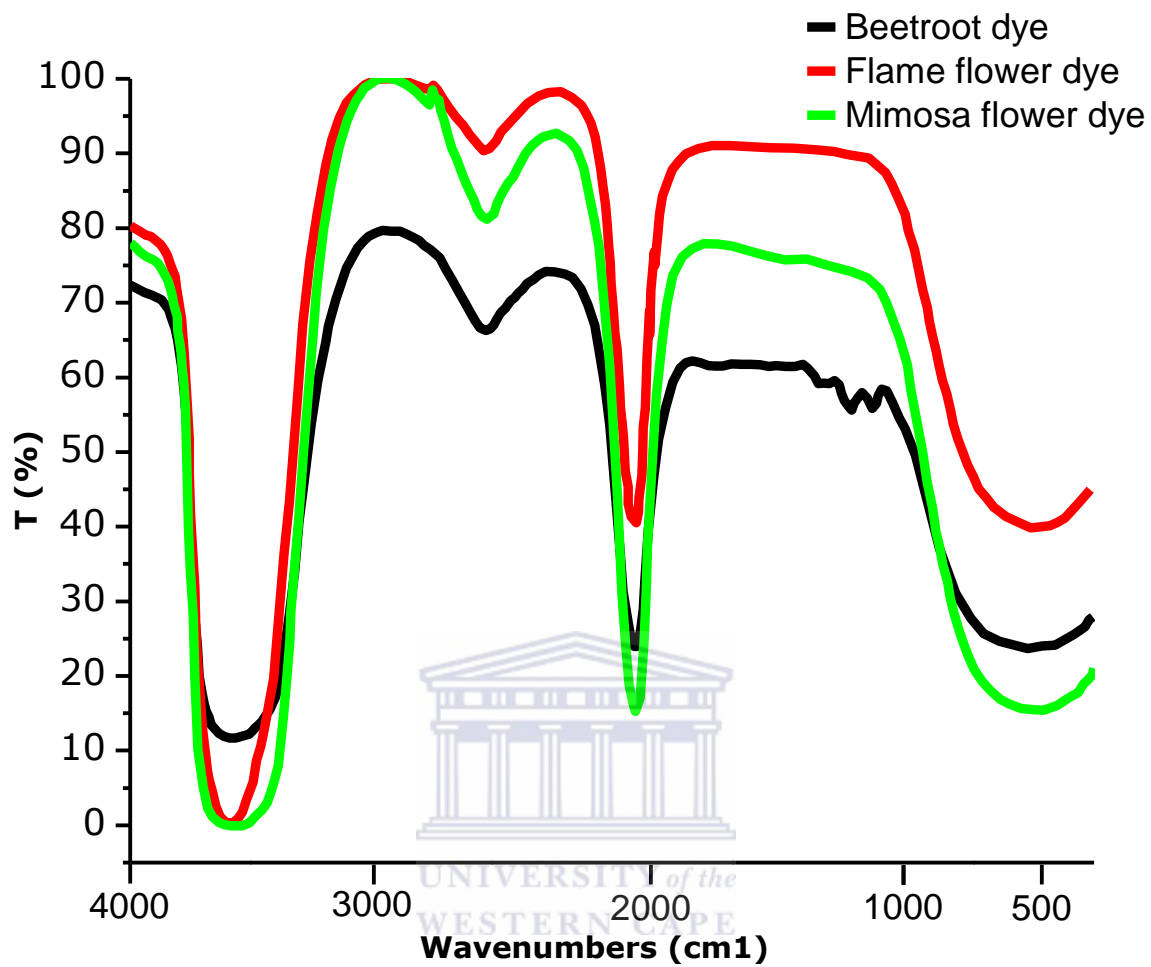


Figure 29: Room temperature IR vibrational spectra of the flame, mimosa yellow flower and beetroot dye solutions.

4.2.2. UV-VIS Spectroscopy and Optical Absorption Properties.

The UV-Vis spectrophotometric analysis was carried out using a standard UV-visible spectrophotometer (CECIL, CE 2021 3000 Series) which covers the spectral range of 200-1100nm. Distilled water contained in 1-cm path cuvette was used as background set up before the measurements. This was followed by similar measurements of the dye solutions in identical cuvettes. The spectra plots were then obtained by computerized spectrophotometer automatically. All the measurements were carried out at room temperature. Figure 30 reports the various optical transmissions T (%) of the mimosa, flame flower and beetroot dye solutions. The spectra indicate that the transmittance of the mimosa flower dye has a cut-off wavelength of about 490 nm while that of the flame flower and beetroot dyes are about 600 and 660 nm respectively, i.e. in the red spectral range. One can distinguish a common absorption around 1020 nm which corresponds to the standard H_2O vibrational mode. The optical transmission is nearly 0% up to the cut-off wavelengths yet for the flame flower dye has a slight distinctive transmission peak at about 447 nm ($T < 2.5\%$). Consequentially, the flame flower and beetroot dye solutions would be exhibiting nonlinear optical properties in the NIR spectral range while the mimosa dye may present an equivalent effect but in the visible spectral region. For a better appreciation and anticipation of nonlinear properties in general and the optical limiting characteristics particularly, it is worth to plot the absorbance spectra instead. The absorbance of the different dye solution samples are plotted in the spectral range of 200-1100 nm (figure 31). As it can be clearly observed, the absorbance profiles are identical in trend. Excluding the absorption peak due to water solvent, they exhibit 3 major absorbance peaks in the considered spectral range i.e. 200-1100nm. They differ in absorbance intensity, width at half maximum as well as in spectral position. In terms of spectral locations, the 1st, 2nd, and 3rd absorbance peaks, they are located roughly at about or within the range of 240nm, 350-400 nm, and 600-800 nm respectively. Concerning the major absorbance peak, it is centered at 360 nm, 374 nm, and 407 nm for mimosa, flame flower and beetroot dye

solutions respectively (figure 31). In view of the absorbance intensity of the 3rd peaks located in the NIR spectral region (600-1000 nm), one could expect indeed an NLO behaviour in the flame and beetroot dye while a weak one in the mimosa dye, if any. Yet, the optical limiting in both flame and beetroot dye solutions would be observed in one excite with an IR femtosecond source, there is a need to explain the origin of the observed absorbance peaks. The light absorption by each dye molecules is correlated through the excitation of electron from low level to excited (high) level of energy within the molecular cycle of each dye. The amount of light absorbed associated to the π -electron delocalization in the conjugated system of the samples. As mentioned before, and like other natural or synthetic dyes, the studied dyes form a class of materials where the organic molecules called chromophores possess an extensive two dimension π -electron system leading to a fast charge delocalization when they are in interaction with varying intense electromagnetic field. The redistribution of the charge not only offers the stability of the conjugated system but also leads to the absorption of specific wavelengths, allowing the investigation of their nonlinear optical properties based on light absorption as well as refractive nonlinearity properties. Hence the observed absorbance peaks can be attributed to the π -electrons delocalization along the conjugated systems, which are correlated to 1-D or 2-D [Rob-2000] electronic distributions. For an excited dye molecule, due to its delocalization, the π -electrons can respond more freely to an electric field and oscillates over the chain at specific wavelength that can produce an optical resonance. As per the nature of the molecular structure of natural dyes, in general, they are governed by π and σ bonds/anti-bonds orbital configurations. Consequentially, their optical absorptions/emissions are governed by an "electronic spectroscopy" and the electronic excitation that may occur is shown in figure 32.

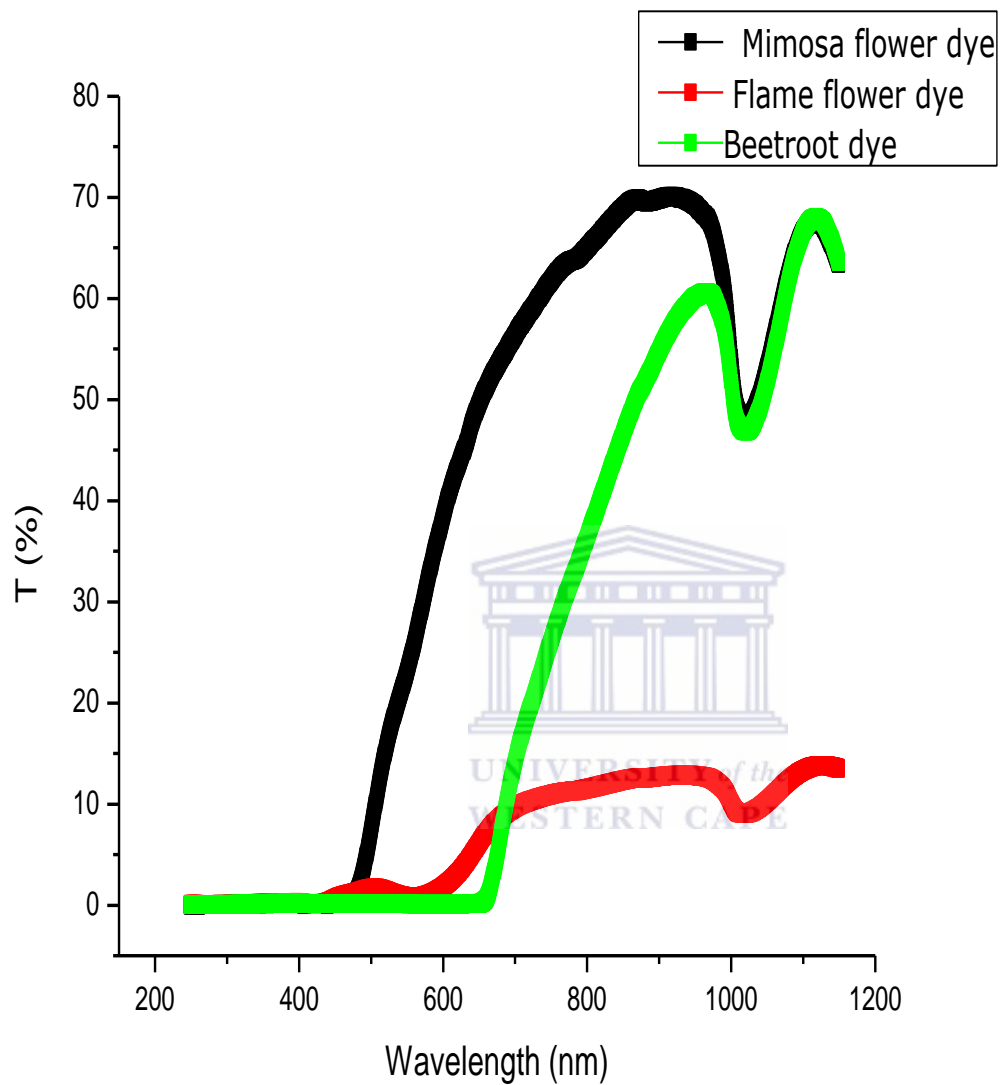


Figure 30: UV-Vis spectra.

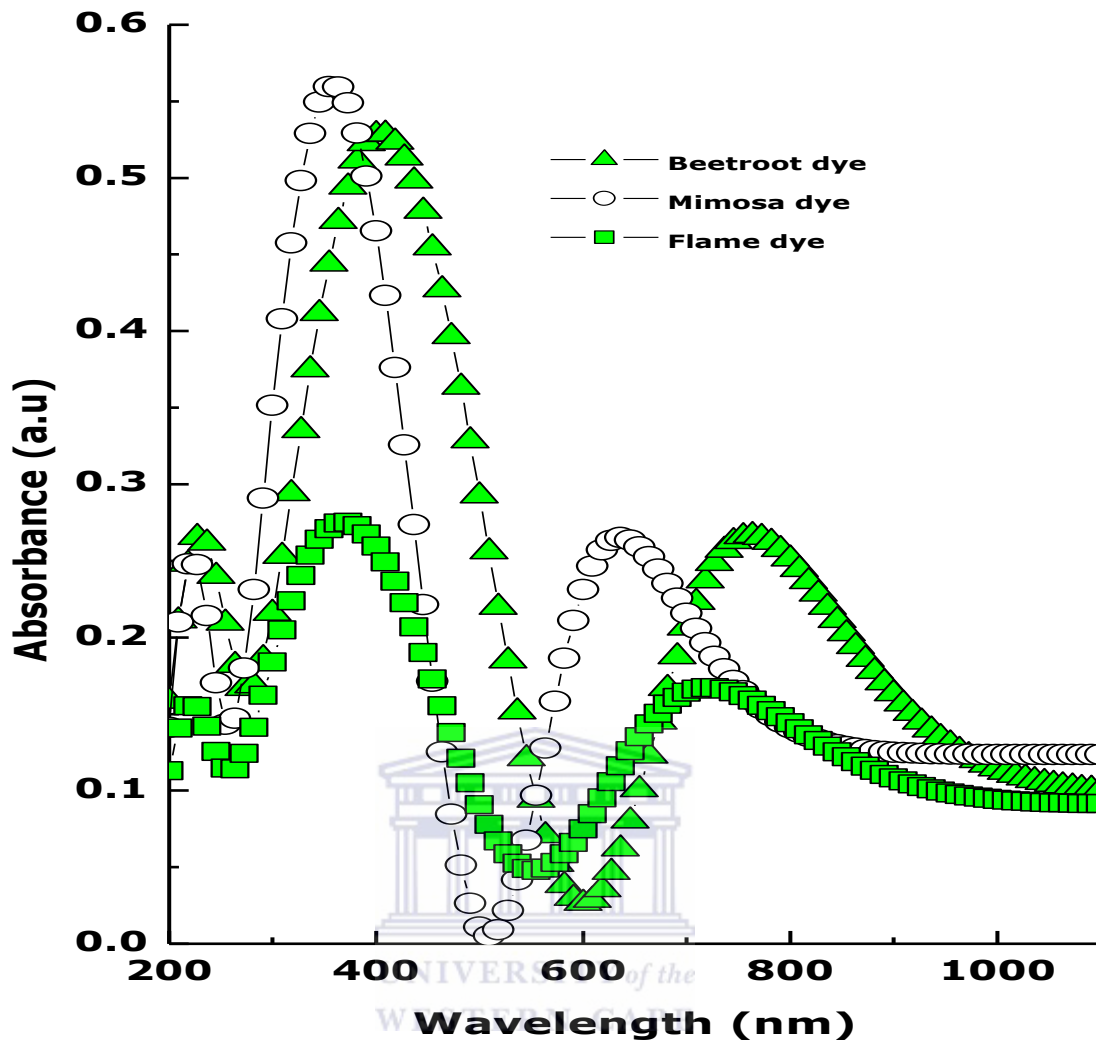


Figure 31: Simulated UV-VIS-NIR optical transmission spectra of the flame, mimosa yellow flower and beetroot dye/H₂O solutions.

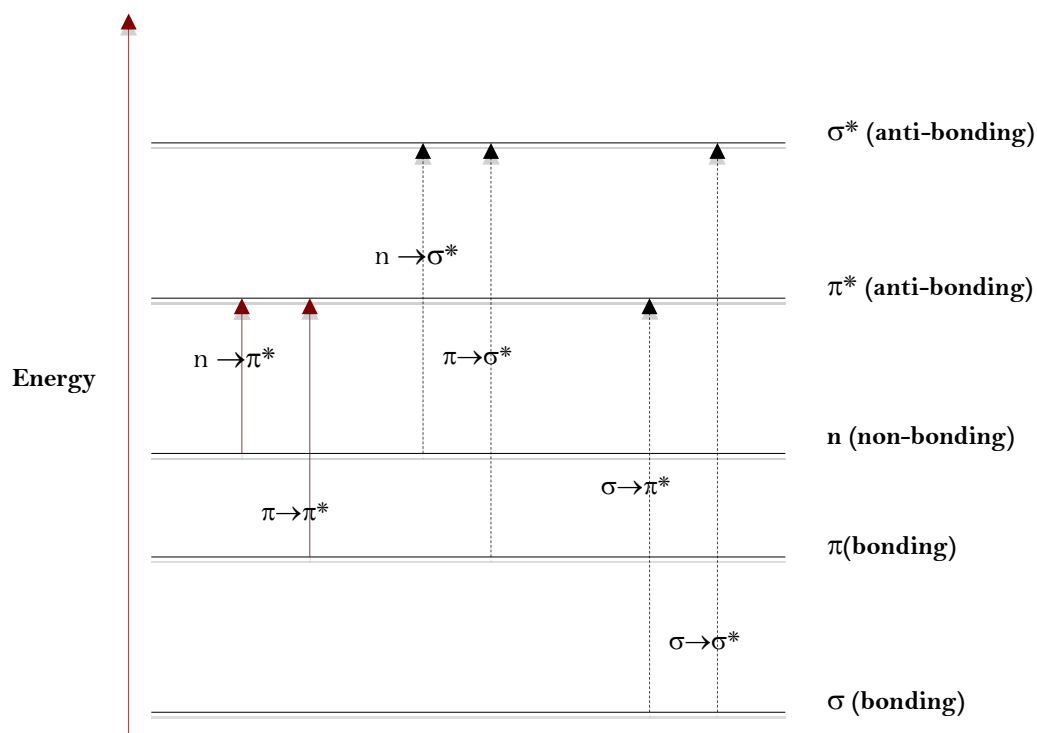


Figure 32: Energy diagram of electronic excitation.



The typical diagram of figure 32 shows the various kinds of electronic excitation that may occur in organic molecules such as our investigated natural dyes molecules. Of the six transitions outlined, only the two lowest energy ones i.e. $\pi \rightarrow \sigma^*$ and $\pi \rightarrow \pi^*$ are achieved by the energies available in the 200 to 800 nm spectrum. As established, energetically favored electron promotion will be from the Highest Occupied Molecular Orbital (HOMO) to the Lowest Unoccupied Molecular Orbital (LUMO). When dye molecules are exposed to light having an energy that matches a possible electronic transition within the dye molecule, some of the light energy will be absorbed as the electron is promoted to a higher energy orbital. Table 5 reports the optical absorbance of a series of standard chromophores. From this table, it can be deduced that the only molecular moieties likely to absorb light in the 200 to 800 nm region are π -electron functions and hetero atoms having non-bonding valence-shell electron pairs. The oxygen non-bonding electrons in alcohols and ethers do not give rise to absorption above 160 nm. Consequentially, based on such

arguments, one could conclude that a priori, the 3 absorbance peaks exhibited by the mimosa, flame flower and beetroot dye solutions are π -electron induced.

Table 5: Optical absorbance of some standard chromophores [Chm-2005].

Chromophore	Example	Excitation	λ_{\max} , nm	ϵ
C=C	Ethene	$\pi \rightarrow \pi^*$	171	15,000
C \equiv C	1-Hexyne	$\pi \rightarrow \pi^*$	180	10,000
C=O	Ethanol	$\pi \rightarrow \pi^*$	290	15
		$\pi \rightarrow \pi^*$	180	10,000
N=O	Nitromethane	$\pi \rightarrow \pi^*$	275	17
		$\pi \rightarrow \pi^*$	200	5,000
C-X	X=Br	$\pi \rightarrow \sigma^*$	205	200
	X=I			

According to the above table, one could certainly conclude that the absorbance peak at about 240 nm for the 3 dye solutions originates indeed from $\pi \rightarrow \pi^*$ transitions. The second and third peaks in the VIS and NIR region are also both due to such $\pi \rightarrow \pi^*$ transitions but are correlated to the high conjugation aspect and the extensive delocalization of electrons pairs in such molecular compounds which are themselves intermediate in character between single and double bonds. An approximate approach to explain the effect of conjugation on the presence of the observed absorbance peaks in the UV and NIR regions is to treat the delocalized electrons within the molecular cycles of the dyes as free particles in a 1-D box of the same length as the chain of alternating single and double bonds. Approximately, in such molecular cycles, the distance from the carbon atom at one end of the conjugated chain to that on the other is about

1.210 nm for vitamin A₂ for example. If one considers the mass of the electron (9.110×10^{-31} kg) moving freely in the box, and considering the basics from quantum mechanics, one can obtain approximate values of the energy levels occupied by such delocalized electrons:

$$E_n = (1/2m_e) (nh/2d)^2 = n^2 (4.11 \times 10^{-20}) \text{ (in Joules)}$$

Therefore, if one considers a molecular cycle with 12 pi free electrons (one for each carbon atom on the conjugate chain) as those present in the flame flower and beetroot cycles (figures 35 & 36), they will occupy the six lowest energetic levels in accord with the Pauli principle. This simple model allows us to calculate the wavelength of the main absorption band in the optical spectra. Hence, if an electron from the highest occupied level ($n = 6$) is excited to the lowest unoccupied level ($n = 7$) (see figure 33), the energy required can be calculated from the equation above:

$$\Delta E = E_7 - E_6 = (7^2 - 6^2) \times 4.11 \times 10^{-20} \text{ J} = 5.34 \times 10^{-19} \text{ J}$$

Corresponding to an absorption wavelength $\lambda = 327$ nm. This is in reasonable agreement with the observed value of the major observed absorbance peaks centered at 360 nm, 374 nm, and 407 nm (figure 37) for mimosa, flame flower and beetroot dyes, considering the approximate nature of the model. As a general rule, the longer a conjugated chain, the longer the wavelength at which it absorbs. Ethene (C₂H₄), for example, has only one double bond and absorbs at 170 nm. Hexatriene (C₆H₈) has three alternating double bonds and absorbs at 265 nm, while vitamin A₂, with six double bonds, absorbs at 350 nm. According to the previous equation, the energy of a level varies inversely with the square of the length of the box. Thus the longer the conjugated chain, the closer the energy levels will be to each other and the less energy a photon need have to excite an electron. Naturally the lower the energy of a photon, the longer its wavelength will be. A similar effect is found for molecules containing several benzene rings (figure 34). Since these correspond to Lewis formulas of alternating double and single bonds, they can also be regarded as conjugated systems containing delocalized electrons. Thus increasing the

extent of electron delocalization increases the wavelength at which a molecule will absorb light, whether the electron is delocalized over rings or chains. An increase of number of atoms along the conjugated path leads to an increase in the wavelength and this is given by $\lambda_{\text{photon}} = (p-1)^2 8m c L^2 / (p+1)^2 h^2$. This behavior of delocalized electrons is important in the preparation of compounds which strongly absorb visible light, i.e. in the preparation of dyes. Very few compounds which are held together by sigma bonds alone are colored. The electrons are so tightly held that a very energetic photon is needed to excite them. In order for an organic molecule to absorb in the visible region of the spectrum, it must usually contain much delocalized pi electrons. Thus most dyes and most colored compounds occurring in living organisms turn out to be large molecules with extensive systems of conjugated double bonds.



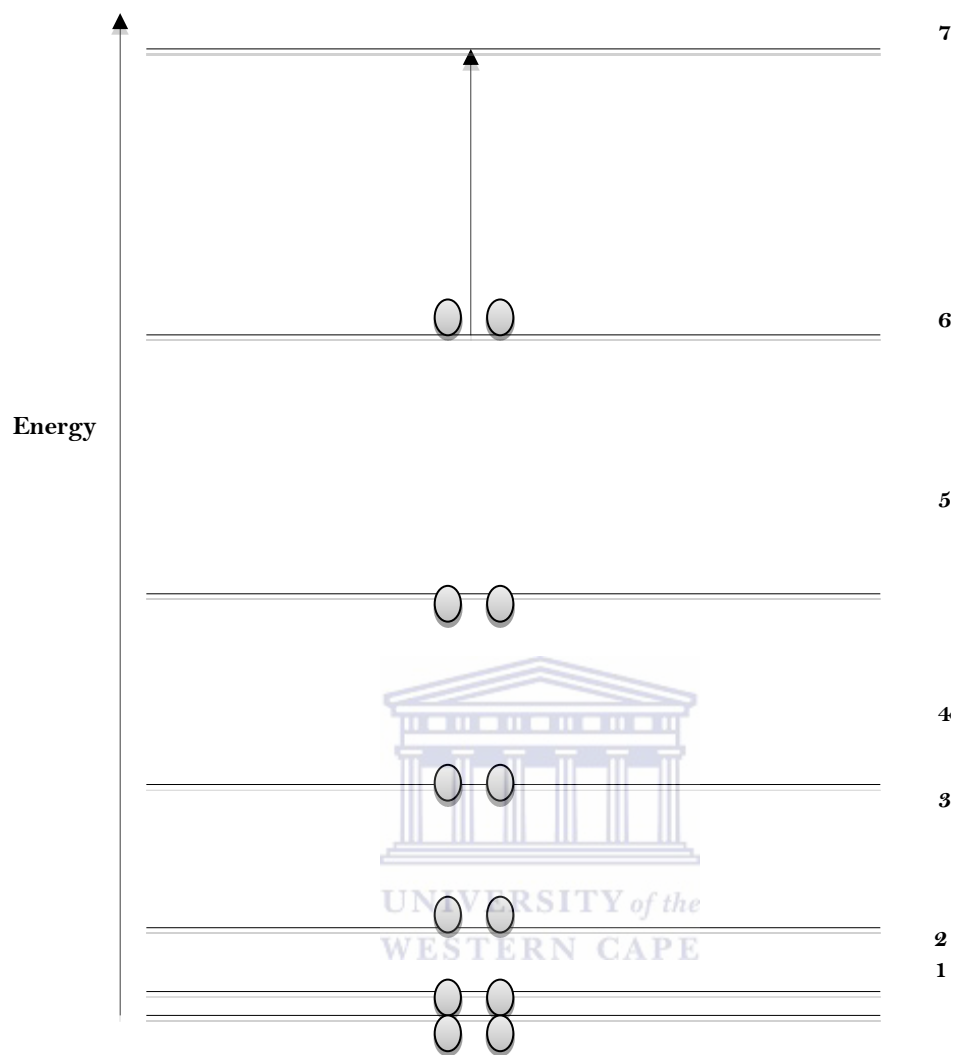


Figure 33: Occupied level of an excited molecule.

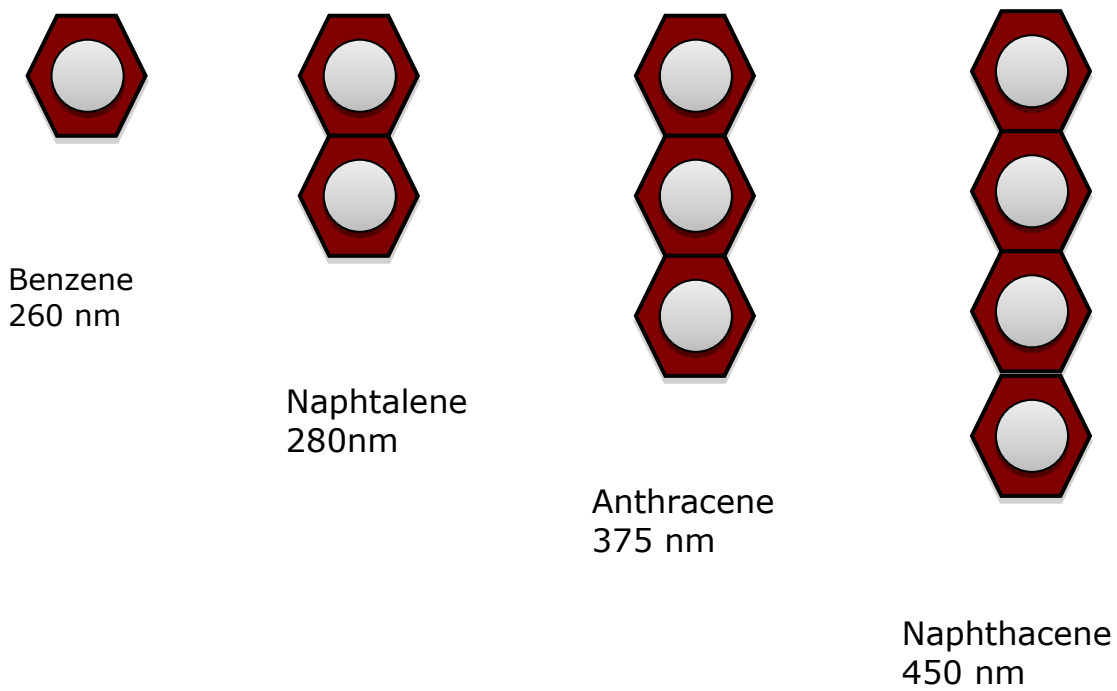


Figure 34: Benzene rings.

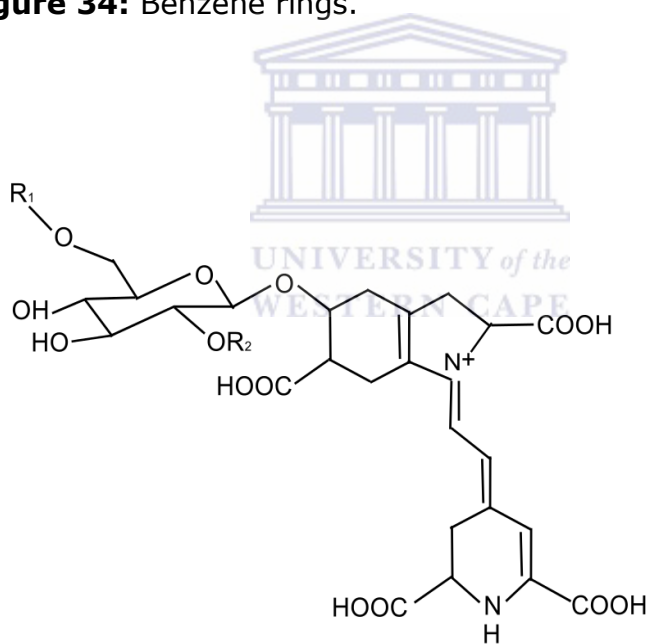


Figure 35: Molecular structure of (Betacyanin) contained in red Beetroot.

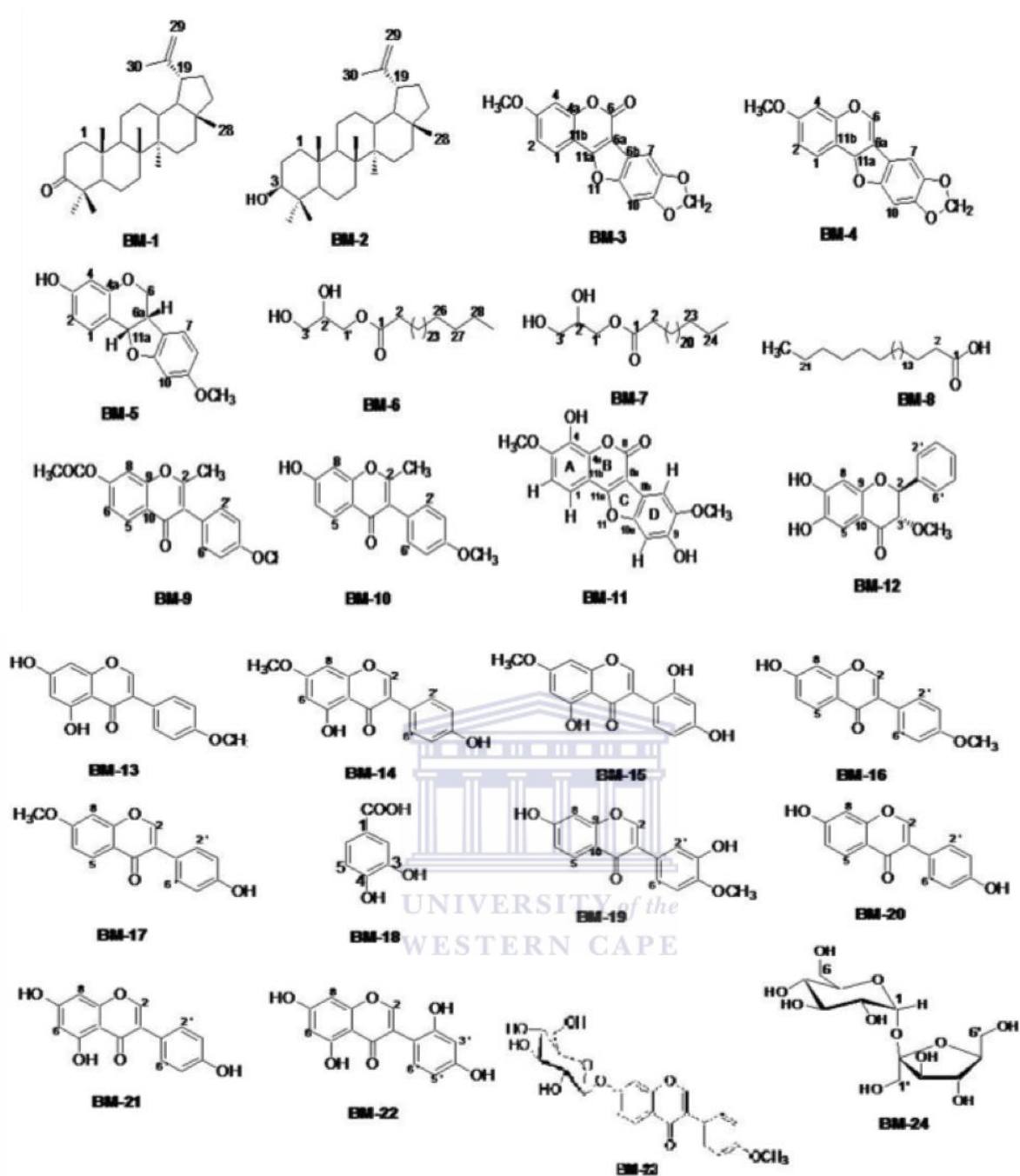


Figure 36: Chemical structures of isolated compounds from *Butea Monosperma* [Pal-2011].

What could explain the shift between the absorbance peaks of the 3 investigated natural dyes as per highlighted in the corresponding figure 32?

To have a direct explanation, it would be sound to use a typical case of the effect of conjugation again in standard chromophores. Generally, and in the so called "electronic" spectroscopy, one can distinguish 4 type of spectral shifts as per the used terminology: (i) Bathochromic (shift to longer λ), Hypsochromic (shift to shorter λ), Hyperchromic (shift to greater absorbance), and Hypochromic (shift to lower absorbance).

As a typical example, figure 37 reports the absorbance of 3 chromophores related all to benzene [Chm-2005]. Benzene exhibits very strong light absorption near 180 nm, weaker absorption at 200 nm and a group of much weaker bands at 254 nm. Only the last group of absorptions is completely displayed because of the 200 nm cut-off characteristic of most spectrophotometers. As one can clearly see, the added conjugation in naphthalene, anthracene and tetracene causes bathochromic shifts of these absorption bands, as displayed in the chart on the left below. All the absorptions do not shift by the same amount, so for anthracene (green shaded box) and tetracene (blue shaded box) the weak absorption is obscured by stronger bands that have experienced a greater red shift. Consequentially, the experimentally observed spectral shift between the absorbance profiles of the mimosa, flame and beetroot dye solutions is correlated to their electron conjugation. More precisely, even without knowing the macro-cycles of all investigated dyes, one could conclude that beetroot dye is more conjugated than flame dye which is more conjugated in its turn to mimosa dye molecular cycle. To understand why conjugation should cause bathochromic shifts in the absorption maxima of chromophores, one needs to look at the relative energy levels of the pi-orbitals again. When two double bonds are conjugated, the four p-atomic orbitals combine to generate four pi-molecular orbitals (two are bonding and two are anti-bonding). In a similar manner, the three double bonds of a conjugated triene create six pi-molecular orbitals, half bonding and half anti-bonding. The energetically most favorable $\pi \rightarrow \pi^*$ excitation occurs

from the highest energy bonding pi-orbital (HOMO) to the lowest energy anti-bonding pi-orbital (LUMO).

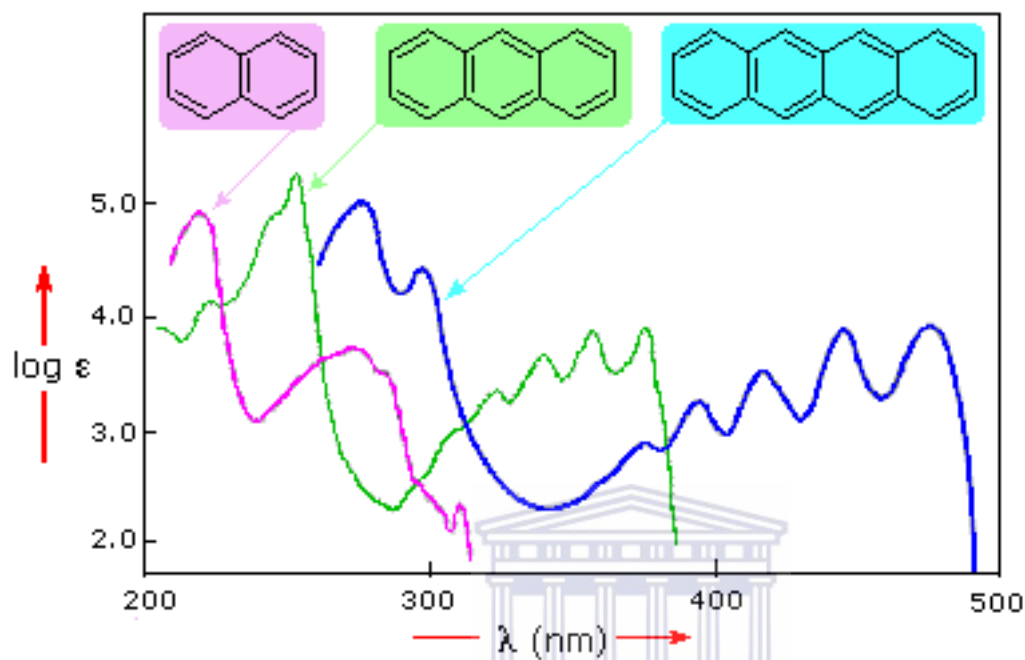


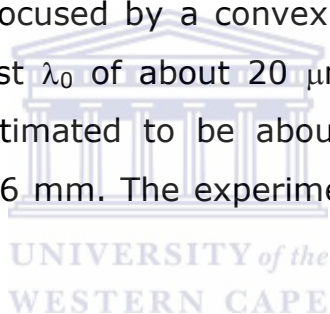
Figure 37: Absorbance in benzene chromophores. [Chm-2005].

4.2.3. Nonlinear Optical Properties and Optical Limiting Investigations

As it was mentioned earlier, the π -electron linear conjugated systems such as the molecular cycles of the investigated dyes can be modelled as a chain (1-D type molecular system) which L as length. The electron re-distribution in response to the externally optical field is therefore measured by the induced polarizability which would generate the targeted large nonlinear optical response such as the optical limiting behaviour. This is a nonlinear optical process which translates itself in a change of the optical transmission versus the electromagnetic input excitation. More precisely, in the optical limiting, after a certain threshold value, the transmitted intensity either stabilize within a plateau or decreases with increased incident light intensity. Optical limiting performance will be enhanced by coupling two or more of the nonlinear optical

mechanisms. Excited state absorption (ESA) and reverse saturable absorption (RSA) are the most common mechanisms for the nonlinear optical behaviour of organic materials similar to the investigated natural dyes [Rek-2010] Indeed, optical limiting was demonstrated in various natural dyes such as Congo red [Rek-2010] and carmine dye for example [Rek-2009]

In view of the optical absorbance resonance exhibited by each of the 3 investigated natural dyes; one has to expect an optical limiting response at least in the femtosecond regime. In this case, a diode-pumped Nd: YAG laser operating at the fundamental wavelength i.e. 1064.8 nm (Fianium FP-1060-5-fs) was used as the excitation source for the optical limiting measurements. The laser source major characteristics are: repetition rate: 78.5 MHz, total power output: 5.6 W, power stability: 0.4%, spectral bandwidth: 12.0 nm, pulse duration: 290 fs with a beam diameter exit of 1.2 mm. The laser of Gaussian beam profile was focused by a convex lens, of focal length $f = 3.5$ cm, to produce a beam waist λ_0 of about 20 μm . The peak intensity of the incident laser beam was estimated to be about $I_0 \sim 4.11 \text{ kW/cm}^2$ with a diffraction length about ~ 2.36 mm. The experimental set-up used is shown in figure 38.



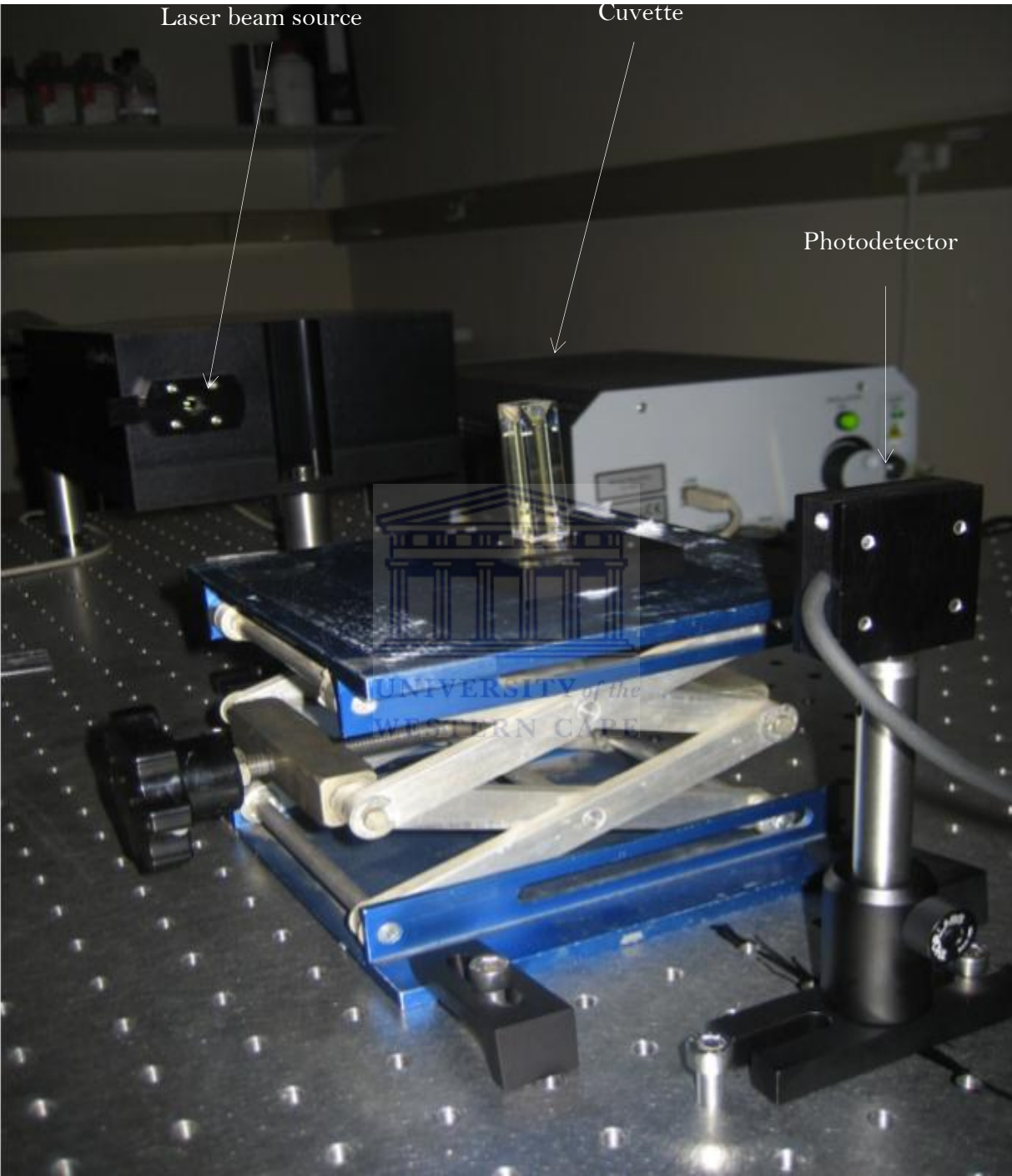


Figure 38: Optical limiting setup.

A ~ 1 mm wide standard optical quartz Y-cell containing the dye solution is translated, at the beginning, across the focal region along the axial direction that is the direction of the propagation laser beam. A variable beam splitter was used to vary the input laser beam power. An aperture of variable diameter is used to control the cross-section of the beam coming out of the sample cuvette. This beam is then made to fall on the photo detector. The input laser intensity is varied systematically and the corresponding output intensity values were measured by the photo detector. At very high peak intensities (closer to the beam focus) we could observe diffraction type pattern with concentric ring structures probably due to self-phase modulation. However, in limiting experiments, it was ensured that there is no ring pattern formation by placing the sample away from focus. The same was repeated for each of the 3 investigated dye solutions.



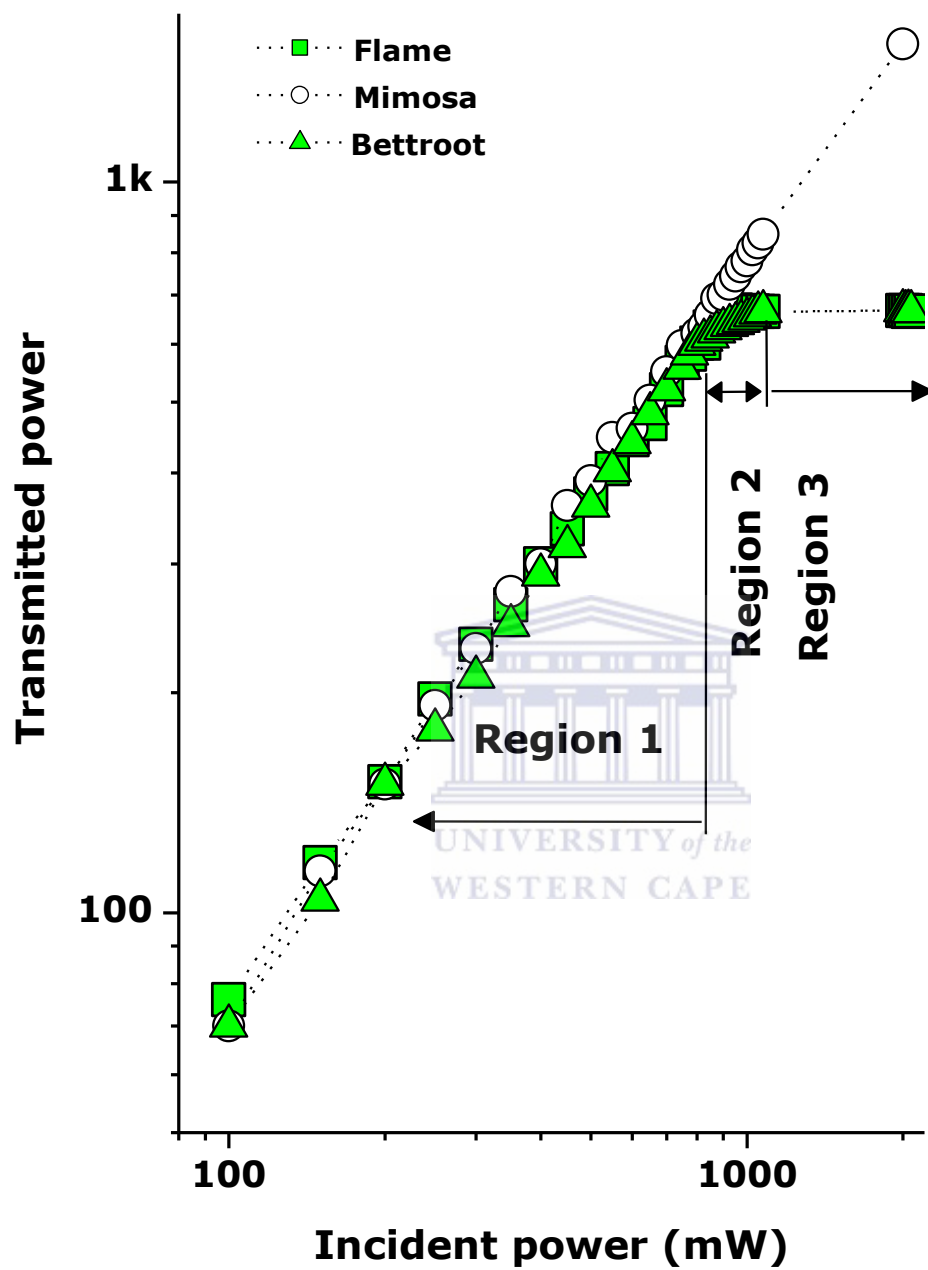


Figure 39: Optic limiting behaviour in the 3 dyes.

Figure 39 reports the experimental transmitted intensity versus the incident laser intensity for the 3 different dyes solutions in a log-log configuration.

As it can be noticed, one can distinguish 3 main spectral regions. In the 1st region which extends up to ~ 802 mW, the output power increases linearly with the input power for all 3 dyes solutions obeying the standard Lambert-Beer law. The 2nd spectral region is proper to the beetroot dye solution and shall be discussed later. In the 3rd region, which starts at a threshold value of about 1078 mW, the transmitted power stabilizes and seems to reach a saturation plateau. More precisely, the transmitted power stabilizes at 1209 mW for both the flame and beetroot dye solutions while still increasing linearly for the mimosa dye. As a conclusion, there is a clear optical limiting behavior for both beetroot and flame flower dyes once excited with IR 1064 nm and not for the mimosa dye. This behavior indicates that the samples start defocusing the beam. More accurately, in such liquid samples, where the thermal expansion is large, high absorbance of the nonlinear material at the corresponding IR wavelength of 1064 nm leads to an increase in temperature and density of the sample. Such a heating due to laser absorption is responsible for changing the absorption coefficient and therefore responsible for the observed optical limiting effect. Concerning region 2 which is approximately limited within the range of 816-1090 mW in terms of the incident power, the variation of the transmitted power is still quasi linear versus the incident power but with a different inclination coefficient. This difference between the optical limiting responses of flame flower and beetroot dye solutions could be assigned to the nature of the phase transitions giving birth to such a NLO behavior; 1st and 2nd order phase transitions for flame and beetroot dye solutions respectively. In view of such, one can deduce that the threshold incident power is about 887 and 1072 mW for the flame flower and beetroot dye solutions respectively if pumped with a Nd: YAG at its fundamental ~ 1064 nm. The curves of the optical limiting measurement are shown in figure 40. reporting the Log-Log variation of the optical transmission versus the laser input energy.

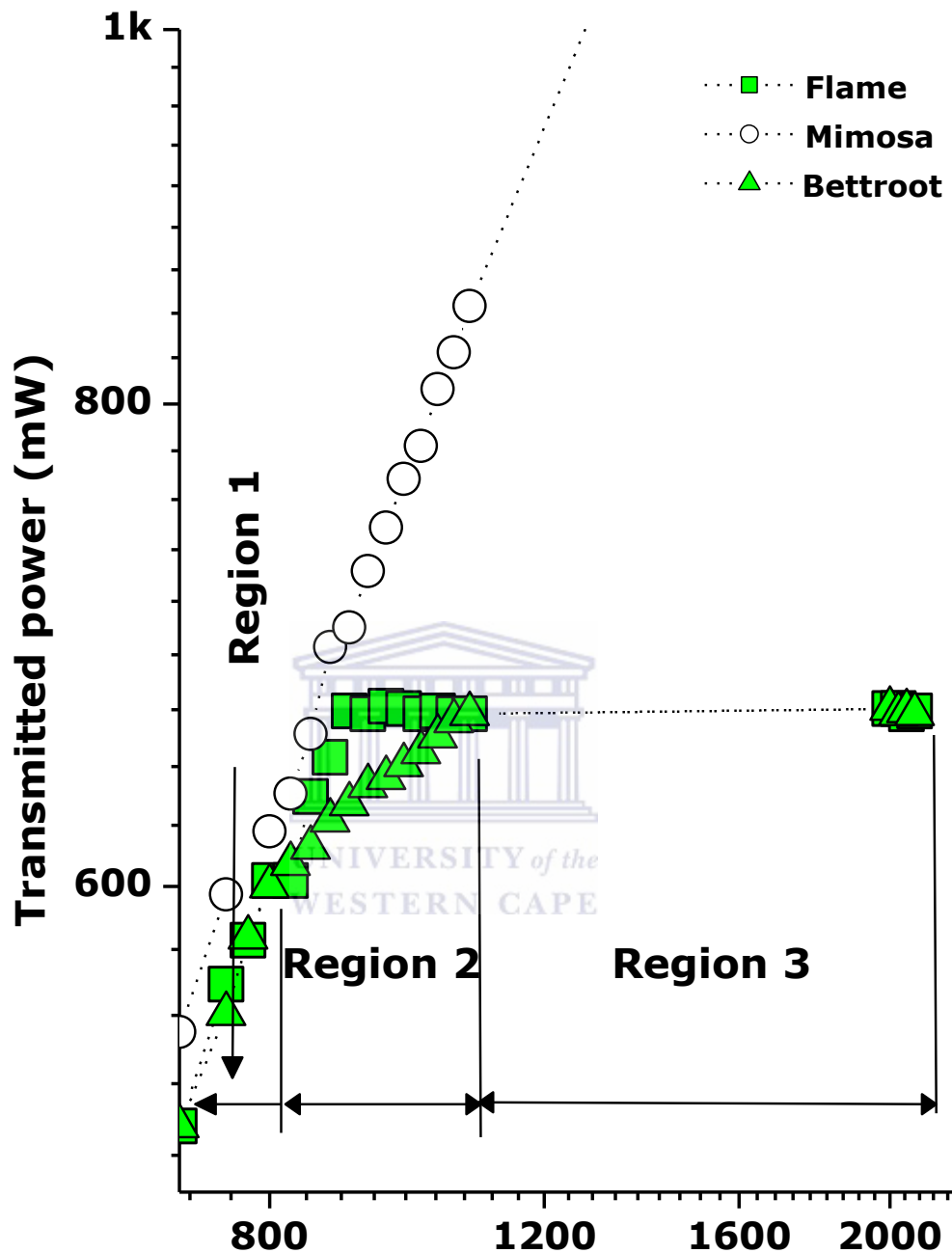


Figure 40: Experimental transmitted intensity versus the incident laser intensity for the 3 different dyes solutions in a log-log configuration.

The output power of the samples increases linearly with the incident power obeying the Beer–Lambert law. The linearity of the curve in the case of the mimosa dye indicates that the transmission is almost total for all the input power intensities. The curves obtained with the flame and beetroot dyes show linear transmission (region 1) from 0 up to 795 mW. Above this value,

transmittance is no longer linear, and a nonlinear relationship can be established between the output and input power. This property of nonlinearity could suggest that the conjugated structures have endowed them with novel optical limiting properties. With a further increase in the incident power, the transmitted power of the flame and beetroot solutions reaches a plateau (corresponding to regions 2 and 3), while the one of the mimosa still increasing. Simultaneously, we also found that the limiting threshold (incident power at which the output power starts to deviate from linearity, around the value of 795 mW, for Beetroot and flame respectively) and amplitude (saturated output intensity) of the dye samples are affected by molecular structure or chemical functional groups (Table 4). Although Beetroot could limit the energy of harsh laser pulses, the optical limiting threshold was still inferior to that of Flame directly connected by conjugated functional group [Yin-2005], which may result from the weakened electronic interactions by spacer between main molecular chains.

In contrast, the transmittance of the mimosa solution continually increases instead of decreasing in the power range of the laser use and this may be due to the laser-induced photolysis of the chemical functional groups chains [Tan-1999] or to the weak ground electronic absorption of mimosa at 1064 nm wavelength as reported in figure 40. Another possible reason that could explain the continuous increase in the transmission of the mimosa solution could be the effect of the concentration of the solution. In fact, G. Balaji *et al.* [Bal-2011], in their study of the effect of the dye's concentration on the optical limiting behaviour, reported that the optical limiting responses of low concentration solutions are generally much weaker than those of high concentrated solutions, while high concentrated solution exhibits strong optical limiting. This indicates that the number density of dye molecules in the laser

beam is the main factor affecting the clamped level. From the threshold intensity for optical limiting for each sample, they reported that the optical power limiting threshold is inversely proportional to the concentration. The data show that as the concentration increases, a reduction in linear transmittance as well as the clamping level is observed. On the other hand,

from theoretical aspect, the low concentration contributes to a reduction of the light absorption [Nic-2004, Dha-2010] if one takes in account the fact that light transmitted is exponentially dependent of the concentration of the dyes. This is expressed according to linear relationships between the concentration and the absorption given by the Beer Lambert's law. The NLO mechanisms for optical limiting of organic compounds can be two-photon absorption (TPA) or reverse saturable absorption (RSA). Generally, TPA can be yielded in principle under the laser irradiation of short pulses. RSA is better achieved on nanosecond or longer pulses, rather than a femtosecond time scale, because of the different excited-state lifetimes involved in a multilevel energy process [Sun-2003]. In this work, the dye solutions are excited by the laser with 290 fs pulse width at 1064 nm. Therefore, we consider that the optical limiting properties of the samples may mainly originate from TPA.



References:

- [Moh-2009] H. Mohamedbakt, and M. Burkitbaev Elaboration and Characterization of Natural Diatomite in Aktyubinsk/Kazakhstan, The Open Mineralogy Journal, 2009, 3, 12-16
- [Ale-2001] Alejandro B. Rodriguez-Navarro, Model of texture development in polycrystalline films growing on amorphous substrates with different topographies, Thin Solid Films 389 288-295 (2001).
- [Bar-1995] P.B Barna , Growth mechanism of Polycrystalline thin, Science and Technology of Thin Films, in FC, (1995)
- [Mat-2007] Mathieu Bouville, Dongzhi Chi, David J. Srolovitz, Grain-boundary grooving and agglomeration of alloy thin films with a slow-diffusing species, Phys. Rev. Lett. 98, 085503 (2007)
- [Jun-1968] H. Junge, M. Musso, Spectrochimica Acta (1968) 24A-1219
- [Kek-2012] Keka Sinha, Papita Das Saha, Siddhartha Datta, Dyes and Pigments 94 (2012) 212-216
- [Ade-2009] G. B. Adebayo, G. A. Olatunji and F. A. Adekola, International Journal of Physical Sciences Vol. 4 (12), (December, 2009) 770-776.
- [Fer-1971] J.R. Ferraron, Plenum Press, New York 85-95 (1971)
- [Oka-1981] E.C. Okafor, Spectrochimica Acta Vol 37A(11) (1981) 945-050
- [Rob-2000] Robert J. Kruhlak, Characterization of Molecular excited State for Nonlinear optics, Dpt. of physical, Washington State University, (2000)
- [Pal-2011] P. Pal and S. Bose Phytopharmacological and Phytochemical Review of Butea monosperma , (2011)
- [Chm-2005] www2.chemistry.msu.edu/faculty/reusch/VirtTxtJml/Spectrpy/UV-Vis/spectrum.htm
- [Rek-2010] Rekha Rathnagiri krishnamurthy, Ramalingam Alkondan, Optica Applicata Vol. XL , No. 1, 2010
- [Yin-2005] S. Yin, H. Xu, W. Shi, Y. Gao, Y. Song, J.W.Y. Lam, Polymer 46 7670-7677, (2005)

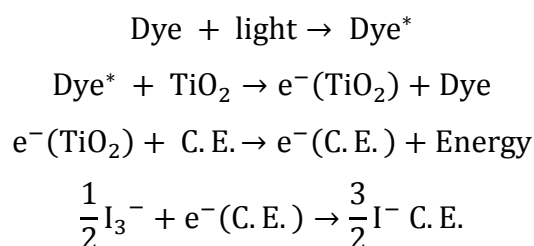
- [Tan-1999] B.Z. Tang, H. Xu, *Macromolecules* 32 (1999) 2569–76
- [Bal-2011] G. Balaji, R.K. Rekha and A. Ramalingam *Acta physica Polonica A*
Vol. 119 (2011)
- [Nic-2004] A. Nicholas Melosh, A. Christian Steinbeck, J. Brian Scott, C. Ryan
Hayward, Patrick Davidson, D. Galen Stucky, and F. Bradley
Chmelka, *J. Phys. Chem. B*, 108, (2004) 11909
- [Dha-2010] M. Dhanam, P. Dheera Devasia, B. Kavitha, B. Maheswari,

Digest Journal of Nanomaterials and Biostructures, Vol. 5, No 3,
587-592, (2010)
- [Sun-2003] W.F. Sun, M.M. Bader, T. Carvalho, *Opt Commun* 215, 185–90,
(2003)



SUMMARY and CONCLUSION

Nonlinearity in optics is evidenced by the change in the optical properties such as absorption coefficient, index of refraction of the medium as the intensity of the applied field increased or when more than one are introduced. Materials that are highly conjugated are very useful for light based applications such as optical limiting, optical switching, optical frequency conversion, data storage and are collectively considered as photonic materials which are characterized by their strong optical nonlinearities. Thus, materials such as organic materials including natural dyes are becoming attracted for their strong conjugated system. In this context, NLO properties investigation for technological applications of such photonic materials becomes a dominant topic in the frontier area of research. This research work was focused on the investigation of the Optical nonlinear optical properties of selected natural dyes such beetroot, flame and mimosa flowers dye. For historical point of view, natural dyes have long been studied for their applications in the food and textile industries. Recently, much work has been done or is being undertaken on natural dyes for their applications in the optical technology. For example, dyes have recently gained interest in the field of the solar cells technology in which the energy conversion follows a process such as.



where C.E. is the counter electrode and Dye^* indicates an excited state of the dye.

The nonlinearity study carried out in this work was focused on the optical limiting property. As described in many reports, the optical limiting is a nonlinear process in which the transmittance of the material decreases with

the increased incident light intensity. Optical limiters are mainly used in the protection of photonic sensors including the human eyes, which have threshold above which they can be damaged. The natural dyes employed for these reasons, were investigated using the femtosecond laser at 1064 nm. The choice of the dyes was based on the fast acting nonlinearity, the synthesis flexibility, and ease processing. As in other organic dyes, they exhibit a conjugated π -electrons system that could be responsible of the optical absorption. Our results have indicated that only the flame flower and the beetroot dyes are promising for optical limiter applications. This could be explained by the fact that the wavelength used was in the range of NIR which matches the red colour. In addition of the optical limiting, the UV-Vis and FTIR spectra were used to identify the main functional groups. The obtained results show that the dyes present some common functional groups such as those mentioned in the table 4, which are responsible of the light absorption. Whereas the liquid forms were unstable for all the dyes, it was found that the dyes embedded in gel were stable for long duration. Any colour change was observed. Therefore the hybrid matrix (i.e. dye-gel) could yield a better optical limiting quality and increases the stability of the dye for long duration. In addition to the optical characterization elemental, crystallographic and morphological analysis were carried out. The intention was to examine the thin film of these dyes and their characteristics.

Future Prospects

In the context of technological applications, organic materials such as natural dyes as well as dye-inorganic hybrid systems, i.e. dye materials-composites have been identified to be promising class of photonic materials. Hybrid materials do possess the synthetic flexibility of dye compounds. For a better understanding of fundamental mechanisms and evolution of nonlinearity phenomena in such material, time resolved measurements, laser flash photolysis experiments under picosecond and femtosecond excitations are required.